

**The Molecular and Electronic Structures of Some  
~~Aromatic and Heteroaromatic~~ Radical Ions**

A Thesis submitted for the degree  
of Doctor of Philosophy in the  
Faculty of Science of the  
University of London

By  
David Victor Avila

The Christopher Ingold Laboratories  
University College London  
20 Gordon Street  
London WC1H 0AJ

July 1990

ProQuest Number: 10608843

All rights reserved

INFORMATION TO ALL USERS

The quality of this reproduction is dependent upon the quality of the copy submitted.

In the unlikely event that the author did not send a complete manuscript and there are missing pages, these will be noted. Also, if material had to be removed, a note will indicate the deletion.



ProQuest 10608843

Published by ProQuest LLC (2017). Copyright of the Dissertation is held by the Author.

All rights reserved.

This work is protected against unauthorized copying under Title 17, United States Code  
Microform Edition © ProQuest LLC.

ProQuest LLC.  
789 East Eisenhower Parkway  
P.O. Box 1346  
Ann Arbor, MI 48106 – 1346

## Acknowledgements

I would like to express my sincere gratitude to Prof Alwyn G. Davies for his guidance and support, and also in his choice of Dr Carl H. Schiesser as post-doctoral fellow whose help and advice has been invaluable.

I would like to thank Dr D. A. Tocher and Prof M. L. Truter for their advice and guidance regarding some of the X-ray crystal structures in Chapter 4.

Many thanks to Dr Robin Hay-Motherwell and Dr Ian Davison who spent time kicking me into shape.

I would like also to thank my colleagues past and present: Karen, Paul, Dang, Pearl, Colin, Kai, Maria, Elizabeth, and Daniel.

There is a night cleaner Claude who has been responsible for making me smile especially at 1 o'clock in the morning when nothing has worked.

My thanks also go to my parents and Eleanor who have supported me and put up with me.

Finally my gratitude goes to the Chemistry Department for the departmental research studentship and to University College for the Thomas Witherton Batt Scholarship. I hope that finances will allow others to benefit from these opportunities as I have done.

## Abstract

This thesis reports an investigation into the molecular and electronic structures of some aromatic and heteroaromatic radical ions (predominantly cations).

The radical ions were identified and characterised by electron spin resonance spectroscopy. Computer-simulated molecular structures of some were optimized by semi-empirical (AM1) and molecular mechanics calculations; these calculations support the experimental observations.

The conformational inversion of the cyclohexene ring in two radical cations containing the benzocyclohexene moiety was observed at a range of temperatures, yielding contrasting barriers to inversion. These were found to be in accord with molecular mechanics calculations on the neutral molecules. The permethylbenzocyclohexenes 9,10-dimethyl-1,2,3,4,5,6,7,8-tetrahydroanthracene and 1,2,3,4-tetramethyl-5,6,7,8-tetrahydronaphthalene exhibited unusual molecular orbital perturbation.

The radical cations and anions of methylated biphenylenes, tetraphenylene, and octa- $\beta$ -methyltetraphenylene were investigated. The pairing principle of alternant  $\pi$ -systems was confirmed in all examples where both radical cations and anions could be studied. The tetra- $\alpha$ -methylbiphenylene exhibited mercurideprotonation when its radical cation was generated in trifluoroacetic acid containing mercury(II) trifluoroacetate. When tetra- $\beta$ -methylbiphenylene in tetrahydrofuran was treated with lithium, reduction and ring opening apparently occurred. The electron distribution observed in the radical cation of octa- $\beta$ -methyltetraphenylene confirmed the prediction of a perturbation of molecular orbitals approach.

The radical cations of a variety of compounds containing the pyrrole moiety are discussed. A series of *p*-phenylene-bis(dialkylpyrroles) showed no hyperfine coupling to the arene unit, and electron release into the pyrrole ring by 2,5-diethyl groups was found to be greater than by 2,5-dimethyl substituents. X-Ray crystallography showed that the 2,2',5,5'-tetramethylbi-(*N*-pyrrolyl) has an orthogonal structure and its radical cation shows the unpaired electron to be delocalised over both rings. The radical cation of 8b,8c-diazapyracyclene, which is isoelectronic with the radical anion of pyracyclene, has been observed and undergoes mercurideprotonation.

The spectrum of the radical cation of 1-phenyl-2,3,4,5-tetramethylarsole is in accord with the photoelectron spectra and calculations which suggest that the heteroatom is pyramidal and that arsoles may be considered as non-aromatic hetero[5]annulenes.

## CONTENTS

	Page
Acknowledgements	2
Abstract	3
Abbreviations	8
1. Introduction	
1.1 Background	9
1.2 Generation of Radical Ions	11
1.3 Mercurideprotonation	12
1.4 Electron Spin Resonance	13
Hyperfine Splitting	
Spin density	
$\alpha$ -Coupling	
Proportionality Constant	
$\beta$ -Coupling	
$\gamma$ -Coupling	
Interpretation of ESR spectra	
1.5 Structural and Molecular Orbital Calculations	20
<i>Ab initio</i>	
Alternant Systems	
Hückel Molecular Orbital Theory	
Molecular Mechanics	
1.6 Single Crystal X-ray Crystallography	22
1.7 Purpose of Work	22
References	23
2. Some Benzocyclohexene and Benzocyclopentene Radical Cations	
2.1 Introduction	25
2.2 Results and Discussion	26
2.2.1 Conformational inversion in the	26

Dodecahydrotriphenylene Radical Cation	
2.2.2 Some Unusual Benzene Ring Distortions	36
References	44
3.1 Radical Cations and Anions of Some Methylated Biphenylenes, Tetraphenylene, and Octa- $\beta$ - methyltetraphenylenes	
3.1 Introduction	46
3.2 Results and Discussion	47
3.2.1 Tetra- $\alpha$ -, Tetra- $\beta$ -, and Octa-methylbiphenylene	47
3.2.2 Tetraphenylene and Octa- $\beta$ -methyltetraphenylene	60
References	70
4. Radical Cations of Some Mono- and Bis-pyrroles and Related Compounds	
4.1 Introduction	72
4.2 Results and Discussion	74
4.2.1 Simple <i>N</i> -Substituted Pyrroles	74
4.2.2 Oligomethylene <i>NN'</i> -Bipyrroles	77
4.2.3 <i>N</i> -Phthalimidopyrrole	80
4.2.4 <i>N</i> -Aminopyrrole	82
4.2.5 <i>N</i> -Arylpyrroles	83
4.2.6 Pyrrolophanes and Some Related Compounds	90
4.2.7 Bis( <i>N</i> -pyrrolyl)	93
4.2.8 Diazapyracyclenes	97
4.2.9 [2.2](2,5)Furano- and Thiopheno-phane	102
4.2.10 Dioxenes	103
4.2.11 1,3,4-Thiadiazoles and 1,3,4-Oxadiazoles	104
4.2.14 1,3 $\lambda^4\delta^2$ ,5,2,4-Trithiadiazepine	105
References	111
5. Arsoles and Other Non-aromatic Hetero[5]annulenes	
5.1 Introduction	113

5.2 Results and Discussion	115
5.3 References	118
6. Experimental	
6.1 Synthesis	119
6.2 Preparation of Samples for ESR spectroscopy	133
6.2.1 Oxidants	133
6.2.2 Reductants	134
6.3 ESR Spectroscopy	135
6.4 NMR Spectroscopy	137
6.5 Semi-empirical MO and Molecular Mechanics	137
Calculations	
6.6 X-Ray Crystallography	137
References	137



### Abbreviations

ESR :-	Electron spin resonance
HOMO :-	Highest occupied molecular orbital
h.p.l.c. :-	High pressure liquid chromatography
IP :-	Ionization potential
LCAO :-	Linear combination of atomic orbitals
MO :-	Molecular orbital
NMR :-	Nuclear magnetic resonance
SOMO :-	Singly occupied molecular orbital
THF :-	Tetrahydrofuran
TFA :-	Trifluoroacetate
TFAH :-	Trifluoroacetic acid
u.p.e. :-	Unpaired electron
$\phi$ :-	A benzene ring irrespective of substituents

## Chapter 1. Introduction

### 1.1 Background

Electron spin resonance (ESR) spectroscopy is the most effective known method of examining the distribution of an unpaired electron (u.p.e.) in a molecule.

The technique was discovered by Zavoiskii<sup>1</sup> in 1945 and has provided detailed structural and electronic information on a variety of paramagnetic compounds.

ESR spectroscopy has the advantage of being very sensitive and free radicals may be detected in concentrations as low as  $10^{-8}$  M. Furthermore no diamagnetic species such as solvent or substrate are detected.

Neutral radicals are usually very reactive species and decay at diffusion-controlled rates. Charged radicals are much less reactive, in part due to their Coulombic repulsion. This intrinsic stability allows higher radical concentrations to be obtained which facilitates detection and observation of such species.

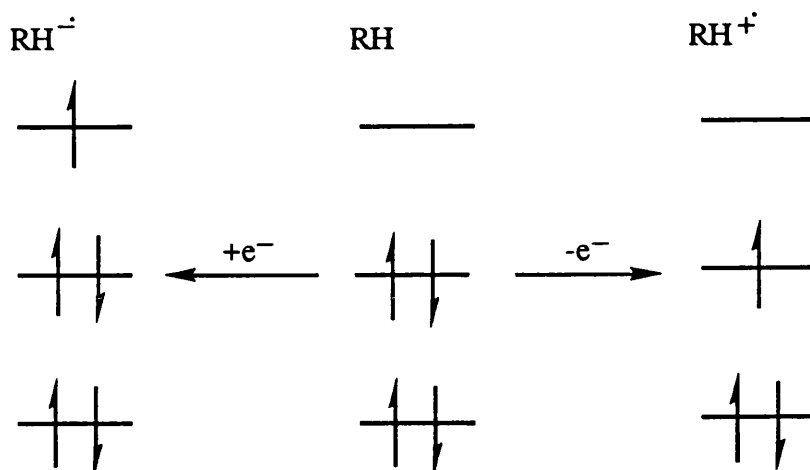


Figure 1.1 Orbital occupancy of a neutral molecule, its radical anion and cation.

The radical anion ( $RH^{-\cdot}$ ) and radical cation ( $RH^{+\cdot}$ ) are generated by reduction and oxidation of  $RH$  respectively. Figure 1.1 illustrates the generation of these radical ions in terms of the molecular orbitals (MO's) involved.

The SOMO of an arene radical cation ( $ArH^{+\cdot}$ ) has the same form as that of the HOMO of its parent ( $ArH$ ). It is this property that makes the radical cations important species in which to study the electronic distribution in the parent.

The information obtained gives insight into reactivities and reaction mechanisms undergone by the parent and related compounds.

The synthetic applications of neutral radicals<sup>2</sup> and of photoexcited<sup>3</sup> states attract more attention than those of the radical ions. Radical cations ( $\text{ArH}^{\cdot+}$ ) form loose complexes with their parent ( $\text{ArH}$ ) by SOMO-HOMO interaction, and then may proceed to form covalent bonds ( $\text{Ar-Ar}$ ) (Figure 1.2, equation 1.1), for example  $\text{C}_6\text{H}_6^{\cdot+} + \text{C}_6\text{H}_6 \rightarrow$  biphenyl radical cation.

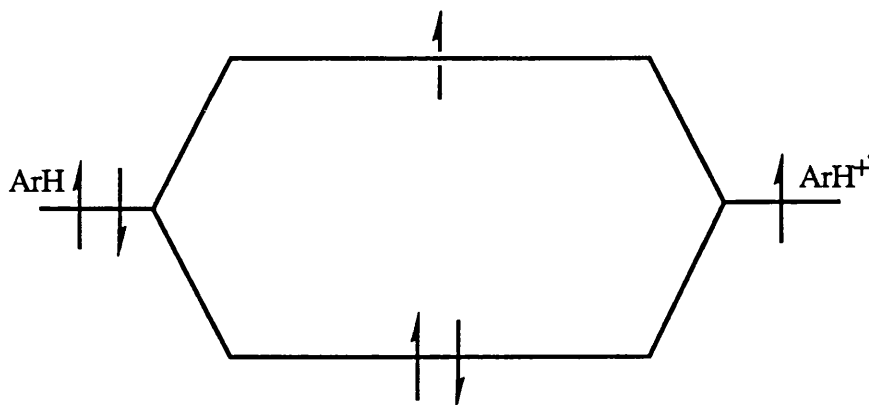
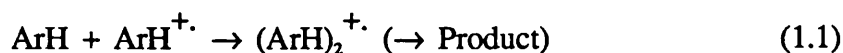


**Figure 1.2** Frontier orbital interaction of  $\text{RH}^{\cdot+}$  and  $\text{RH}$ .

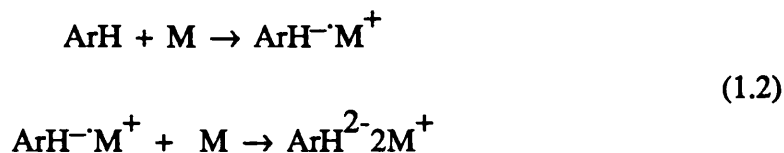


When two orbitals of very similar energy interact, the stabilising interaction is greater than when two orbitals of dissimilar energy interact. This is part of the reason why radical anions are often less reactive than their corresponding radical cations. The SOMO of a radical anion is of higher energy and is more diffuse due to electrostatic repulsion, and the interaction with its parent [ $\text{ArH}^{\cdot-} + \text{ArH} \rightarrow (\text{ArH})_2^{\cdot-}$ ] is not observed.

The Diels-Alder dimerization of cyclohexa-1,3-diene<sup>4</sup> has been shown to be catalysed by an oxidizing agent and is believed to involve the diene radical cation acting as a dienophile. The increased reactivity is probably due to better orbital interaction between diene and dienophile.

## 1.2 Generation of Radical Ions

Aromatic compounds with sufficient electron affinity react with alkali metals to form mono or divalent salts (Equations 1.2).



The reaction is promoted by polar aprotic solvents such as tetrahydrofuran and dimethoxyethane which can effectively solvate the metal cations. Sometimes the addition of a suitable crown ether is required to facilitate the reaction by chelating the metal ion.

If the diamagnetic dianion is formed, the use of an alkali metal with a higher ionisation potential (IP), or a limited contact with the reductant may prevent this. In some cases it is possible to photoeject an electron from the diamagnetic dianion producing the paramagnetic radical anion (Equation 1.3).



Aromatic compounds with sufficiently low IP's do not always form ESR-observable radical cations. Polymerisation may be a problem with compounds ArH with high electron densities at any one point. Electrophilic attack of the radical cation upon its parent, probably the route by which polymerization occurs, is reduced by alkylation at positions of high electron density. In the five-membered heteroaromatics it is necessary to have the 2 and 5 positions alkylated to observe their radical cation species in liquid solution.

Radical cations may be generated by  $\gamma$ -radiolysis of dilute (*ca.*  $10^{-3}$  M) solutions of the parent in a Freon matrix,<sup>5,6</sup> usually at liquid nitrogen temperatures. The IP of the substrate needs only to be lower than that of the matrix, and polymerization does not occur. As the molecules are not tumbling, the hyperfine coupling and *g*-value are anisotropic, generally leading to broad lines in which small couplings cannot be observed. Other physical methods for oxidation include photoionisation, pulse radiolysis, and electrolysis.

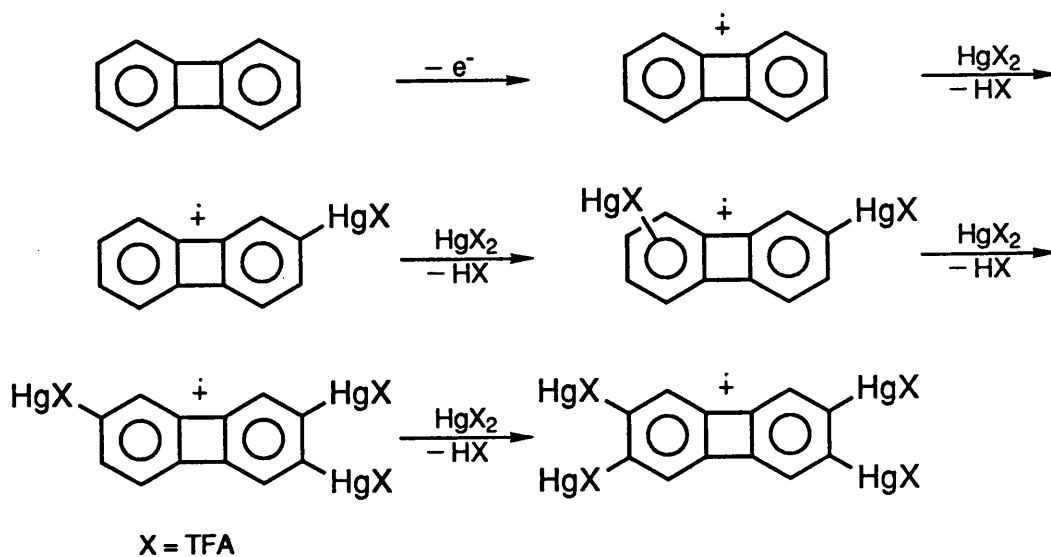
In our laboratories chemical methods have been used most frequently for radical cation generation. Historically, sulphuric acid was the first oxidant used, but now a variety of reagents are available, such as certain Lewis acids, e.g.  $\text{AlCl}_3$  and  $\text{SbCl}_5$ , using  $\text{CH}_2\text{Cl}_2$  as the solvent; the metal salts of trifluoroacetic acid (TFAH) with variable oxidation states, e.g.  $\text{Hg}^{2+}$ ,  $\text{Tl}^{3+}$ ,  $\text{Co}^{3+}$  or  $\text{Ce}^{4+}$ , with or without varying degrees of ultraviolet (u.v.) irradiation; or a solution of  $\text{HFSO}_4$  in liquid  $\text{SO}_2$ .

### 1.3 Mercurideprotonation

Mercurideprotonation<sup>7,8</sup> was first observed within this group when the radical cations of some hydrocarbon  $\pi$ -electron systems were generated in trifluoroacetic acid containing mercury(II) trifluoroacetate. This was detected by the occurrence of  $^{199}\text{Hg}$  satellites about the central feature of the ESR spectrum. Mercury has two magnetically active nuclei  $^{199}\text{Hg}$  (natural abundance 16.84%)( $I = 1/2$ ) and  $^{201}\text{Hg}$ , (natural abundance 13.22%)( $I = 3/2$ ). No  $^{201}\text{Hg}$  coupling has been observed in NMR or ESR spectra in fluid solution, probably because of quadrupolar effects. The best documented case of mercurideprotonation is that of biphenylene where its radical cation becomes mono- $\beta$ -mercurated and proceeds progressively through to tetra- $\beta$ -mercurated species as shown in Scheme 1.1.

After observing mercurideprotonation in a series of compounds, Davies *et al.* have put forward the following principles:

1. Mercurideprotonation occurs at the aromatic position where the proton ESR coupling is highest i.e. at the position of greatest electron density in the SOMO of the radical cation.
2. When the mercuriation occurs, the coupling constants of the remaining protons remain unaffected i.e.  $\rho_{\alpha}$  remains constant.
3. The ratio between the coupling constant of the mercury substituent and the proton it displaces,  $a(^{199}\text{Hg})/a(^1\text{H})$ , is ca 20.6:1.
4. Mercurideprotonation of an aromatic species always leads to a reduction in the  $g$ -value of the radical cation and if progressive mercuriation occurs, there is a corresponding progressive reduction in the  $g$ -values of the radical cations.



Scheme 1.1

#### 1.4 Electron Spin Resonance

The theory and practice of ESR spectroscopy are described and reviewed in many texts.<sup>9,10</sup>

ESR is restricted to paramagnetic species, and many methods (Section 1.2) have been developed for generating these from their diamagnetic precursors.

Hyperfine coupling  $a(X)$  arises where there is a net unpaired electron (u.p.e.) spin density at magnetically active nuclei (X). The magnitude of such coupling is dependent upon the degree of interaction between the orbital the u.p.e. occupies and the nucleus.

The spin density ( $\rho_i$ ) in conjugated molecules is a function of many electrons and is defined as the difference between the total probability of electrons with spin  $M_s = +1/2$  ( $\alpha$ ) and  $M_s = -1/2$  ( $\beta$ ) where the densities are normalized to unity over the whole molecule (equation 1.4).

$$\rho_i = \rho_i(\alpha) - \rho_i(\beta) \quad (1.4)$$

$\rho_i$  is the spin density in the region  $i$  of the molecule and  $\rho_i(\alpha)$  and  $\rho_i(\beta)$  the total probability of electrons with  $\alpha$  and  $\beta$  spin respectively in the region  $i$ .

$\alpha$ -Coupling can arise by the mechanism of spin polarization. Consider the methyl radical where there are two possible electronic configurations as shown in Figure 1.3a and b.

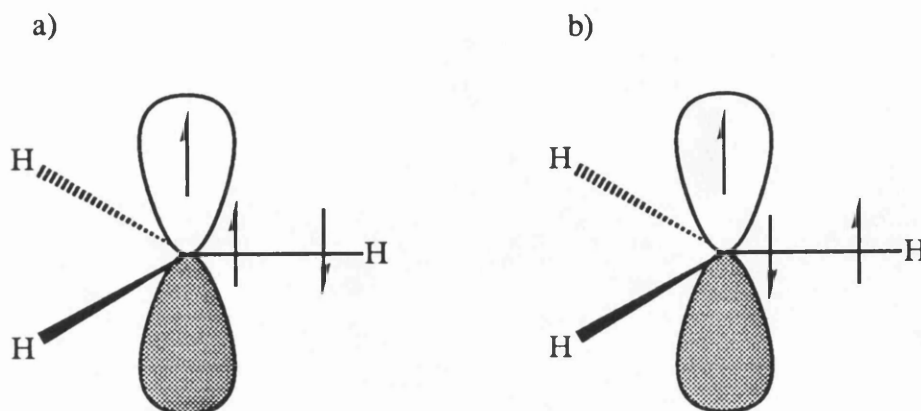


**Figure 1.3** Possible configurations of electron spin in the  $\sigma$ -orbital bonding the hydrogen atom of a methyl radical, for  $\alpha$ -spin in the  $2p_z$  orbital of carbon.

If there were no u.p.e. in the  $2p_z$  orbital the spin orientations of the electrons in the  $\sigma$ -bonds of a) and b) would be equally probable and at the hydrogen atom  $\rho_H(\alpha) = \rho_H(\beta) \therefore \rho_H = 0$ . Hund's rule of maximum multiplicity states that electrons with parallel spins have lower energy than a corresponding pair with opposed spins, hence configuration a) is the energetically more favourable. Thus there is a net negative spin density on the  $\alpha$ -hydrogen [ $\rho_H(\beta) > \rho_H(\alpha)$ ] and the coupling constant is negative.  $\alpha$ -Coupling is described by the McConnell equation<sup>11</sup> (Equation 1.5).

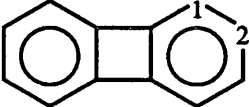
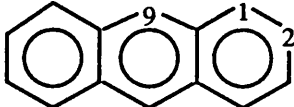
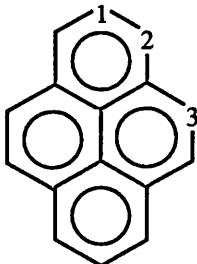
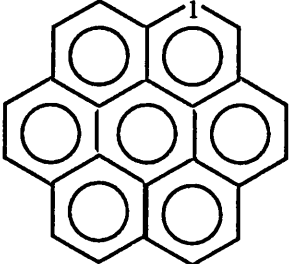
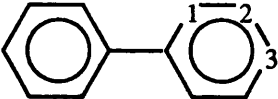
Figure 1.3a indicates that the spin density of a C-H fragment should be negative if the spin density in the adjacent  $2p_z$  orbital is positive. The sum of the spin polarization contributions from surrounding  $2p_z$  orbitals can be zero, positive, or negative.

The sign of hyperfine splitting constants can be determined from the nuclear magnetic resonance (NMR) shifts for paramagnetic molecules. The NMR lines must be narrow enough relative to the magnitudes of the line shifts to permit the measurement of the latter.

$$a(X) = \rho_i Q \quad (1.5)$$

$a(X)$  Is the magnitude of coupling (in Gauss),  $\rho_i$  is the spin density on atom  $i$ , and  $Q$  is the proportionality constant.

There is considerable variation in  $Q$ , especially between corresponding negative and positive charged species. The  $\pi$ -spin densities for corresponding positions in the radical cation and anion of a given alternant hydrocarbon should be identical (Section 1.4). The fact that the hydrocarbon cation splittings are generally larger than those of the corresponding anion implies that the  $Q$  value is dependent on the charge at the carbon atom.<sup>12,13</sup> Table 1.1 gives a comparison of coupling constants ( $G$ ) in radical ions of some alternant hydrocarbons.

Radical ion of	X	Cation		Anion	
		$a(H_X)$ ArH	$a(H_X)$ ArH	$a(H_X)$ ArH	$a(H_X)$ ArH
	1	0.21		0.21	
	2	3.69		2.86	
	1	3.06		2.74	
	2	1.38		1.51	
	9	6.53		5.34	
	1	5.38		4.75	
	2	1.18		1.09	
	3	2.21		2.08	
	1	1.53		1.47	
	1	3.15		2.73	
	2	0.51		0.43	
	3	6.30		5.46	

**Table 1.1** : The coupling constants  $a(H_X)/G$  of ring protons in the radical ions of some alternant hydrocarbons.



Coupling to  $\beta$ -protons is frequently larger than to  $\alpha$ -protons, for example, in the ethyl radical  $\text{CH}_3\text{CH}_2\cdot$ ,  $a(2\text{H}_\alpha) = 22.2 \text{ G}$  but  $a(3\text{H}_\beta) = 26.9 \text{ G}$ . The  $\beta$ -coupling is principally due to hyperconjugation but also has a small contribution from spin polarization. Figure 1.4a illustrates that spin polarization makes only a small contribution to  $\beta$ -coupling because it has to be transmitted through two bonds, and Figure 1.4b shows how the u.p.e. in a  $2p_z$  orbital may interact effectively with the electrons of a  $\beta$  C-H bond.

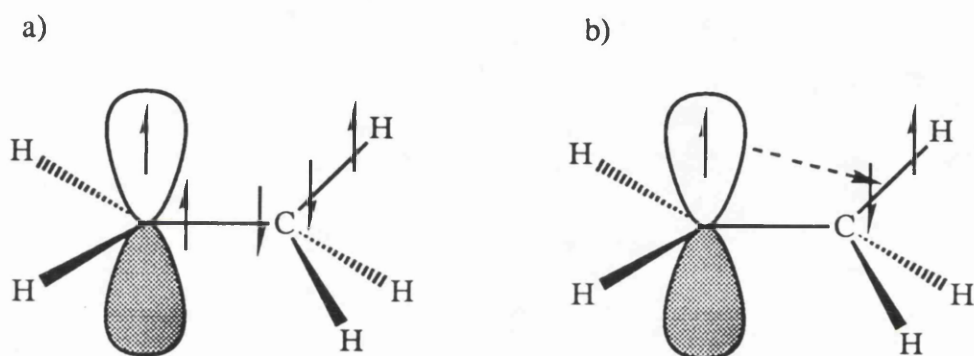


**Figure 1.4** Qualitative representation of (a) spin polarisation and (b) hyperconjugation involving the  $\sigma$ -bond of a  $\beta$ -hydrogen atom and the u.p.e. ( $\alpha$ -spin) in the  $2p_z$  orbital of the ethyl radical.

A quantum mechanical description of hyperconjugation considers the three  $\sigma$ -bonds of a methyl group. Three MOs are formed, one of which has a non-zero net overlap with the  $2p_z$  orbital (Figure 1.5).

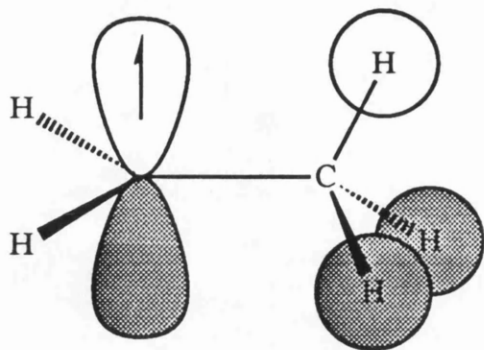


**Figure 1.5** Schematic representation of a three-hydrogen-atom molecular orbital of the same symmetry as the  $\pi$ -orbital in a ethyl radical.

Figure 1.5 illustrates this  $p\pi$ - $\sigma$  interaction allowing partial delocalisation, and hence stabilization of the radical.  $\beta$ -Proton coupling is dependent on the dihedral angle,  $\theta$ , that the plane of symmetry of the MO of the methyl group subtends with that of the  $2p_z$  orbital as illustrated in Figure 1.6. This relationship is described by the Heller-McConnell<sup>14</sup> equation (equation 1.6).

$$a(H_\beta) = \rho_{C\alpha}(A + B\cos^2\theta) \quad (1.6)$$

$A$  (ca. 1 G) And  $B$  (ca. 54 G) are the constants relating to spin polarization and hyperconjugation respectively.

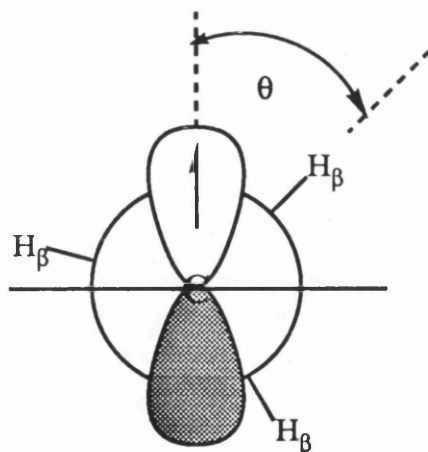
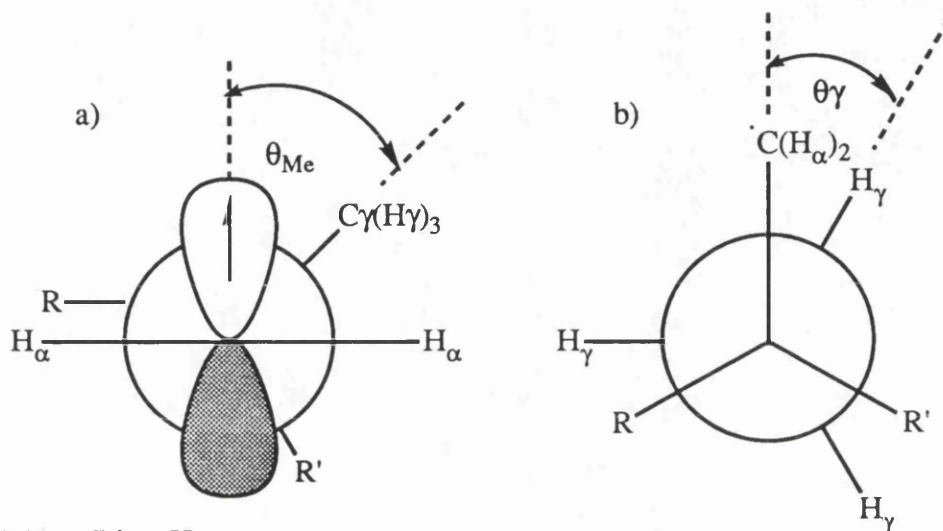


**Figure 1.6** The orientation of a methyl group with respect to the  $2p_z$  orbital in a  $\pi$ -radical.

*Ab initio* calculations of the conformational dependence of  $\gamma$ -coupling for the *n*-propyl radical<sup>15</sup> (1), are supported by the experimental results on (1), and on isobutyl (2) and neopentyl (3) radicals.<sup>16</sup> The magnitude of  $a(H_\gamma)$  is strongly dependent upon  $\theta_{Me}$  (Figure 1.7a), the dihedral angle between the  $C_\beta$ - $C_\gamma$  group and the  $2p_x$  orbital and upon  $\theta_\gamma$ , the dihedral angle  $H_\gamma C_\gamma C_\beta C_\alpha$  (Figure 1.7b).



- 1)  $R = R' = H$
- 2)  $R = H, R' = Me$
- 3)  $R = R' = Me$

**Figure 1.7** Illustration of  $\theta_{Me}$  and  $\theta_\gamma$  as described in text.

$\gamma$ -Coupling can rise from near zero to a predicted maximum of *ca.* 8G in the **W-plan** arrangement, which allows greater  $2p$ - $\sigma$  delocalisation between the back lobe of the  $H_\gamma$   $\sigma$ -bond and the  $2p_x$  orbital (Figure 1.8).

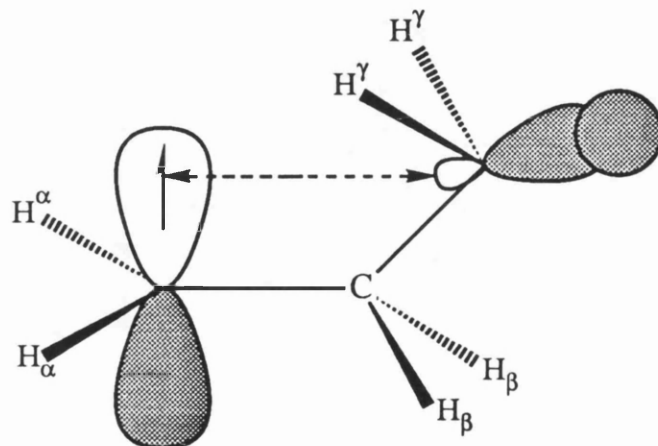


**Figure 1.8** The **W-Plan** arrangement.

This hyperconjugation can account for large values of  $a(H_\gamma)$ . Table 1.2 gives a comparison of measured  $\gamma$ -hydrogen couplings ( $G$ ) with those calculated for the  $n$ -propyl radical in the appropriate conformation.

Radical	$\theta_{Me}$	$a(H_\gamma)$ ( $\theta_\gamma = 180^\circ$ )		$a(H_\gamma)$ ( $\theta_\gamma = 60^\circ$ )	
		Measured	Calculated	Measured	Calculated
1	90°	0.10	0.26	0.59	0.27
2	60°	1.45	0.89	0.72	0.49
3	45°	4.04	2.06	0.62	0.48
	0°	-	4.37	0	0.69

**Table 1.2** . Measured and calculated values of  $a(H_\gamma)/(G)$ .

$^{13}\text{C}$ -Hyperfine coupling in aromatic compounds is observed under favourable circumstances although  $^{13}\text{C}$  has a natural abundance of only *ca.* 1.1%. Coupling to other nuclei, such as  $^{14}\text{N}$ ,  $^{17}\text{O}$ ,  $^{33}\text{S}$  etc has been observed. When such nuclei are part of the aromatic framework the theory of the magnitude of their couplings is more complex than when proton couplings are considered. Figure 1.9 illustrates the number of terms involved for  $^{13}\text{C}$  couplings as opposed to those of  $\alpha$ -proton coupling for the  $\text{C}_2'\text{CH}$  fragment. The numbered interactions are (1)  $Q_{\text{CH}}^{\text{H}}$ , (2)  $S^{\text{C}}$ , (3)  $Q_{\text{CH}}^{\text{C}}$ , (4,5)  $Q_{\text{CC}}^{\text{C}}$ , and (6,7)  $Q_{\text{C'C}}^{\text{C}}$ , and combination of these contributions leads to equation 1.7,<sup>17</sup>  $a_i^{\text{C}}$  being the term for carbon coupling, where the atoms  $X_j$  are bonded to the carbon atom  $i$ .

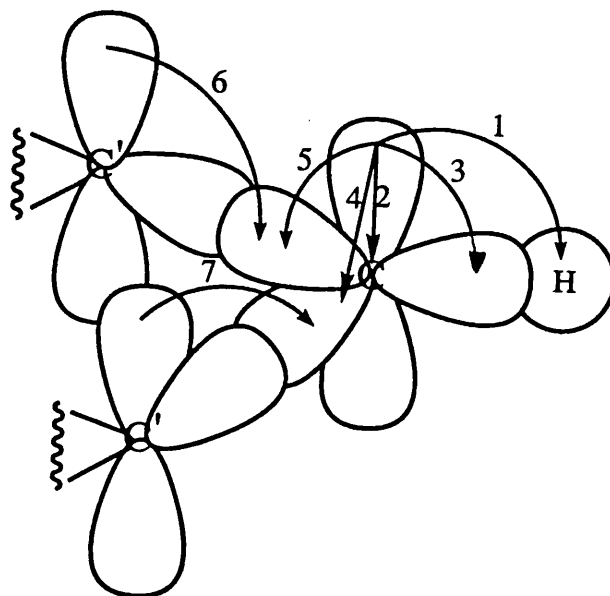


**Figure 1.9** Spin polarization contributions to the  $^{13}\text{C}$  and to the proton hyperfine splittings in a  $\text{C}_2'\text{CH}$  fragment.

$$a_i^c = \left( S^c + \sum_{j=1}^3 Q_{\text{CX}_j}^c \right) \rho_i + \sum_{j=1}^3 Q_{\text{X}_j\text{C}}^c \rho_j \quad (1.7)$$

### 1.5 Structural and Molecular Orbital Calculations

*Ab initio* calculations are quantum mechanical calculations using the Schrödinger wave equation, which do not rely upon experimental data for solution. Such solutions require much computational time and at the moment are limited to simple molecules.

MO Theory without electron repulsion is computationally rather simple because the Hamiltonian then only consists of kinetic energy, electron-nuclear attraction, and nuclear-nuclear repulsion terms. These Hamiltonian integrals can be calculated with relative ease.

Hückel Molecular Orbital (HMO) theory<sup>18</sup> is the simplest for calculating  $\pi$ -electron spin densities, where  $\pi$  and  $\sigma$  bonds are treated as wholly independent. Thus it is possible to construct an energy level scheme involving only the  $\pi$ -electrons. The molecular orbitals are written as linear combinations of atomic orbitals (LCAO). The LCAO approximation is justified in that: a) at the point where a molecule is "pulled apart" into its component atoms the set of molecular orbitals

must transform smoothly into a set of atomic orbitals, and: b) the effective potential for an electron in a molecule is so dominated by the potential due to that nucleus that all other potentials are negligible in comparison. It follows that the functional form of a molecular orbital near to a nucleus must be similar to the functional form of an atomic orbital of that atom.

Alternant  $\pi$ -systems are those in which stars may be placed on alternate atoms so that no two starred or unstarred atoms are directly bonded. Some examples are given in Figure 1.10. An important property of the Hückel-derived  $\pi$ -orbitals of alternant molecules is that they occur in pairs with energies equal to  $(\alpha \pm x\beta)$ . Such pairs have the same numerical values of coefficients but with sign changing for every alternate atom on going from bonding to antibonding MOs.

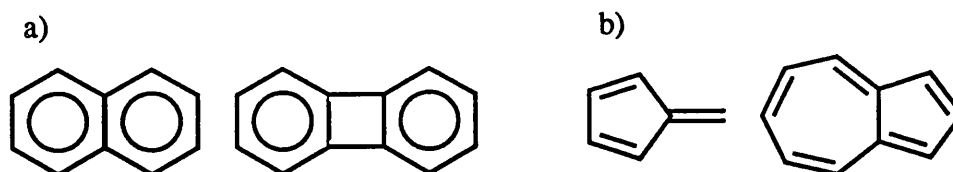


Figure 1.10 a) Alternant

b) Non-alternant.

HMO Theory is extended to heteroatoms by the use of modified coulombic integrals.

The Dewar group has developed and conveniently packaged an increasingly sophisticated series of programs for performing semi-empirical calculations, the most recent using the PM3<sup>19</sup> semi-empirical Hamiltonian. Throughout this thesis we have predominantly used the previous AM1 Hamiltonian, using the unrestricted Hartree-Fock (UHF) level for open shell calculations. Hyperfine coupling constants were obtained from INDO<sup>21</sup> calculations on the AM1/UHF optimised geometries.

Molecular mechanics is parameterised completely from data available experimentally, treating atoms and bonds as balls and springs. This method, despite being crude in comparison to *ab initio* and semi-empirical methods, reproduces the geometries and strain energy differences of many ground state molecules with very good reliability. The MM2-type programs have no insight for orbitals or

conjugation, but the MMP2-type<sup>22</sup> programs have been developed for ground state conjugated systems.

Where we needed to calculate energy strain differences using MM2<sup>22</sup> for molecules containing aromatic carbon atoms, extra bond length and torsional parameters were added for  $sp^2$  carbons.

### 1.6. Single Crystal X-Ray Diffraction<sup>23</sup>

A fundamental characteristic of the crystalline state is a high state of order, that is the molecules or atoms are arranged in a regular way which is repeated over and over in all directions. When a narrow beam of X-rays hits a single crystal it is diffracted in a regular pattern, and the X-ray diffraction pattern is recorded electronically or photographically. This diffraction technique has to be used because X-rays cannot be focused by any known lens. The recombination of the diffracted beam is done mathematically with the aid of a computer, to produce a three-dimensional model of the molecule.

Since its first application by W. H. Bragg to determine the structure of sodium chloride, and later by Kathleen Lonsdale to show that benzene is a structure not of alternate single and double bonds, many advances have been made. These are in the hardware, such as the electronic detection of the X-ray diffracted beam, the computer power, and the development of software packages for solving the diffraction patterns.

These developments now allow the non-specialist to collect and solve the data for simple crystal structures.

### 1.7 Purpose of Work

ESR Spectroscopy is the most sensitive known method for determining the electronic distribution and geometries of a radical. The technique may also be used to obtain kinetic data from radical reactions. It is therefore an excellent tool for obtaining practical data to compare with the results of MO theory.

We have decided to study the ESR spectra of the radical ions (predominantly cations) of selected aromatic and heteroaromatic compounds, for two reasons, firstly to observe and report the novel spectra obtained, and secondly to test whether the selected radical ions would exhibit any of the characteristics described above or

undergo other novel processes which could be observed by ESR.

With the above in mind the ESR spectra were interpreted by measurement of hyperfine couplings, and the relative signal intensities, and were checked by comparison with computer simulations. Where necessary hyperfine couplings were assigned to specific nuclei by comparison with the values calculated by AM1/INDO methods. Where possible, relevant single crystal X-ray structures were also determined.

### References

1. E. Zavoisky, *J. Phys., USSR*, **1945**, *9*, 221.
2. D. I. Davies and M. J. Parrott, "Free Radicals in Organic Synthesis.", Springer-Verlag, Berlin, 1978.
3. J. G. Calvert and J. N. Pitts, "Photochemistry.", John Wiley and sons, Inc, 1966
4. D. J. Bellville, D. D. Wirth, and N. L. Bauld, *J. Am. Chem. Soc.*, **1981**, *103*, 718.
5. T. Shida, Y. Egawa, H. Kubodera, and, T. Kato, *J. Chem. Phys.*, **1980**, *73*, 5963.
6. M. C. R. Symons, *Chem. Soc. Rev.*, **1984**, *13*, 393.
7. J. L. Courtneidge, A. G. Davies, P. S. Gregory, D. C. McGuchan, and S. N. Yazdi, *J. Chem. Soc., Chem. Commun.*, **1987**, 1192.
8. A. G. Davies and D. C. McGuchan, *Organometallics.*, in the press.
9. F. Gerson, "High resolution E.S.R. Spectroscopy.", John Wiley and Sons Ltd., Verlag Chemie, 1970.
10. J. E. Wertz, and J. R. Bolton "Electron Spin Resonance: Elementary Theory and Practical Applications.", Chapman and Hall Ltd., U.S.A., 1986.
11. H. M. McConnell and D. B. Chestnut, *J. Chem. Phys.*, **1958**, *28*, 107.
12. J. R. Bolton, *J. Chem. Phys.*, **1965**, *43*, 309.
13. J. P. Colpa, and J. R. Bolton, *Mol. Phys.*, **1963**, *6*, 273.
14. C. Heller, and H. M. McConnell, *J. Chem. Phys.*, **1960**, *32*, 1535.
15. Y. Ellinger, A. Rassat, R. Subra, and G. Berthier, *J. Am. Chem. Soc.*, **1973**, *95*, 2272.
16. K. U. Ingold and J. C. Walton *J. Am. Chem. Soc.*, **1982**, *104*, 616.

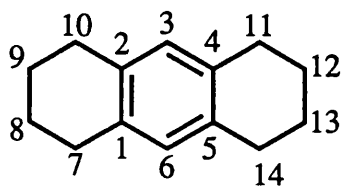
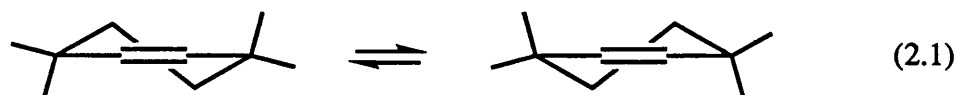


17. M. Karplus and G. K. Fraenkel, *J. Chem. Phys.*, **1961**, *35*, 1312.
18. A. Streitwieser Jr., "Molecular Orbital Theory for Organic Chemists.", J. Wiley and Sons, Inc., New York, 1961.
19. J. J. P. Stewart *J. Comp. Chem.*, **1989**, *10*, 209 and J. J. P. Stewart, *J. Comp. Chem.*, 1989, *10*, 221.
20. M. J. S. Dewar, E. G. Zoebisch, E. F. Healy, and J. J. P. Stewart, *J. Am. Chem. Soc.*, **1985**, *107*, 3902.
21. J. A. Pople, and D. L. Beveridge, "Approximate Molecular Orbital Theory.", McGraw-Hill, New York, 1970.
22. N. L. Allinger, and H. L. Flanagan, *J. Comp. Chem.*, **1983**, *4*, 339.
23. J. P. Glusker and K. N. Trueblood., "Crystal Structure Analysis: a Primer.", Oxford University Press., New York, 1985.

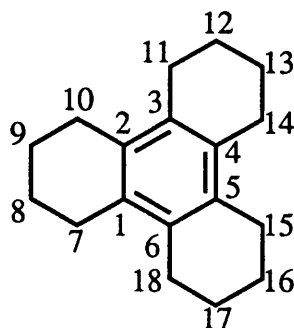
## Chapter 2. Conformational Inversion in the Dodecahydrotriphenylene Radical Cation and Some Unusual Ring Distortions

### 2.1 Introduction

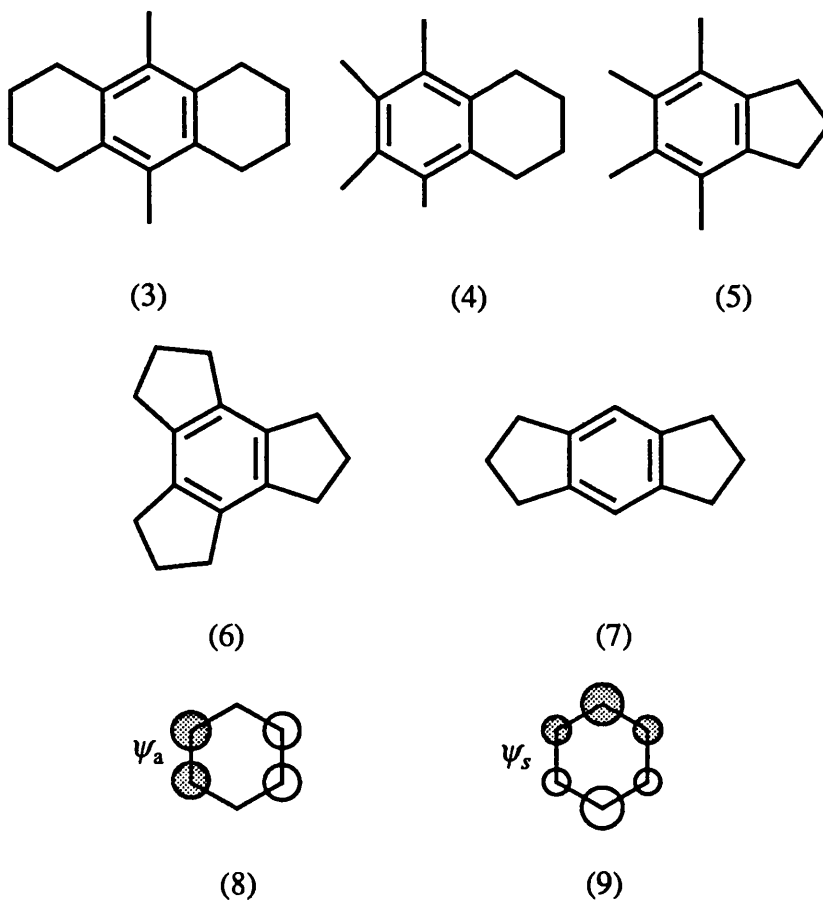
Conformational inversion in the cyclohexene ring of a radical ion containing a benzocyclohexene moiety can in principle be studied by monitoring the temperature dependence of the hyperfine coupling of the exchanging axial and equatorial protons (equation 2.1), but as far as we can determine there is no report of this having been done for either a radical cation or radical anion. We describe here a variable temperature ESR study of the radical cations of octahydroanthracene (1) and dodecahydrotriphenylene (2), which has provided the inversion barrier in (2<sup>+</sup>). The experimental observations are supported by molecular mechanics calculations and the potential energy profiles are traced out when the cyclohexene moieties in (1) and (2) undergo ring inversion.



(1)



(2)



The radical cations of 9,10-dimethyl-1,2,3,4,5,6,7,8-octahydroanthracene (3), 4,5,6,7-tetramethylindane (5), and 1,2,3,4-tetramethyl-5,6,7,8-tetrahydronaphthalene (4) exhibit an unusual electronic distribution. This is rationalized in terms of distortion of the aromatic framework and the results are discussed with respect to the radical cations of (1), (2), trindane (6), and some other symmetrically alkylated benzenes.

Compounds (4), (5), (6), and (7) were prepared by Elizabeth Li, a 3rd year undergraduate student under my supervision.

## 2.1 Results and discussion

### 2.2.1 Conformational Inversion in the Dodecahydrotriphenylene Radical Cation

The ESR spectra of (1<sup>+</sup>) [ $a(8H\beta)$  15.5 G] and of (2<sup>+</sup>) [ $a(12H\beta)$  10.1 G] have been observed previously by Dessau and Shih<sup>1</sup> who oxidised (1) and (2) with

the cobaltic ion in trifluoroacetic acid in a rapid mixing flow system at room temperature, but this technique cannot readily be adapted for studies at low temperature. We have generated the radical cations by photolysis with Pyrex-filtered u.v. light of a static solution in the ESR cavity of the appropriate hydrocarbon in dichloromethane containing aluminium chloride.

Octahydroanthracene (1) showed a spectrum of the radical cation ( $1^{+\cdot}$ )  $a(8H\beta)$  15.5 G,  $g$  2.0029 (Figure 2.1). The spectrum of ( $1^{+\cdot}$ ) showed no significant line-width effect down to the lowest temperature (190 K) which could be reached in this solvent, but with a mixture of dichloromethane and fluorodichloromethane, relatively poor spectra could be obtained down to 168 K. Alternate lines broadened at *ca.* 180 K and then split into separate signals (Figures 2.1) corresponding to  $a(4H\beta_{ax})$  20.15 G and  $a(4H\beta_{eq})$  10.85 G. Only the spectrum at 180 K was of sufficient quality to warrant simulation, and this gave a rate constant for axial-equatorial exchange of *ca.*  $9.6 \times 10^7 \text{ s}^{-1}$  at 180 K. If  $\log A$  is taken to be 12.6 as it is for the dodecahydrotriphenylene radical cation (see below), this would correspond to an activation energy of *ca.*  $4.0 \text{ kcal mol}^{-1}$ .

Dodecahydrotriphenylene (2) in dichloromethane at room temperature showed a spectrum of ( $2^{+\cdot}$ ) with  $a(12H\beta)$  10.24 G,  $g$  2.0028, and at lower temperature a further splitting of *ca.* 1 G could be detected because of coupling to the  $\gamma$ -protons (Figure 2.2). Between *ca.* 213 K and 183 K alternate lines in the 13-line multiplet broadened and resolved into two signals so that at low temperature the spectra could be analysed in terms of  $a(6H\beta_{ax})$  13.31 G and  $a(6H\beta_{eq})$  7.17 G (Figure 2.3) [In order to obtain a set of spectra of ( $2^{+\cdot}$ ) consistently without the small coupling illustrated in Figure 2.2, the spectra were recorded with a modulation amplitude of *ca.* 2 G.]. Computer simulation of these spectra gave the rate constants for the ring inversion process which are shown in the Arrhenius plot in Figure 2.4, which is described by equation 2.2, where  $R = 1.986 \times 10^{-3} \text{ kcal deg}^{-1} \text{ mol}^{-1}$ , and at 180 K,  $k = 9.3 \times 10^6 \text{ s}^{-1}$ .

$$\log_{10}(k/s^{-1}) = (12.8 \pm 0.3) - (4.8 \pm 0.3)/2.303RT \quad (2.2)$$

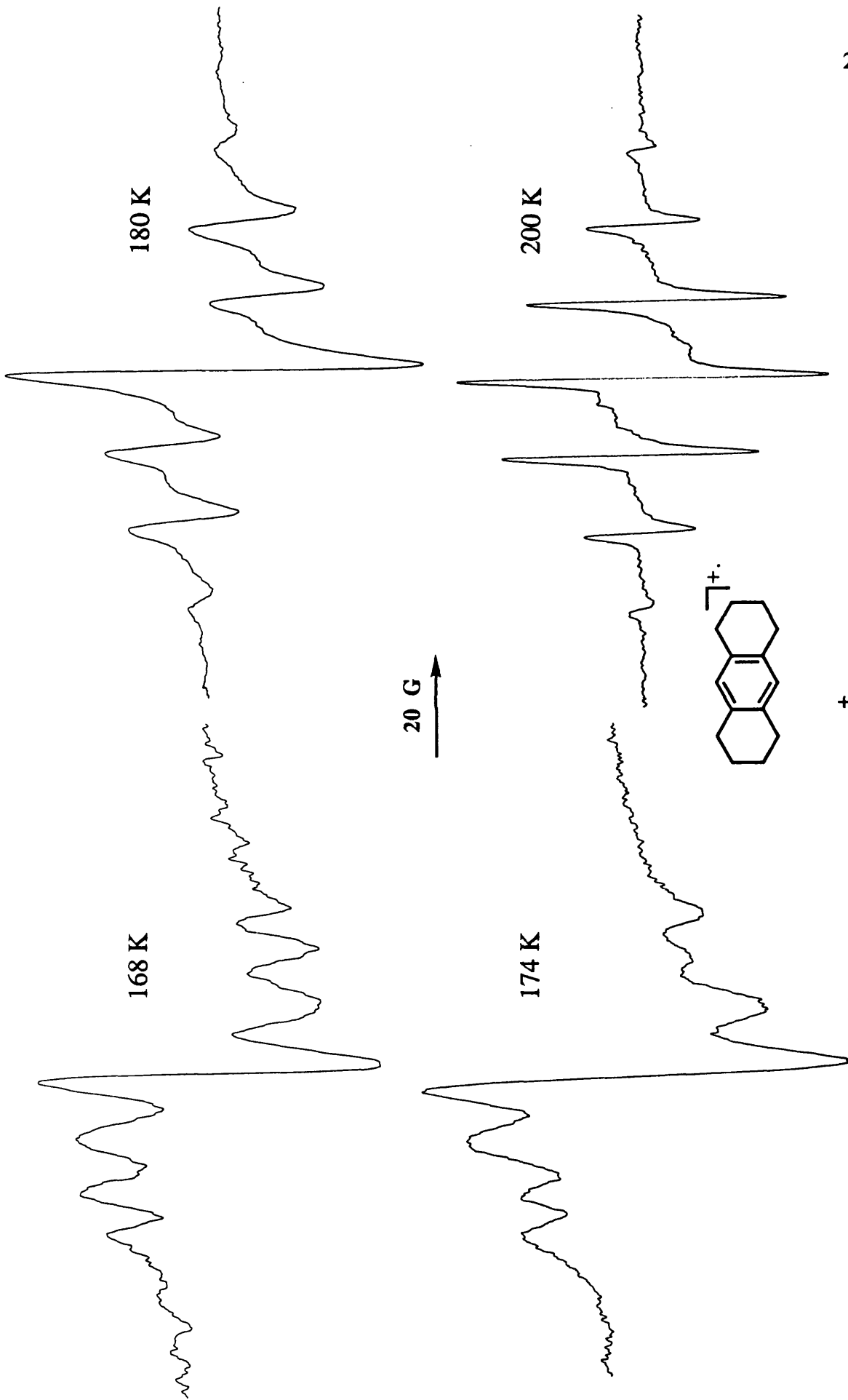


Figure 2.1 ESR Spectra of ( $1^+$ ) at various temperatures in  $\text{CH}_2\text{Cl}_2$  (200 K) or  $\text{CH}_2\text{Cl}_2/\text{CHFC}_2$  (other temperatures).

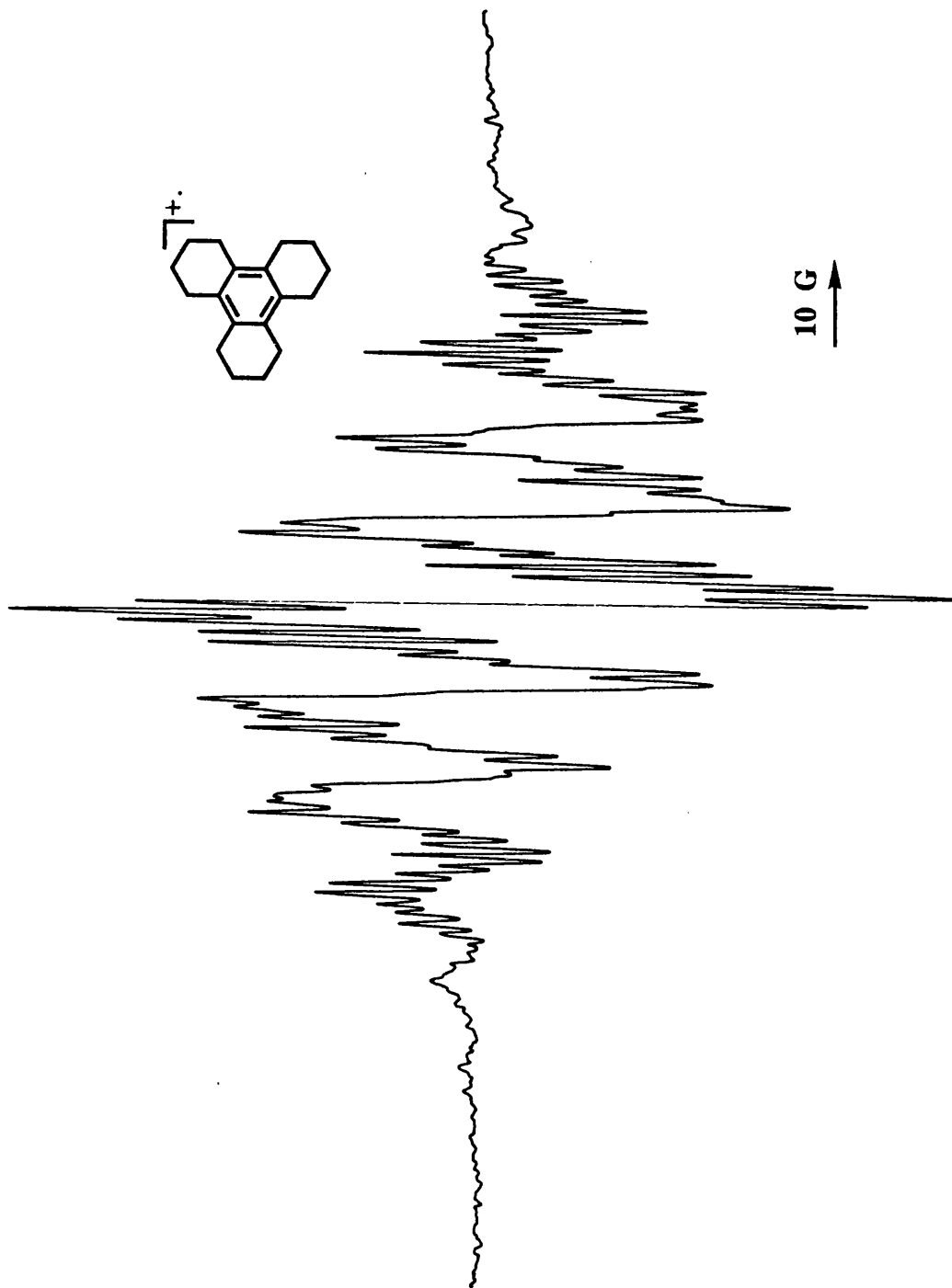


Figure 2.2 ESR Spectrum of ( $2^{+}$ ) in  $\text{CH}_2\text{Cl}_2$  at 200 K.

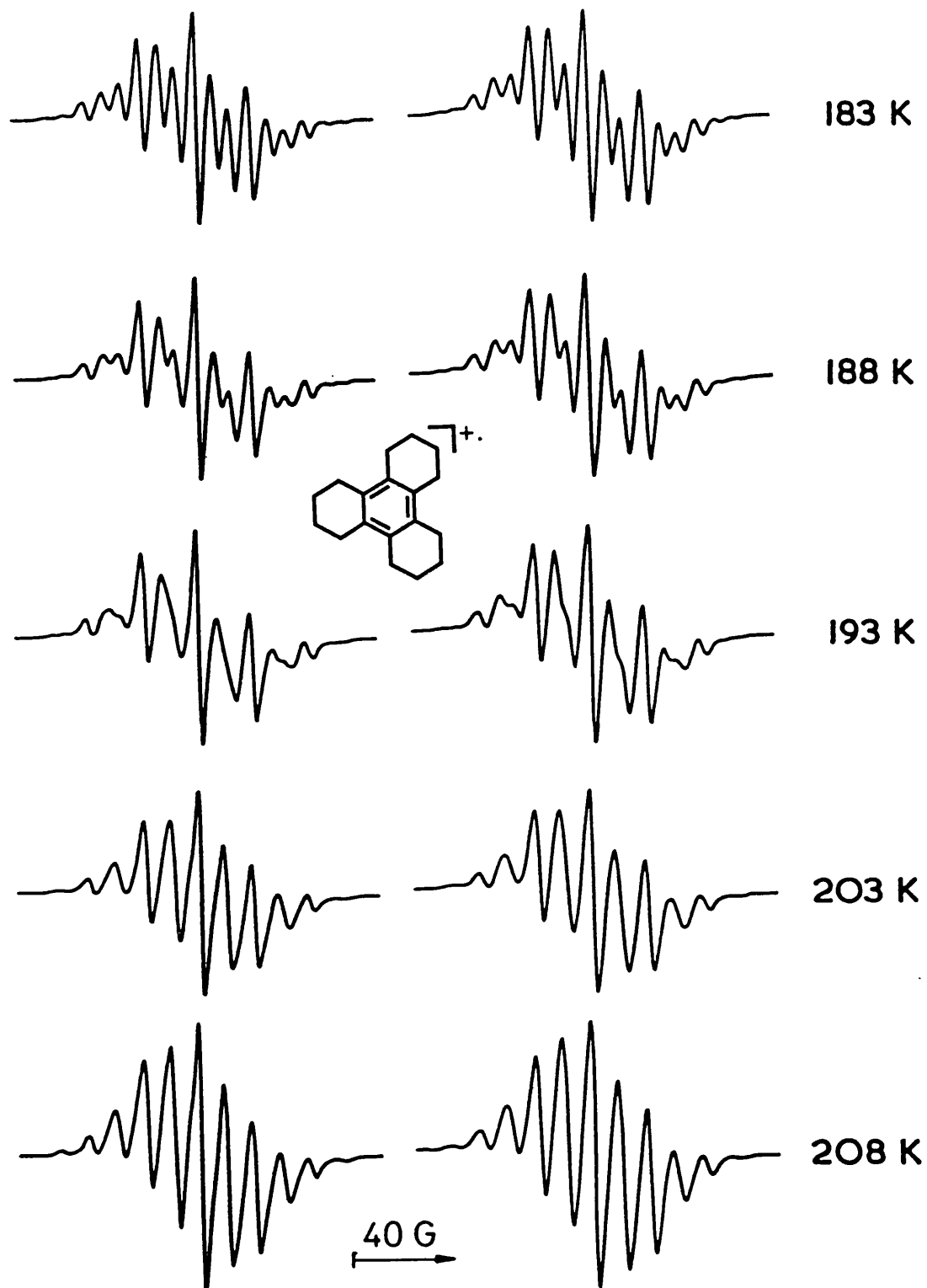


Figure 2.3 ESR Spectra (left) of  $(2^+)$  in  $\text{CH}_2\text{Cl}_2$ , and computer simulations (right).

J. E. Anderson of this department recorded the 400 MHz  $^1\text{H}$  NMR spectrum of (2) in  $\text{CHF}_2\text{Cl}$  containing 20%  $\text{CD}_2\text{Cl}_2$  down to 133 K. The methylene groups gave signals at  $\delta$  1.772 and 2.572, and these showed no sign of broadening and separating into individual signals for axial and equatorial protons even at the lowest temperature. If the separation between the signals for  $\text{H}_{\text{ax}}$  and  $\text{H}_{\text{eq}}$  were say 10 Hz, this would imply that the activation energy to ring inversion is less than 6.2 kcal  $\text{mol}^{-1}$ .

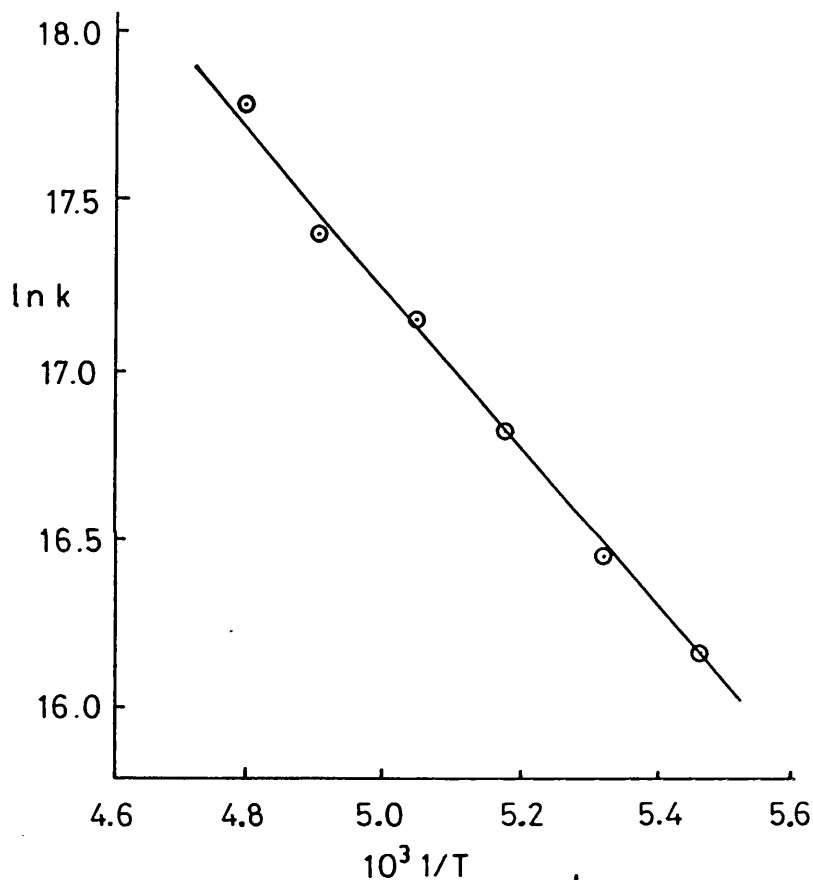


Figure 2.4. Arrhenius plot for the inversion of  $(2^{+\cdot})$  (equation 2).

The high value of  $a(\text{H}\beta)$  in  $(1^{+\cdot})$  and the absence of any resolvable coupling to the protons in the aromatic ring shows that the 1,2,4,5-tetraalkylation has raised the energy of the  $\psi_{\text{A}}$  MO (8) above that of the  $\psi_{\text{S}}$  MO (9) so that the unpaired electron is located solely in  $\psi_{\text{A}}$ . For comparison, the radical cation of 1,2,4,5- $\text{Me}_4\phi$  shows  $a(12\text{H}\beta)$  10.70, and  $a(2\text{H}\alpha)$  0.8 G.<sup>2</sup> In  $(2^{+\cdot})$ , the  $\psi_{\text{A}}$  and  $\psi_{\text{S}}$  MOs should remain degenerate leaving equal electron distribution around the aromatic ring. For comparison,  $\text{Me}_6\phi^{+\cdot}$  shows  $a(18\text{H})$  6.45 G,<sup>2</sup> and  $\text{Et}_6\phi^{+\cdot}$  shows  $a(12\text{H}\beta)$  2.65, and  $a(18\text{H}\gamma)$  0.73 G at 253 K.<sup>3</sup>



The most interesting point to come out of these measurements however is that the barrier to ring inversion in the dodecahydrotriphenylene radical cation is apparently greater than that in the octahydroanthracene radical cation.

Dodecahydrotriphenylene (2) provides an interesting example of a family of compounds which has attracted much attention,<sup>4</sup> where steric interaction occurs between alkyl groups bonded to a planar framework. This might be expected to lead to correlated rotation between the alkyl groups in what has been termed a gear or cogwheel effect, but it appears that with simple alkyl groups, stepwise rather than correlated rotations usually occur.<sup>5</sup> We can find no record of (2) being discussed in this context.

We have investigated by molecular mechanics calculations (MM2) the potential energy profiles which are traced out when the cyclohexene moieties in (1) and in (2) undergo ring inversion. These calculations were carried out using the parameters  $l_0$  1.3937 Å and  $k$ , 8.0667 mdyn Å<sup>-1</sup> for the C<sub>sp</sub>-C<sub>sp</sub> bonds.<sup>5</sup>

We find in agreement with Koningsveld and Baas<sup>6</sup> that the two possible structures (A) and (E) of (1) with the cyclohexene rings in half-chair conformations have equal stability as shown in Figure 2.5. The two X-ray diffraction studies which have been carried out<sup>6,7</sup> have identified the centrosymmetric conformer (A) with a C<sub>2</sub> axis of symmetry.

Operation of the dihedral driver on one cyclohexene ring generated the potential energy profile shown in Figure 2.5, in which two semiplanar transition states (B) and (D) separate the half-chair reactants (A) and (E) from the boat intermediate (C) by an inversion barrier of 5.58 kcal mol<sup>-1</sup>. Steric energies and some dihedral angles are given in Table 2.1. In cyclohexene itself (partially deuteriated) the activation enthalpy is found by NMR spectroscopy to be about 5.3 kcal mol<sup>-1</sup>, and the boat conformation is generally believed to be the transition state.<sup>8</sup> As a check on the calculations, the energy profile for the inversion of cyclohexene itself was computed, and showed minimised strain energies for the chair, transition state, and boat structures of 4.19, 10.26, and 10.26 kcal mol<sup>-1</sup> implying an inversion barrier of 6.07 kcal mol<sup>-1</sup>. This is to be compared with the values in the literature of 5.97,<sup>9</sup> 6.1,<sup>10</sup> 6.39,<sup>11</sup> and 6.64<sup>12</sup> kcal mol<sup>-1</sup>.

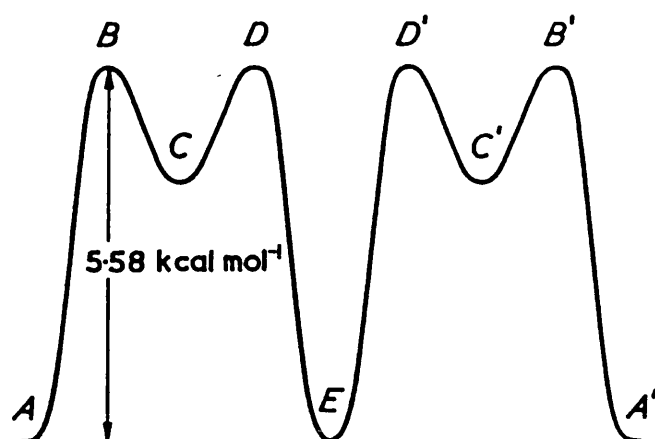
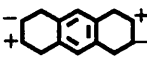
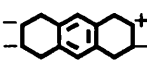
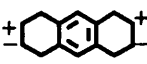


Figure 2.5 MM2-Derived energy profile for the inversion of a cyclohexene ring in octahydroanthracene (1).

Table 2.1 MM2 Steric energies and dihedral angles for various conformations of (1) shown in Figure 2.5.

	Conformational Steric Energy <sup>b</sup> $\Delta E_s / \text{kcal Mol}^{-1}$	Dihedral angle <sup>a</sup> / $^\circ$		
		3-2-10-9	6-1-7-8	7-8-9-10
A 	0.00	+163.06	+164.41	-64.83
B	5.58	+178.48	-165.10	-31.57
C 	3.84	+133.08	-132.27	+1.92
D	5.57	-179.00	-164.49	+31.56
E 	0.00	-163.91	-163.49	+64.82

<sup>a</sup> The positions are numbered as shown in (1). A positive angle indicates clockwise rotation on the formulae, and a positive sign indicates that the methylene group is above the plane of the benzene ring.

<sup>b</sup> Relative to the ground state structure A which was calculated to have a total strain energy  $E_s$  of  $4.06 \text{ kcal mol}^{-1}$ .

A similar examination of (2) showed the most stable conformation (*F*) to be that with a  $C_3$  axis of symmetry, minimising steric interactions between vicinal benzylic methylene groups. No complete X-ray diffraction study of (2) has yet been carried out<sup>13</sup>, but the ligand (2) has this symmetry in the complex  $[(\eta^6-2)\text{Mn}(\text{CO})_3][\text{BF}_4]$ .

Inversion of one cyclohexene ring traces out the energy profile shown in *F* to *J* in Figure 2.6. The conformer (*J*) is now substantially less stable than (*F*) because of the destabilising interaction between two vicinal pairs of methylene groups. The boat conformer (*H*) again appears as an intermediate, and there is little change in the conformations of the other two rings, that is there is no cogwheel effect. The transition state (*G*) is semiplanar, but the second transition state (*I*) is not. Steric energies and some dihedral angles are given in Table 2.2.

Rotation of a second ring (*J* to *L*) then proceeds over a second rather lower barrier. The complete lowest profile which could be located is shown in Figure 2.6 and detailed in Table 2.2. These calculations thus suggest a barrier of 7.50 kcal mol<sup>-1</sup> for the exchange of axial and equatorial  $\beta$ -protons in (2), higher than that calculated for (1).

If (1) and (2) can be taken to be satisfactory models for (1<sup>+</sup>) and (2<sup>+</sup>) in the context of this ring inversion, this steric interaction between adjacent non-bonded methylene groups might provide the origin of the higher inversion barrier which we observe in (2<sup>+</sup>). However there is a second, more subtle, factor that should be taken into account that would not be recognised by the molecular mechanics model.

The single crystal X-ray diffraction studies of octahydroanthracene (1)<sup>6,7</sup> show that the bonds from the central aromatic ring to adjacent methylene groups are not coplanar but subtend a dihedral angle of 3.8°. Our MM2 calculation of the structure of (1) gave the dihedral angle 1-6-5-4 as 0.19°, but van Koningsveld and Baas' calculation<sup>6</sup> did reproduce this effect, giving the angle as 2.8°.

If the structure of (1<sup>+</sup>) is similar, and if this implies that the axes of the  $2p$  orbitals on the adjacent aromatic ring atoms in the  $\psi_A$  MO (8) are not coparallel in the ground state, the activation energy for ring inversion might be reduced because during the inversion, the dihedral angle between these two AOs, which are in a locally bonding region of the MO, becomes zero.

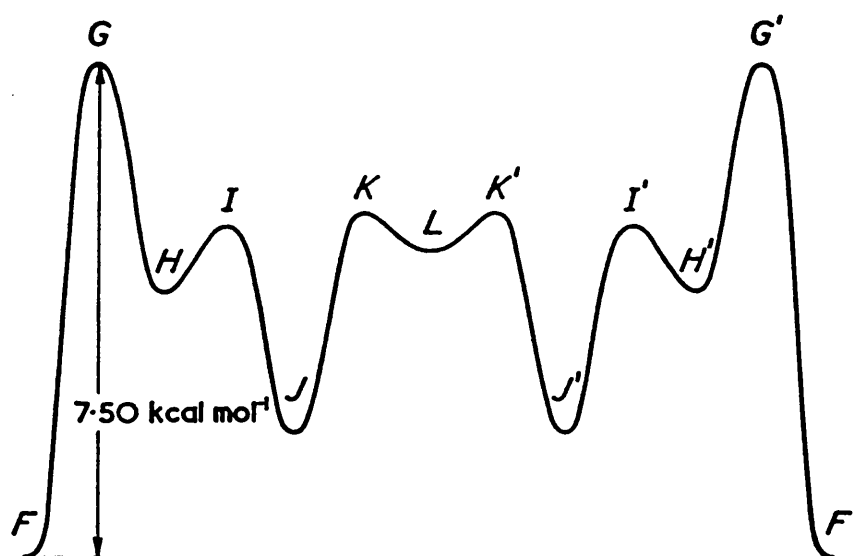


Figure 2.6 MM2-Derived energy profile for the inversion of a cyclohexene ring in dodecahydrotriphenylene (2).

Table 2.2 MM2 Steric energies and dihedral angles for the various conformations of (2) shown in Figure 2.6.

	Conformational Steric Energy <sup>b</sup> $\Delta E_s/\text{kcal mol}^{-1}$	Dihedral angle <sup>a</sup> / $^\circ$		
		3-2-10-9	6-1-7-8	7-8-9-10
<i>F</i>	0.00	+163.00	+164.06	-65.13
<i>G</i>	7.50	+163.44	-177.59	-26.60
<i>H</i>	4.15	+130.82	-129.43	-2.16
<i>I</i>	4.98	-137.43	+157.15	+38.15
<i>J</i>	1.62	-164.59	-163.39	+64.78
		2-3-11-12	5-4-14-13	11-12-13-14
<i>K</i>	5.24	-152.71	+136.57	-35.10
<i>L</i>	4.73	-130.75	+131.31	+1.61

<sup>a</sup> The positions are numbered as shown in (2). See also foot note *a* to Table 2.1.

<sup>b</sup> Relative to the ground state structure *F* which was calculated to have a total strain energy  $E_s$  of  $11.83 \text{ kcal mol}^{-1}$ .

A rather similar argument has been used to account for the deuterium isotope effect on the ESR spectra of deuteriobenzene radical anions.<sup>15</sup> Even if the bonds to the central ring in ( $2^+$ ) were not coplanar, the above effect would not be important because the  $\psi_A$  and  $\psi_S$  MOs are degenerate.

### 2.2.2 Some Unusual Benzene Ring Distortions.

Trindane (6) when dissolved in TFAH/Tl(TFA)<sub>3</sub> gave rise to an ESR spectrum (Figure 2.7) with the following characteristics:  $a(12H)$  11.48 and  $a(6H)$  0.34 G,  $g$  2.0026.

9,10-Dimethyl-1,2,3,4,5,6,7,8-octahydroanthracene (3) when oxidized in TFAH with the thallium salt gave an intense but complicated ESR spectrum (Figure 2.8). Similar spectra were obtained in TFAH/Hg(TFA)<sub>2</sub> and AlCl<sub>3</sub>/CH<sub>2</sub>Cl<sub>2</sub>. The spectrum has not been fully analysed but the methyl coupling  $a(2Me)$  9.27 G and that of the  $\beta$ -ring protons  $a(8H\beta)$  3.65 G,  $g$  2.0027 are discernible. What is apparent from these couplings is that the methyl substituents destabilise  $\psi_A$  preferentially with respect to  $\psi_S$ , implying that electron release from the methyl groups is more effective than that of the cyclohexene rings.

This unexpected apparent MO perturbation was reproduced when we oxidized [TFAH/Tl(TFA)<sub>3</sub>] 1,2,3,4-tetramethyl-5,6,7,8-tetrahydronaphthalene (4) which gave an exceptionally strong and well resolved ESR spectrum (Figure 2.9); the computer simulation is in excellent accord. The coupling constants are  $a(6H)$  9.34,  $a(6H)$  2.39,  $a(4H\beta)$  3.75, and  $a(4H\gamma)$  1.38 G,  $g$  2.0027.

The radical cation of 4,5,6,7-tetramethylindane (5) could be generated in either TFAH/Tl(TFA)<sub>3</sub> or TFAH/Hg(TFA)<sub>2</sub> with u.v. photolysis. The spectrum was far less persistent than that of ( $4^+$ ) and had the following coupling constants:  $a(12H)$  8.73 and  $a(6H)$  0.68 G,  $g$  2.0027. It is noteworthy that all the methyl groups of (5) appear equivalent in the highfield NMR (200 MHz) as they do in the ESR spectrum of its radical cation. We cannot reconcile these couplings with the structure of (5) and are not certain whether the ESR spectrum shown in Figure 2.10 is an authentic spectrum of ( $5^+$ ).

Not only do the radical cations of (3), (4), and (5) appear to show unusual MO perturbations, but the ESR spectral width is also reduced.

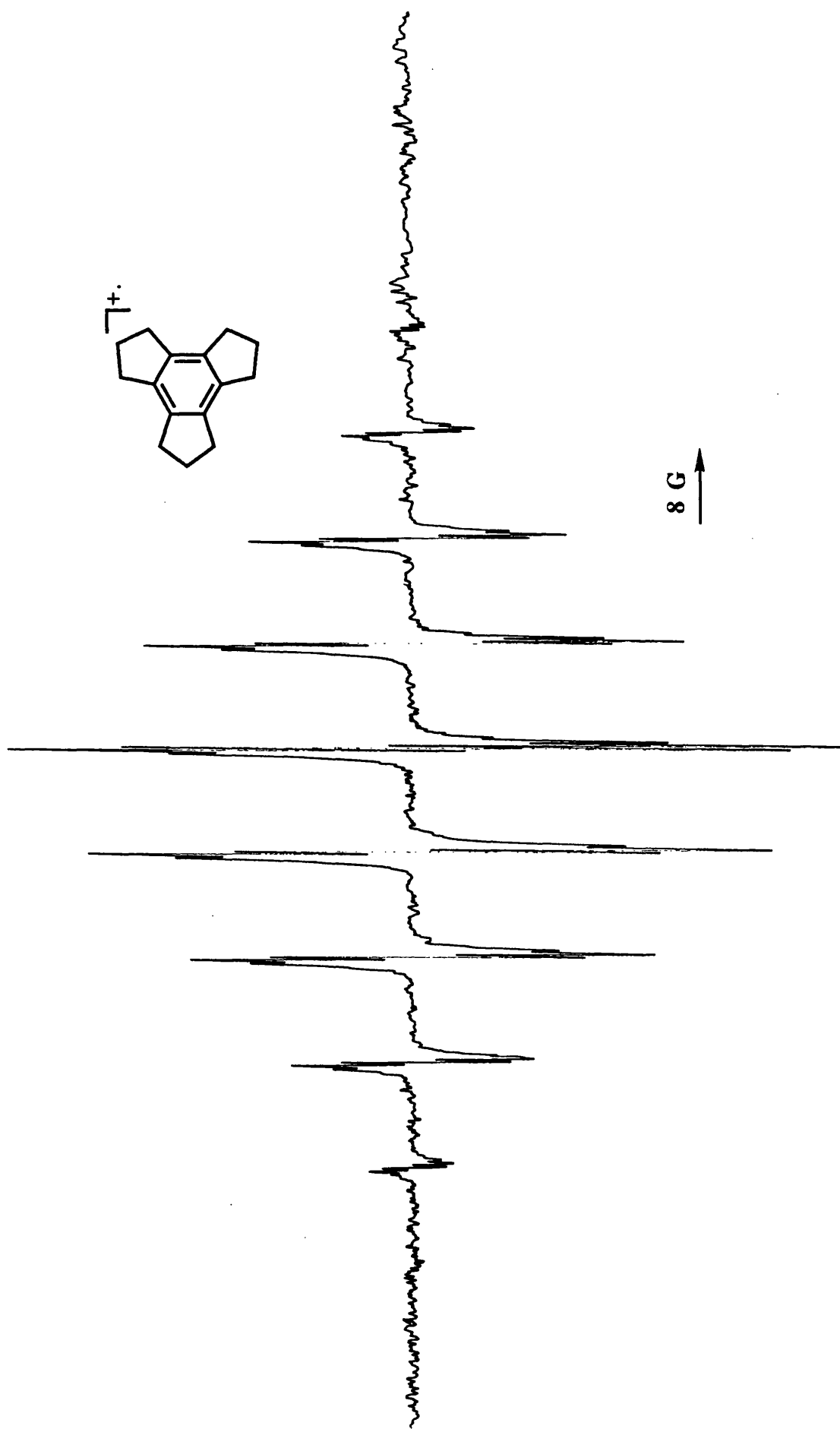


Figure 2.7 ESR Spectrum of ( $6^{+\cdot}$ ) in TFAH/Tl(TFA)<sub>3</sub> at 260 K.

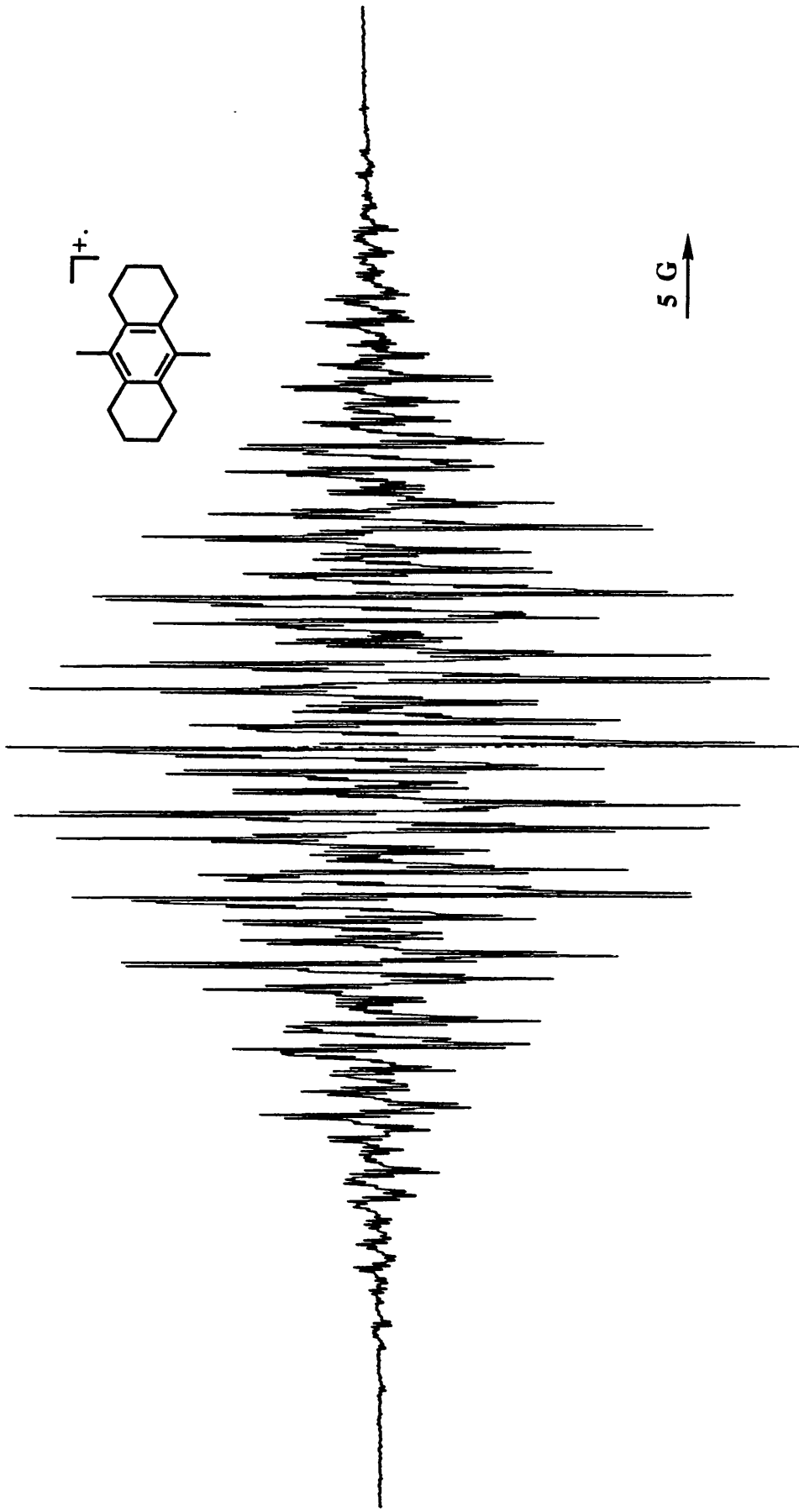
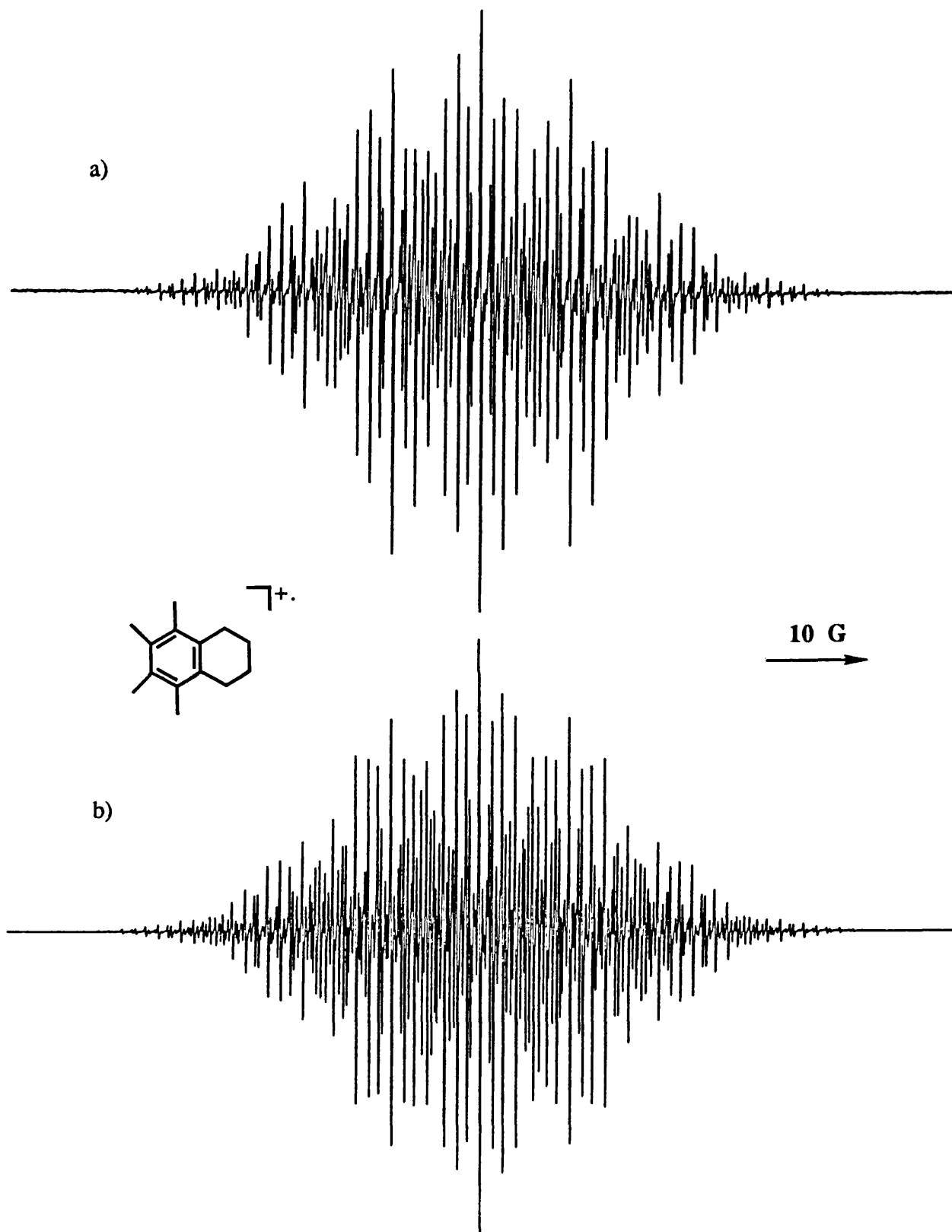


Figure 2.8 ESR Spectrum of ( $3^{\cdot+}$ ) in TFAH/Tl(TFA)<sub>3</sub> at 260 K.



**Figure 2.9** (a) ESR Spectrum of ( $4^+$ ) in TFAH/Tl(TFA)<sub>3</sub> at 260 K. (b) Computer simulation of (a).



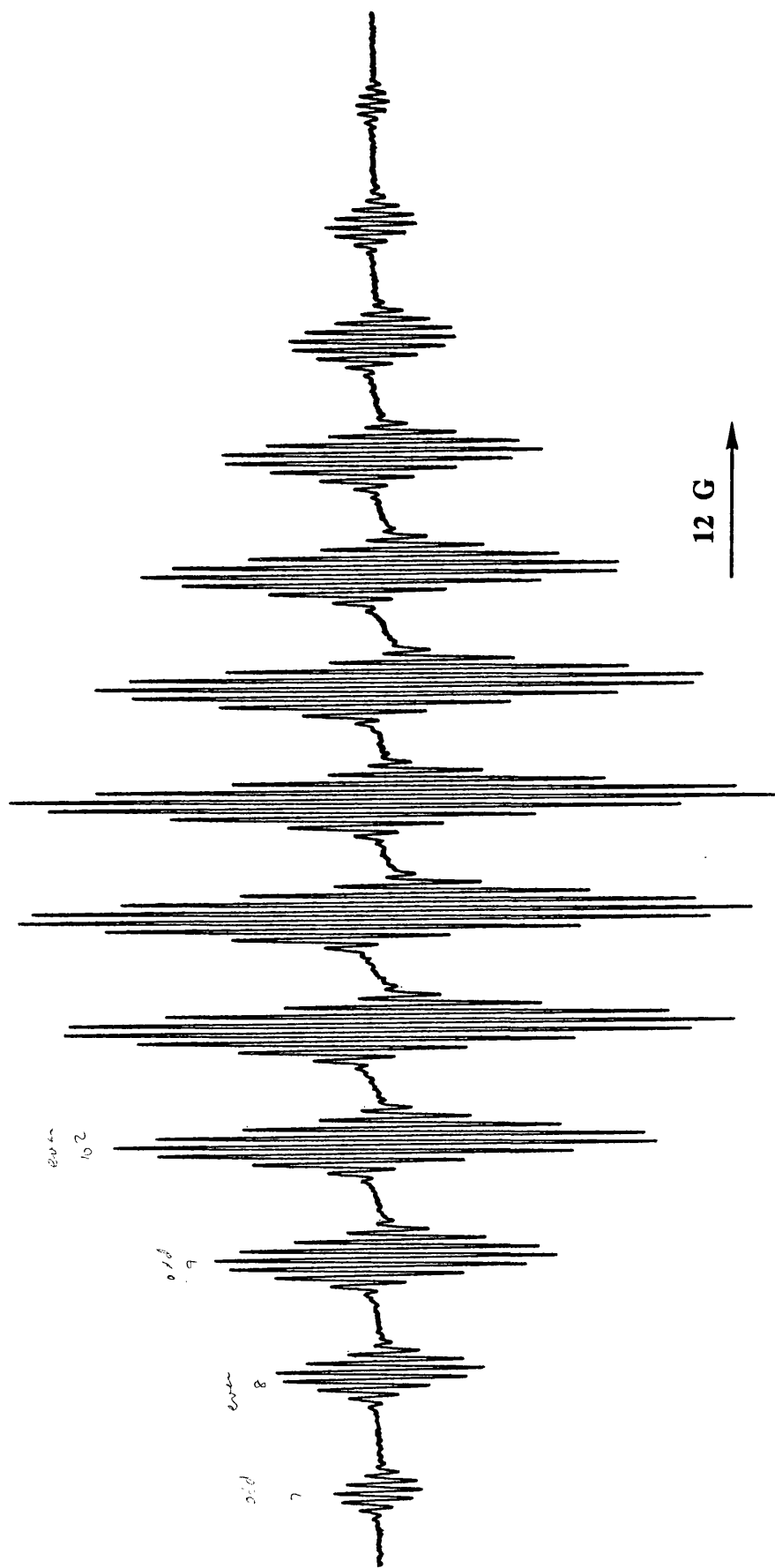


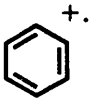
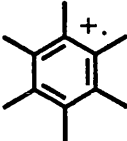
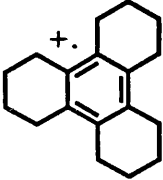
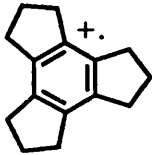
Figure 2.10 ESR Spectrum obtained when (5) was dissolved in TFAH/PI(TFA)<sub>3</sub> at 260 K.

The reduction in overall width gives the appearance of the magnetically active nuclei coupling with less than an unit electron.

A comparison can be made of calculated proportionality constants,  $Q$ , (section 1.4) which are useful in comparing the electronic effect in similarly alkylated aromatics. More importantly it is possible to estimate the apparent total unpaired electron density of some alkylated benzenes using the calculated  $Q$ -values of benzene and uniformly peralkylated benzenes. The  $Q$ -value is defined in the McConnell equation (equation 1.5) for coupling to  $\alpha$ -protons and also corresponds to the  $(A + B\cos^2\theta)$  term in the Heller-McConnell equation (equation 1.6) for coupling to  $\beta$ -protons.

For example, the benzene radical cation shows an ESR spectrum characterized by  $a(6H)$  4.43 G. The  $Q$ -value can be calculated by multiplying the coupling constant by the number of substituents, hence for the benzene radical cation  $Q_{H\alpha} = 26.6$  G (for all the  $Q$ -values discussed the benzene ring is assumed to have  $D_{6h}$  symmetry). A series of relevant  $Q$ -values are given in Table 2.3.

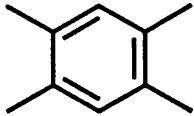
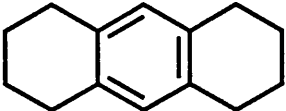
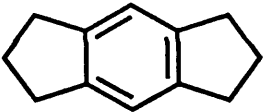
Table 2.3  $Q$ -values of some benzene derivatives.

				
$a/G$	4.43 (6H)	6.45 (6Me)	10.1 (6CH <sub>2</sub> )	11.48 (6CH <sub>2</sub> )
$Q/G$	26.6	38.7	60.6	68.8

In the 1,2,4,5-tetraalkylated benzenes the  $\psi_1$  MO is perturbed with respect to the  $\psi_2$ , and in the radical cation the SOMO takes the form  $\psi_1$ . The apparent u.p.e. density can be estimated for the 1,2,4,5-tetramethylbenzene radical cation using the calculated  $Q$ -values of the hexamethylbenzene and benzene radical cations. The coupling constant of the four methyl groups in 1,2,4,5-Me<sub>4</sub>φ<sup>+</sup> [ $a(4Me)$  10.7 G] when divided by the  $Q$ -value of Me<sub>6</sub>φ<sup>+</sup> ( $Q_{HB} = 38.7$  G) gives a figure (0.276) for

the apparent u.p.e. density at each of the 1,2,4,5 positions. Similarly using the coupling constant of the two protons [ $a(2H)$  0.8 G] and the  $Q$ -value of  $\phi^+$  ( $Q_{H\alpha} = 38.7$  G) gives a value (0.03) for the apparent u.p.e. density at the 3 and 6 positions. Hence the total apparent u.p.e. density is 1.17. A series of calculated total apparent u.p.e. densities are given in table 2.4.

**Table 2.4** Calculated u.p.e. densities of some 1,2,4,5-tetraalkylated benzenes.

	$\sum \rho_{c\alpha} = \sum a/Q =$	1.17
		1.08
		1.12

We will now use those  $Q$ -values to determine the total electron density in some cyclic compounds where the ESR spectra of their radical cations apparently have reduced spectral widths; see Table 2.5.

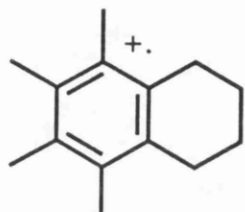
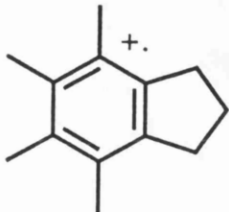
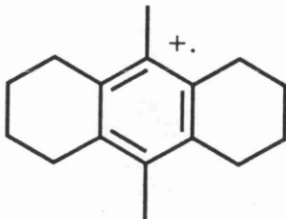
The apparent total u.p.e. densities of ( $3^+$ ), ( $4^+$ ), and ( $5^+$ ) are significantly less than unity, namely 0.721, 0.730, and 0.922 respectively. These calculated low values of the u.p.e. density may possibly be accounted for by distortion of the benzene rings from planarity.

The most definitive information about the degree of non-planarity of the benzene would be from its  $^{13}\text{C}$ -couplings, but the ESR spectra are unfortunately too complicated to determine any  $^{13}\text{C}$ -couplings. We believe however, that the reduction in spectral width arises because of distortion of the benzene rings.

The  $^{13}\text{C}$ -coupling of a carbon-centered radical will increase as the radical deforms from planarity and becomes more tetrahedral (acquiring more  $s$ -character). However the  $\alpha$ - and  $\beta$ -proton coupling decreases as a result of this distortion from planarity.

When a radical has some  $s$ -character, the  $\alpha$ -coupling has two contributions: spin polarization (a negative contribution) and an interaction arising from direct orbital overlap (a positive contribution). Hence  $\alpha$ -coupling can vary from a small negative value to a large positive value. These contributions are destructive, and small or zero net couplings can sometimes arise.

**Table 2.5** Calculated u.p.e. densities of some alkylated benzenes that are significantly below unity.

		$\rho_{C\alpha}$
	$a(2Me) \longrightarrow$	0.483
	$a(2Me) \longrightarrow$	0.123
	$a(2CH_2) \longrightarrow$	0.124
	$\Sigma \rho_{C\alpha} =$	<u>0.730</u>
		
	$a(4Me) \longrightarrow$	0.902
	$a(2CH_2) \longrightarrow$	0.020
	$\Sigma \rho_{C\alpha} =$	<u>0.922</u>
		
$a(2Me) \longrightarrow$		0.480
$a(4CH_2) \longrightarrow$		0.241
$\Sigma \rho_{C\alpha} =$		<u>0.721</u>

No way!!

For example the cyclopropyl radical<sup>16</sup> [ $a(H\alpha)$  6.7 G] which is *pyramidal* [ $a(^{13}C\alpha)$  95.9 G] has a much smaller  $\alpha$ -proton coupling than the ethyl radical<sup>17</sup> [ $a(2H\alpha)$  22.4 G] which is essentially planar [ $a(^{13}C\alpha)$  39.07 G].

As the radical becomes more *pyramidal*,  $\beta$ -proton coupling decreases as a

consequence of less effective hyperconjugation between the  $sp^3$  hybridized orbital and the C-H bonds of the methyl group.

For example the 1-methylcyclopropyl radical<sup>16</sup> [ $a(3H\beta)$  19.5 G and  $a(^{13}C\alpha)$  98.0 G], and the 1,1-difluoroethyl radical [ $a(3H\beta)$  13.99 G] which are tetrahedral all have a much smaller  $\beta$ -proton coupling than the ethyl radical<sup>17</sup> [ $a(3H\beta)$  26.9 G].

To conclude, the X-ray crystal structure of octahydroanthracene (1) shows the benzene ring to be distorted by  $3.8^\circ$  and it is most likely that the structures of (3) and (4) are distorted to the same degree, if not more severely.

### References

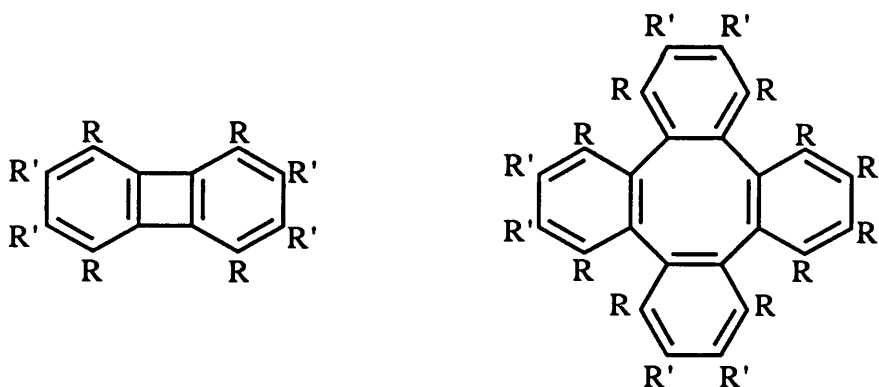
1. R. M. Dessau and S. Shih, *J. Chem. Phys.*, **1972**, *57*, 1200.
2. R. M. Dessau, S. Shih, and E. I. Heiba, *J. Am. Chem. Soc.*, **1970**, *92*, 412.
3. M. K. Carter and G. Vincow, *J. Chem. Phys.*, **1970**, *92*, 302.
4. U. Berg, T. Liljefors, C. Roussel, and J. Sandstrom, *Acc. Chem. Res.*, **1985**, *18*, 80.
5. J. Siegel, A. Gutierrez, W. B. Schweizer, O. Ermer, and K. Mislow, *J. Am. Chem. Soc.*, **1986**, *108*, 1569.
6. H. van Koningsveld and J. M. A. Baas, *Acta Cryst.*, **1984**, *40C*, 311.
7. M. A. Wilson, A. M. Vassallo, M. I. Burgaer, P. J. Collin, B. W. Skelton, and A. H. White, *Phys. Chem.*, **1986**, *90*, 3944.
8. F. R. Jensen and C. H. Bushweller, *J. Am. Chem. Soc.*, **1969**, *91*, 5774. and F. A. L. Anet and M. Z. Haq, *J. Am. Chem. Soc.*, **1965**, *87*, 3147.
9. G. Favini, G. Buemi, and M. Raimondi, *J. Mol. Struct.*, **1968**, *2* 137.
10. R. Bucourt, *Topics in Stereochem.*, ed. E.L. Eliel and N.L. Allinger, **1974**, *8*, 159-244, esp. pp. 183.
11. N. L. Allinger and J. T. Sprague, *J. Am. Chem. Soc.*, **1972**, *94*, 5734.
12. F. A. L. Anet and I. Yavari, *Tetrahedron*, **1978**, *34*, 2879.
13. S. L. Chorghade, *Proc. Natl. Acad. Sci. India.*, **1944**, *14A*, 30. F. Halla, H. H. Jagodzinski, and W. R. Ruston, *Acta Cryst.*, **1953**, *6*, 478.
14. L. H. P. Gommans, L. Main, and B. K. Nicholson, *J. Organomet. Chem.*, **1985**, *284*, 345.
15. R. G. Lawler and G. K. Fraenkel, *J. Chem. Phys.*, **1968**, *49*, 1126.
16. K. U. Ingold and L. J. Johnston, *J. Am. Chem. Soc.*, **1986**, *108*, 2343.

17. O. W Howarth and G. K. Fraenkel, *J. Chem. Phys.*, **1970**, *52*, 6258.

**Chapter 3. Radical Cations and Anions of Some  
Methylated Biphenylenes, Tetraphenylene,  
and Octa- $\beta$ -methyltetraphenylene**

### 3.1 Introduction

Derivatives of biphenylene (1) and tetraphenylene (2) have an important place in radical ion and di-ion chemistry. Biphenylene readily undergoes oxidation and reduction to show strong, simple, persistent ESR spectra of the radical cation and anion, and this provided early support for the pairing theorem.<sup>1</sup> Hart has used the broadening of NMR signals which results from electron exchange between radical ion and substrate to show the formation of the radical cations of methylated biphenylenes in the presence of acids.<sup>2</sup> The biphenylene radical cation provides the best example of the mercurideprotonation reaction which occurs with some arenes in trifluoroacetic acid containing mercury(II) trifluoroacetate (Section 1.3).<sup>3</sup>



- 1a R = R' = H  
1b R = Me, R' = H  
1c R = H, R' = Me  
1d R = R' = Me

- 2a R = R' = H  
2b R = Me, R' = H  
2c R = H, R' = Me  
2d R = R' = Me

Solutions of biphenylene and the methylated biphenylenes in superacids yield the dications which can be detected by  $^1\text{H}$  and  $^{13}\text{C}$  NMR spectroscopy,<sup>4</sup> and similarly reduction with lithium yields the dianions<sup>5,6</sup> which may then undergo ring opening to give 2,2'-dilithiobiphenyls.

Much less work has been carried out on the tetraphenylenes which are less readily available than the biphenylenes, but the molecular structure of the

dianion is thought to be different from that of the neutral molecule,<sup>7</sup> and Huber has shown that two radicals with different ESR spectra can be obtained from tetraphenylene, and has suggested that these two species again have different structures.<sup>8,9</sup>

Some of these points are discussed in more detail in this chapter. Against this background we have carried out an ESR study of the radical cations and anions obtained from tetra- $\alpha$ -methyl-, tetra- $\beta$ -methyl-, and octamethyl-biphenylene, the radical cation of tetraphenylene, and the radical cation of the new octa- $\beta$ -methyltetraphenylene. Details of the spectra which have been observed are given in the Table 3.1.

Compounds (1b), (1c), (1d), (2a) and (2c) were prepared by Marisa Girbal or by Kai Ng, 3rd year undergraduate students, under my supervision.

## 3.2 Results and discussion

### 3.2.1 Tetra- $\alpha$ -methylbiphenylene, Tetra- $\beta$ -methylbiphenylene and Octamethylbiphenylene

The best ESR spectra of the tetra- $\alpha$ -methylbiphenylene (1b) radical cation were obtained from the light red solutions which (1b) forms in TFAH/Tl(TFA)<sub>3</sub>, without photolysis (Figure 3.1a); the spectra were rapidly lost if the sample was irradiated. The spectrum appears as a 1:4:6:4:1 quintet due to coupling to the 4 $\beta$ -protons, and any coupling to the 12 protons of the  $\alpha$ -methyl groups was lost in the line width of ca. 0.15 G. All couplings constants and  $g$ -values are summarized in Table 3.1.

Three of the four possible <sup>13</sup>C satellites could be observed. As hyperfine coupling to the protons of the methyl groups is probably less than 0.02 G, the spin density at C $\alpha$  is probably less than 0.001. In the ethyl radical,  $a(^{13}\text{C}_\beta)$  is ca. 13 G, thus in (1b<sup>+</sup>), hyperfine coupling to the protons of the methyl groups would be expected to be not greater than ca. 0.01 G, and this would be within the line width. We therefore tentatively assign the <sup>13</sup>C coupling constants of 3.04, 2.35, and 2.25 G to the  $\alpha$ ,  $\beta$ , and  $\gamma$  <sup>13</sup>C atoms respectively. These assignments are based upon the relative magnitudes of calculated <sup>13</sup>C couplings for the biphenylene radical cation (1a<sup>+</sup>).<sup>3,10</sup> The calculations are carried out by the Karplus-Fraenkel method<sup>11</sup> [ $a(^{13}\text{C}\alpha)$



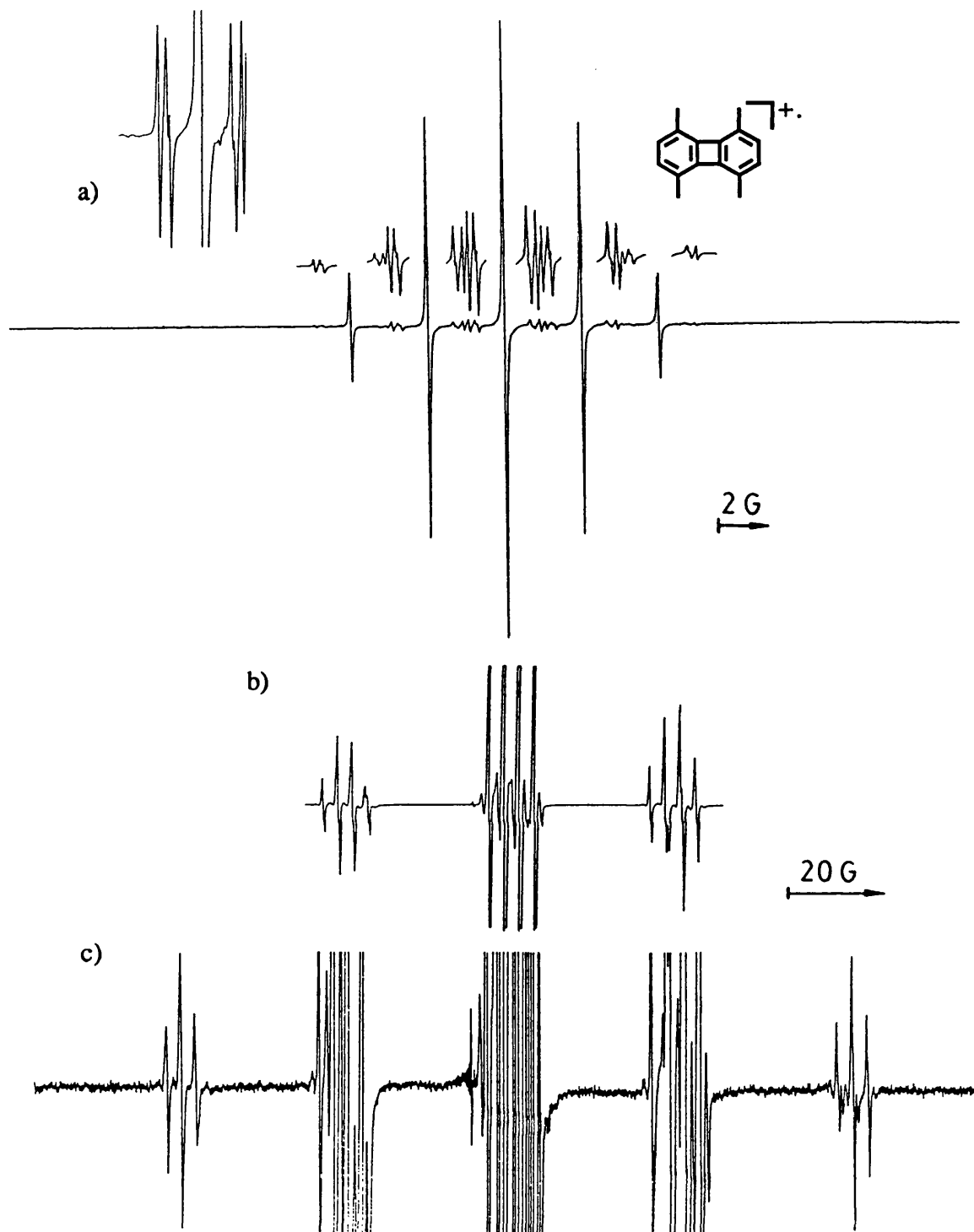
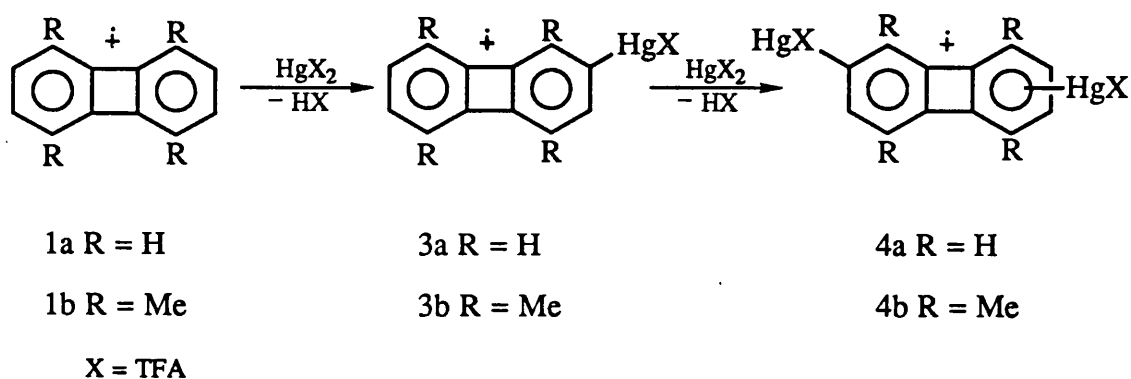


**Figure 3.1** ESR Spectrum derived from (1b) in TFAH at 262 K. (a) In the presence of  $\text{Tl}(\text{TFA})_3$ , giving  $(1b)^+$ . The insets show the  $^{13}\text{C}$  satellites at increased gain, and the  $^{13}\text{C}$  satellites about the first line of the spectrum at increased gain and expansion. (b) In the presence of  $\text{Hg}(\text{TFA})_2$ . The principal species present is the monomercuriated radical cation ( $3^+$ ); the central feature and the  $^{199}\text{Hg}$  satellites are mainly quartets, with some triplet character due to the presence of some ( $4^+$ ). (c) In the presence of  $\text{Hg}(\text{TFA})_2$ . Further mercuriation has occurred to give principally the dimercuriated species ( $4^+$ ); the secondary  $^{199}\text{Hg}$  triplet satellites arise from molecules containing two  $^{199}\text{Hg}$  atoms.

-2.14,  $a(^{13}\text{C}\beta)$  1.53, and  $a(^{13}\text{C}\gamma)$  -0.01 G] and by the Yonezawa-Kawamura-Kato model<sup>12</sup> [ $a(^{13}\text{C}\alpha)$  -2.56,  $a(^{13}\text{C}\beta)$  1.98, and  $a(^{13}\text{C}\gamma)$  -0.95 G] (which is better for ring strained hydrocarbons).

We could see no evidence for the formation for a dimer radical cation  $(1b)_2^+$  equivalent to the familiar  $(1a)_2^+$ ; the methyl groups probably sterically prevent the close approach of the two molecules. Reference 2 reports that (1b) in chloroform containing TFAH gave a broad ESR spectrum ( $\Delta H_{pp}$  8 G) which showed some splitting at -70 °C.

When (1b) was dissolved in TFAH/ $\text{Hg}(\text{TFA})_2$  it showed the same quintet spectrum of  $(1b)^+$ . When this sample was irradiated with u.v. light which was attenuated to 10% of its intensity by a neutral filter and passed through Pyrex glass, the spectral intensity was enhanced and mercurideprotonation occurred (Scheme 3.1).



**Scheme 3.1.**

Figure 3.1b shows the spectrum after 10 min. The initial quintet ( $g$  2.0025) has been largely transformed into a quartet ( $g$  2.0014). The reduction in the  $g$ -value causes the quartet to be superimposed at an intermediate stage on the upfield four lines of the initial quintet. Mercury contains a natural abundance of 16.84%  $^{199}\text{Hg}$ ,  $I = 1/2$ , and  $^{199}\text{Hg}$  satellites can be observed which reflect the quartet character of the central signal. Further photolysis reduces the central feature to a triplet ( $g$  2.0007), with triplet primary  $^{199}\text{Hg}$  satellites, and secondary satellites (Figure 3.1c) appear. Spectroscopic data are given in the Table 3.1, together with those for the monomercury and the dimercury derivatives of biphenylene itself for comparison.<sup>3</sup>

We assign the quartet central spectrum and quartet satellites to the

monomercuriated species ( $3b^+$ ), and the triplet central spectrum and triplet primary and secondary satellites to the dimercuriated species ( $4b^+$ ) (Scheme 3.1) which probably comprises both the 2,6- and 2,7-dimercuriated isomers.<sup>3</sup> These two mercuriation steps appear to be faster than those in biphenylene itself (1a) to give the corresponding mono- and di-mercuriated derivatives,<sup>3</sup> but further reaction to give tri- and tetra-mercuriation is clearly slower with (1b) than with (1a), probably because of the steric congestion involving the methyl groups which develops.

Davies and coworkers<sup>3</sup> have observed the progressive mercurideprotonation which occurs in the  $\beta$ -position of the biphenylene radical cation. Monomercuriation and dimercuriation appear to occur more rapidly with (1b) than with (1a), and it was difficult to obtain a clean ESR spectrum of monomercuriated ( $1b^+$ ), uncontaminated by the spectrum of any dimercuriated species.

Davies *et al.*<sup>13</sup> observe that in a series of aromatic hydrocarbons, mercuriation occurs preferentially at the position of highest spin density, and that the ratio  $a(^{199}\text{Hg})/a(^1\text{H})$  for the groups involved in the substitution is ca. 20.6. For the mono- and di-mercuriation of (1b), this ratio is 21.6 and 21.7 respectively, within the range of values previously observed.

When (1b) was treated with lithium in tetrahydrofuran, the solution developed a light blue then a brown colour, and the spectrum of the radical anion as shown in Figure 3.2 was observed. The McConnell constant for coupling to the aromatic protons is less than it is in the corresponding radical cation, as would be expected,<sup>14</sup> but now a significant coupling to the methyl groups can be observed, and the complexity which this confers allowed only the largest  $^{13}\text{C}$  coupling constant to be identified. The spectrum in Figure 3.3 under higher resolution showed a further small hyperfine coupling, presumably to the lithium counterion, but a good simulation of the spectrum could not be obtained.

When the reduction was carried out with potassium at 243 K, counterion coupling at ca. 0.7 G could be observed (Figure 3.4), but again the simulation was unsatisfactory.

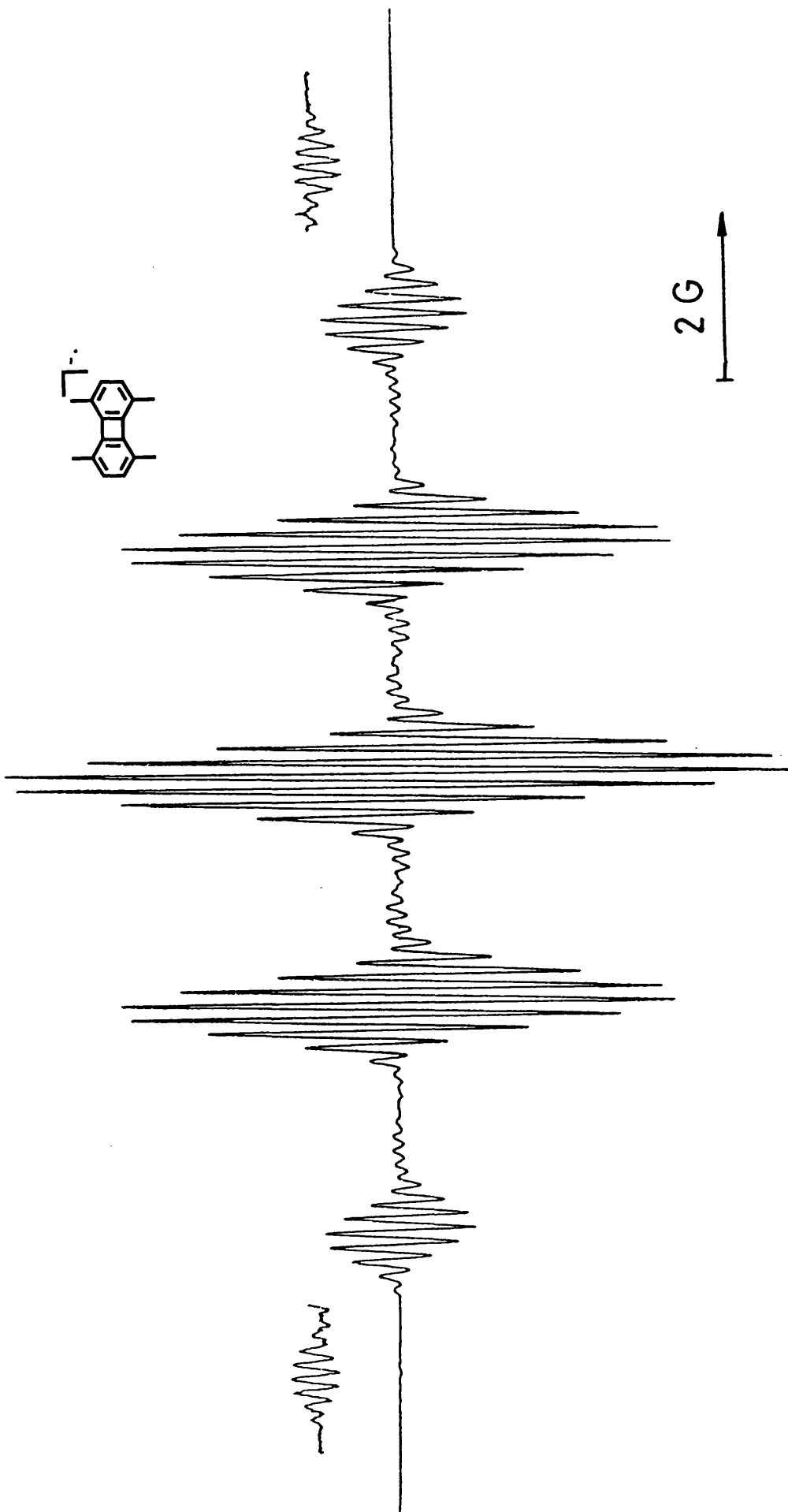


Figure 3.2 ESR Spectrum of (1b<sup>+</sup>) Li<sup>+</sup> in THF at 243 K showing (inset) the <sup>13</sup>C satellites.

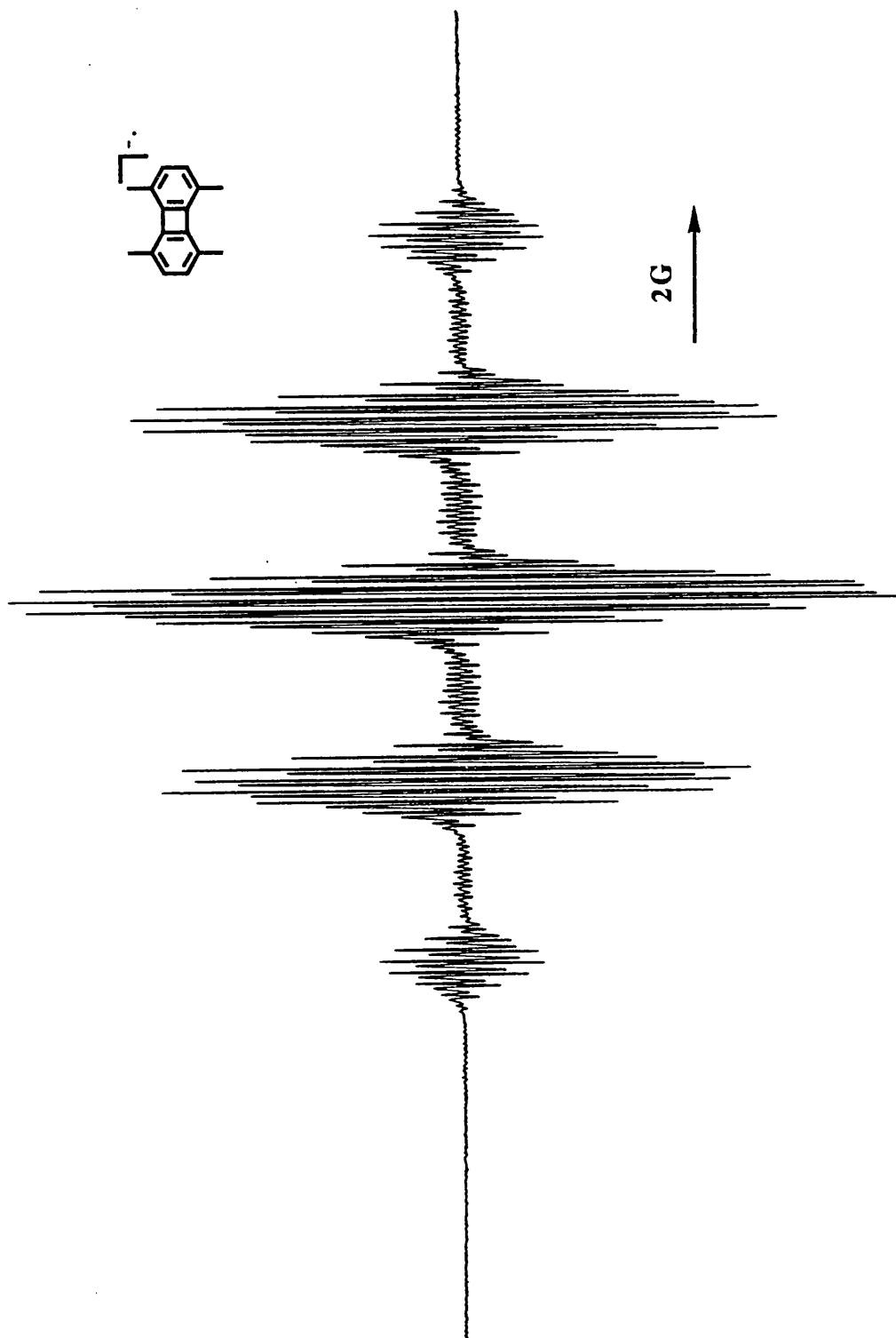


Figure 3.3 ESR Spectrum of  $(1b^-) Li^+$  in THF at 243 K, showing  ${}^7Li^+$  coupling.

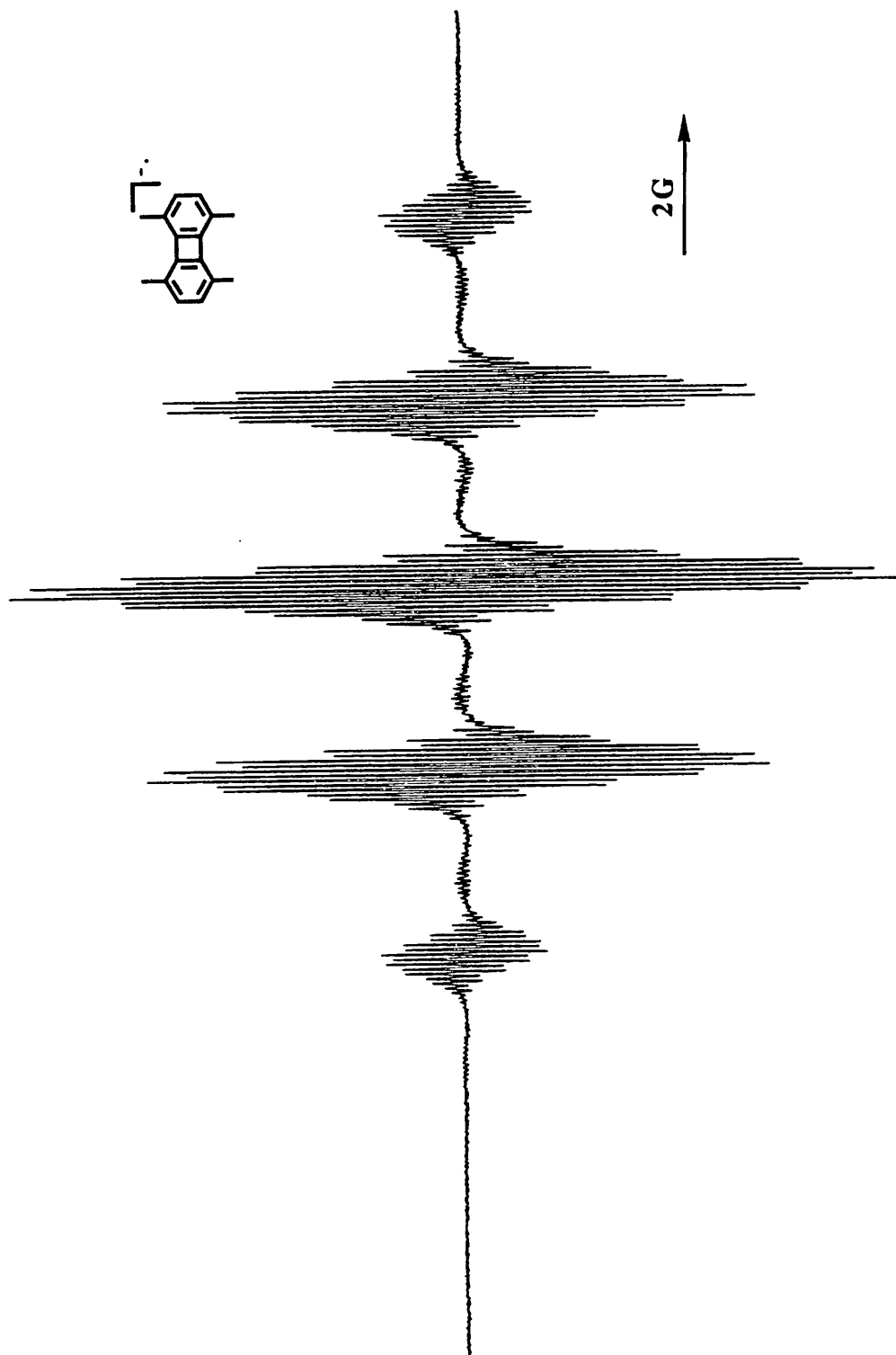


Figure 3.4 ESR Spectrum of (1b<sup>-</sup>) K<sup>+</sup> in THF at 243 K, showing <sup>39</sup>K<sup>+</sup> coupling.

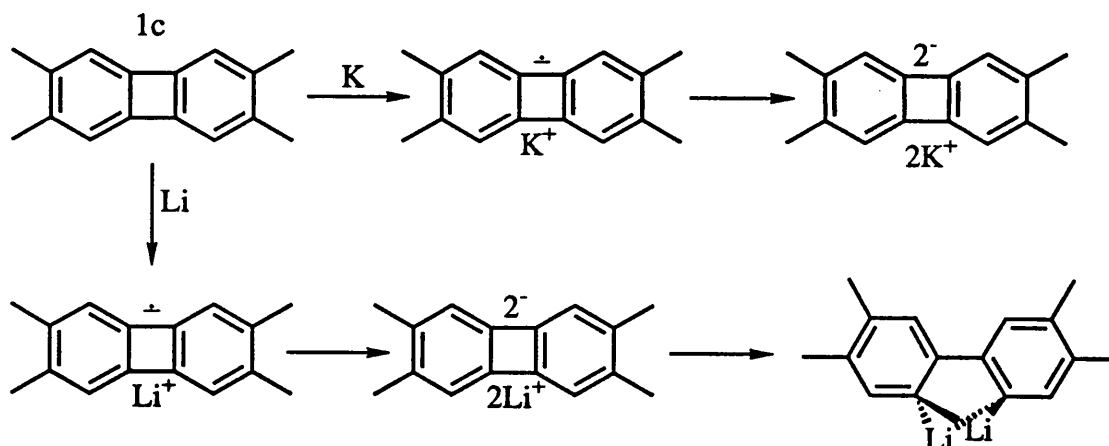
Thermolysis of biphenylene (1a) at 400 °C gives tetraphenylene (2a) in almost quantitative yield,<sup>15</sup> but we were unable to isolate octa- $\alpha$ -methyltetraphenylene (2b) from the thermolysis of tetra- $\alpha$ -methylbiphenylene (1b).

The ESR spectrum of the radical cation of tetra- $\beta$ -methylbiphenylene (1c<sup>+</sup>) in TFAH/Tl(TFA)<sub>3</sub> is shown in Figure 3.5, and the spectral data are given in the Table. The solutions are light yellow in colour. Similar spectra were obtained in SO<sub>2</sub>/FSO<sub>3</sub>H, in TFAH/Hg(TFA)<sub>2</sub>, and in AlCl<sub>3</sub>/CH<sub>2</sub>Cl<sub>2</sub>, but the quintet coupling by the 4 aromatic protons was less well resolved. The outer pair of <sup>13</sup>C satellites with *a* 3.5 G can be assigned to the  $\alpha$  positions of the aromatic rings. The inner pair with a separation of 2.5 G appear to result from the overlap of two signals, which could arise from the  $\beta$ ,  $\gamma$ , or methyl carbon atoms.

Reference 2 reports that a solution of (1c) in chloroform containing TFAH at room temperature gave a broad signal, which resolved into a 17-line spectrum at -60 °C, with *a*(H) 2 G, but such a spectrum could relate to (1c<sup>+</sup>) only in the unlikely circumstance where hyperfine coupling by the protons at the  $\alpha$ -positions and by the methyl groups at the  $\beta$ -positions were equal.

When (1c) in THF was treated with lithium it gave a deep blue solution which showed only the complex spectrum shown in Figure 3.6, which could not be analysed, and it is likely that our spectrum relates to a ring-opened species.

Olah and Schleyer<sup>6</sup> have shown that (1c) is particularly sensitive to undergoing ring opening to give 2,2'-lithiobiphenyl when it is treated with lithium (Scheme 3.2), and this reaction is probably the cause of the complication which we observe, though the exact nature of the radical anion which is formed is not clear.



Scheme 3.2.

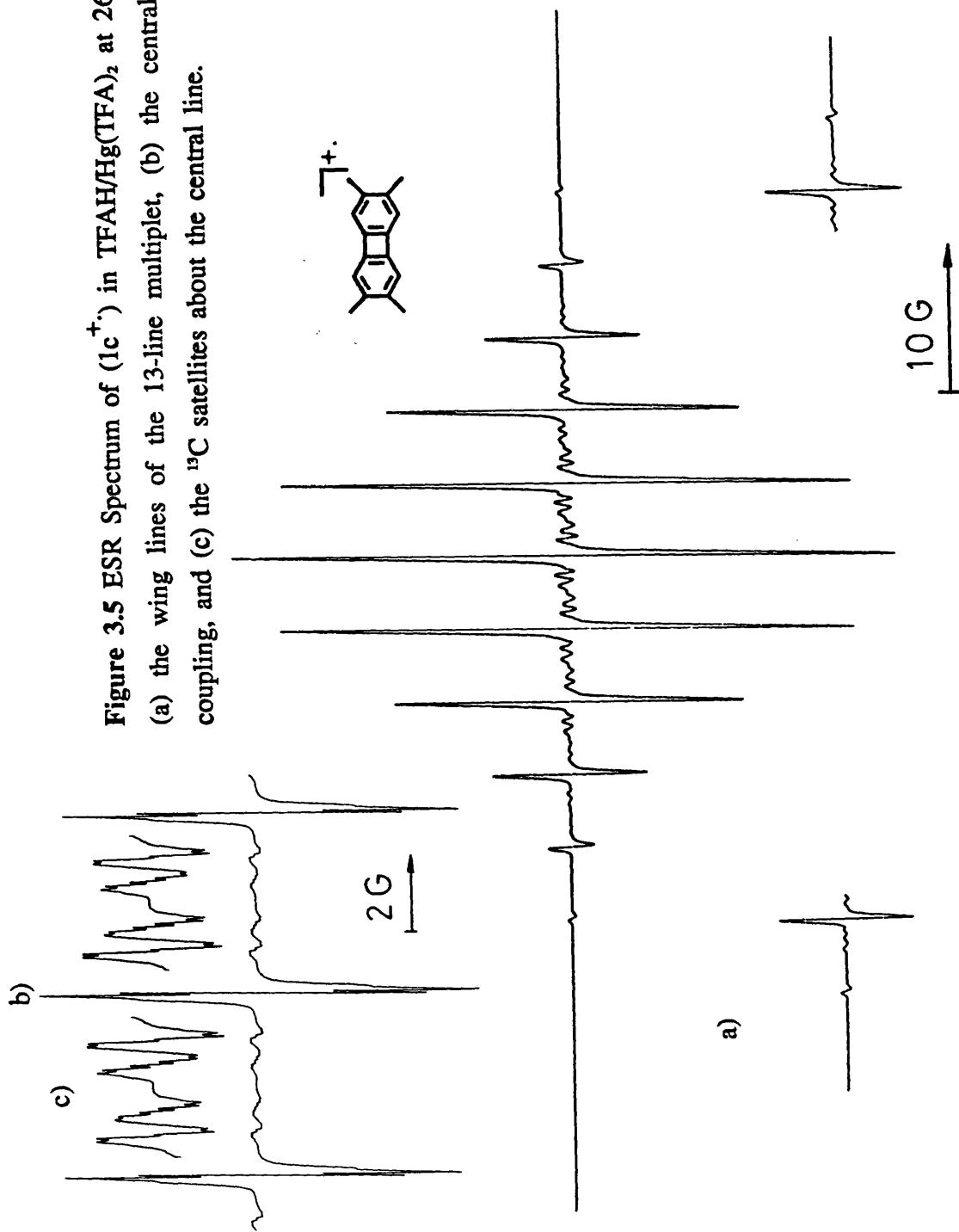


**Figure 3.5** ESR Spectrum of  $(1c^+)$  in TFAH/Hg(TFA) $_2$  at 261 K, showing inset (a) the wing lines of the 13-line multiplet, (b) the central lines with quintet coupling, and (c) the  $^{13}\text{C}$  satellites about the central line.



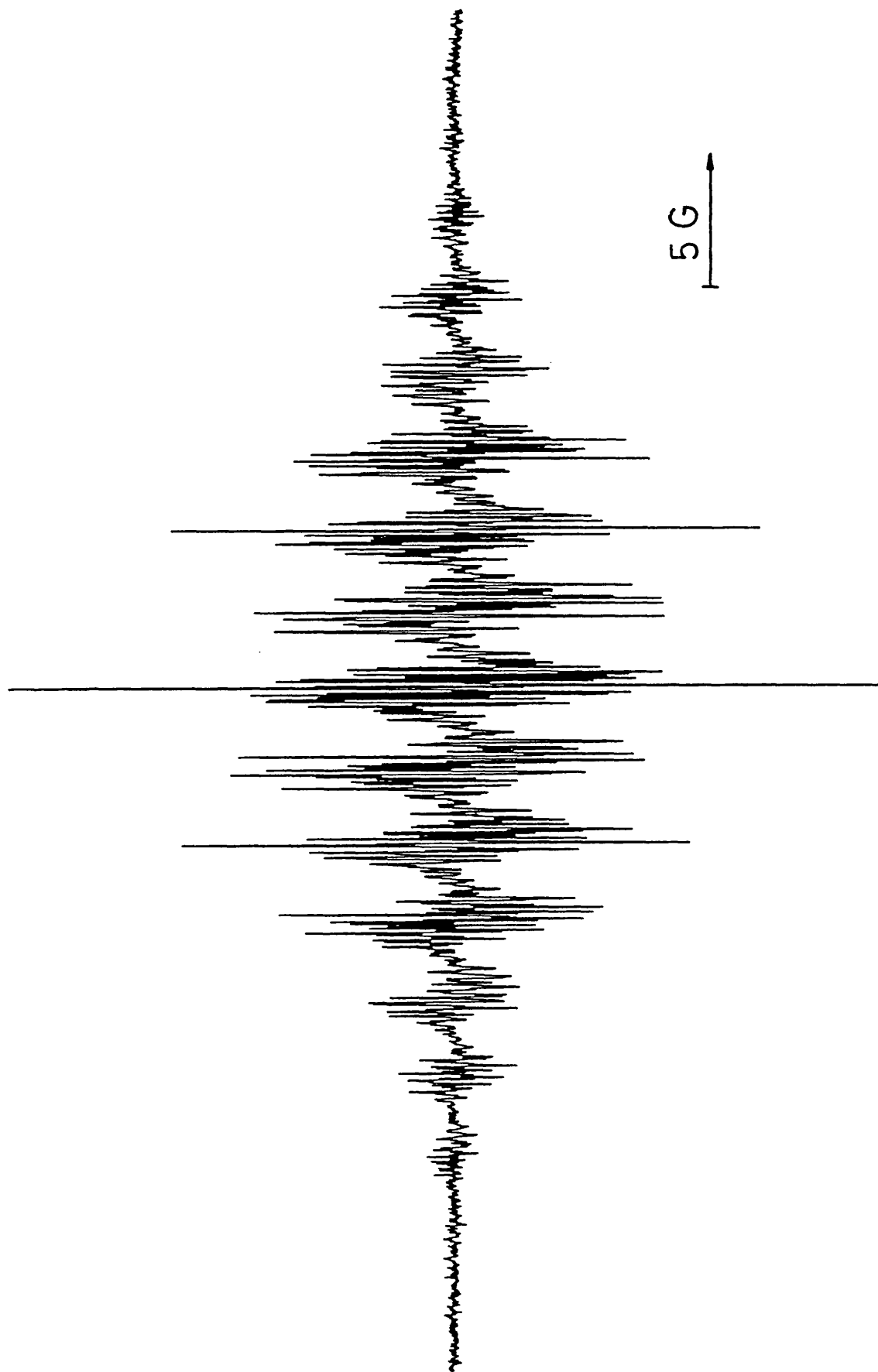


**Figure 3.6** ESR Spectrum of the radical anion formed by the reaction of lithium with (1c) in THF at 243 K. This spectrum was unchanged after 2 days.

Treatment of (1c) in tetrahydrofuran (THF) with potassium gave a brown solution which we believe to contain the dianion ( $1c^{2-}$ ). Photolysis of this gave the weak, short-lived spectrum of the radical anion ( $1c^{\cdot-}$ ) as shown in Figure 3.7. Presumably the reaction involves photoejection of an electron from the dianion ( $1c^{2-}$ ) (Equation 3.1). Davies and coworkers have observed a similar reaction previously for the dianions of pentalene<sup>16</sup> and fulvalene,<sup>17</sup> and Huber<sup>9</sup> has reported the equivalent reaction for the dianions of fluorene and of tetraphenylene.



Thermolysis of tetra- $\beta$ -methylbiphenylene (1c) at 400 °C gave the corresponding octa- $\beta$ -methyltetraphenylene (2c), which was isolated in low yield as a crystalline solid; this compound has not been described previously.

Octamethylbiphenylene (1d) in TFAH has been reported to show a poorly resolved 13-line-multiplet ESR spectrum which has been assigned to the radical cation of (1d). We believe this to be incorrect and have observed and analysed the authentic ESR spectrum of ( $1d^{\cdot+}$ ).

In TFAH/Tl(TFA)<sub>3</sub>, octamethylbiphenylene (1d) gives a deep blue solution which shows a strong spectrum of the radical cation ( $1d^{\cdot+}$ ) (Figure 3.8). The hyperfine coupling constants  $a(12H\alpha)$  0.17 and  $a(12H\beta)$  4.50 G are in accord with the predictions based upon the spectrum of ( $1a^{\cdot+}$ ) and the assumption that permethylation does not substantially effect the electron distribution.

The <sup>13</sup>C hyperfine couplings arise in principle from the superposition of five sets of triadecaplets (13-lines), and cannot be fully analysed in detail, but the largest <sup>13</sup>C coupling which can be identified is *ca.* 3.2 G. Hyperfine coupling to <sup>13</sup>C $\beta$  is usually less than to <sup>13</sup>C $\alpha$  [eg in CH<sub>3</sub>CH<sub>2</sub><sup>·</sup>,  $a(^{13}C\alpha)$  39.07,  $a(^{13}C\beta)$  13.57 G].<sup>18</sup> Hence the largest coupling probably relates to a ring carbon atom, and correlates well with the largest <sup>13</sup>C coupling in ( $1a^{\cdot+}$ ) of 3.21 G.

It is this analysis of the ESR spectrum of ( $1d^{\cdot+}$ ) that makes us believe that Hart's interpretation was incorrect. It is possible that Hart may have been observing the dimer radical cation ( $1d$ )<sub>2</sub><sup>·+</sup> which has been observed for ( $1a$ )<sub>2</sub><sup>·+</sup>.<sup>3</sup> We have been unable to observe any dimer species of ( $1d$ )<sub>2</sub><sup>·+</sup> in our

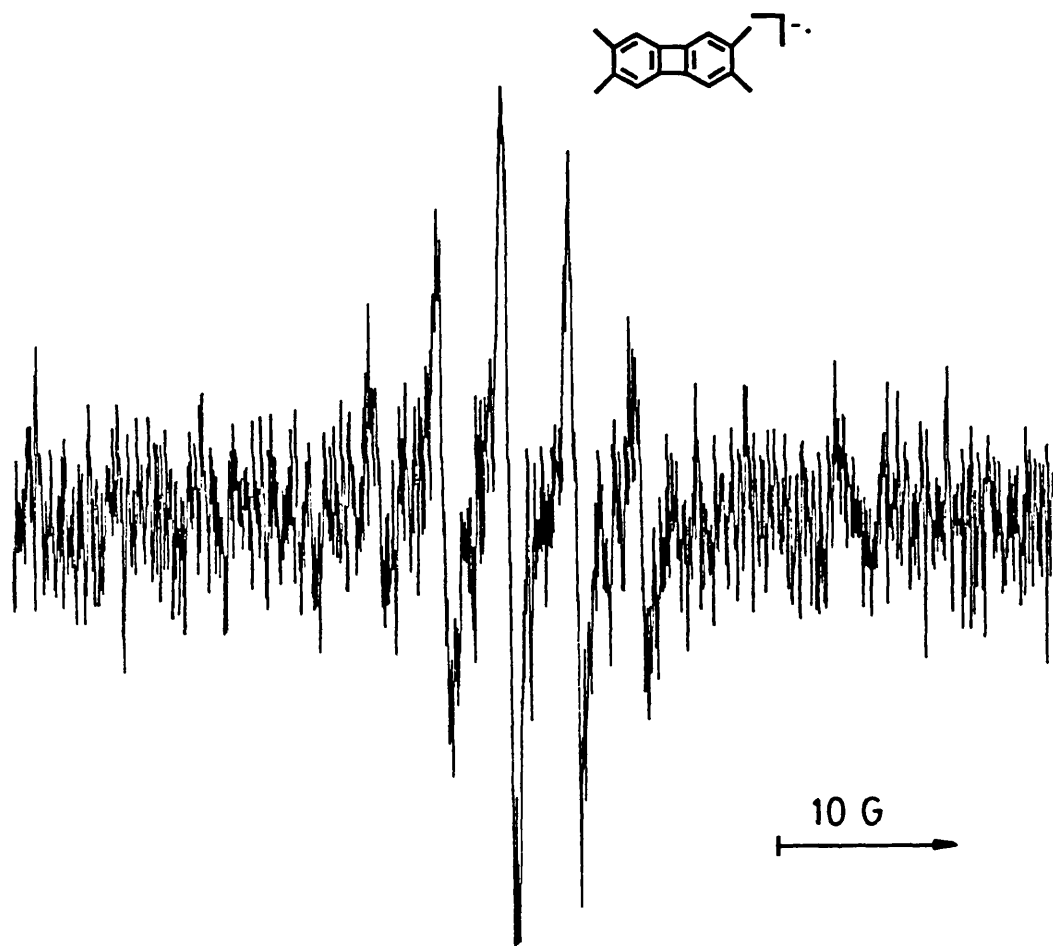
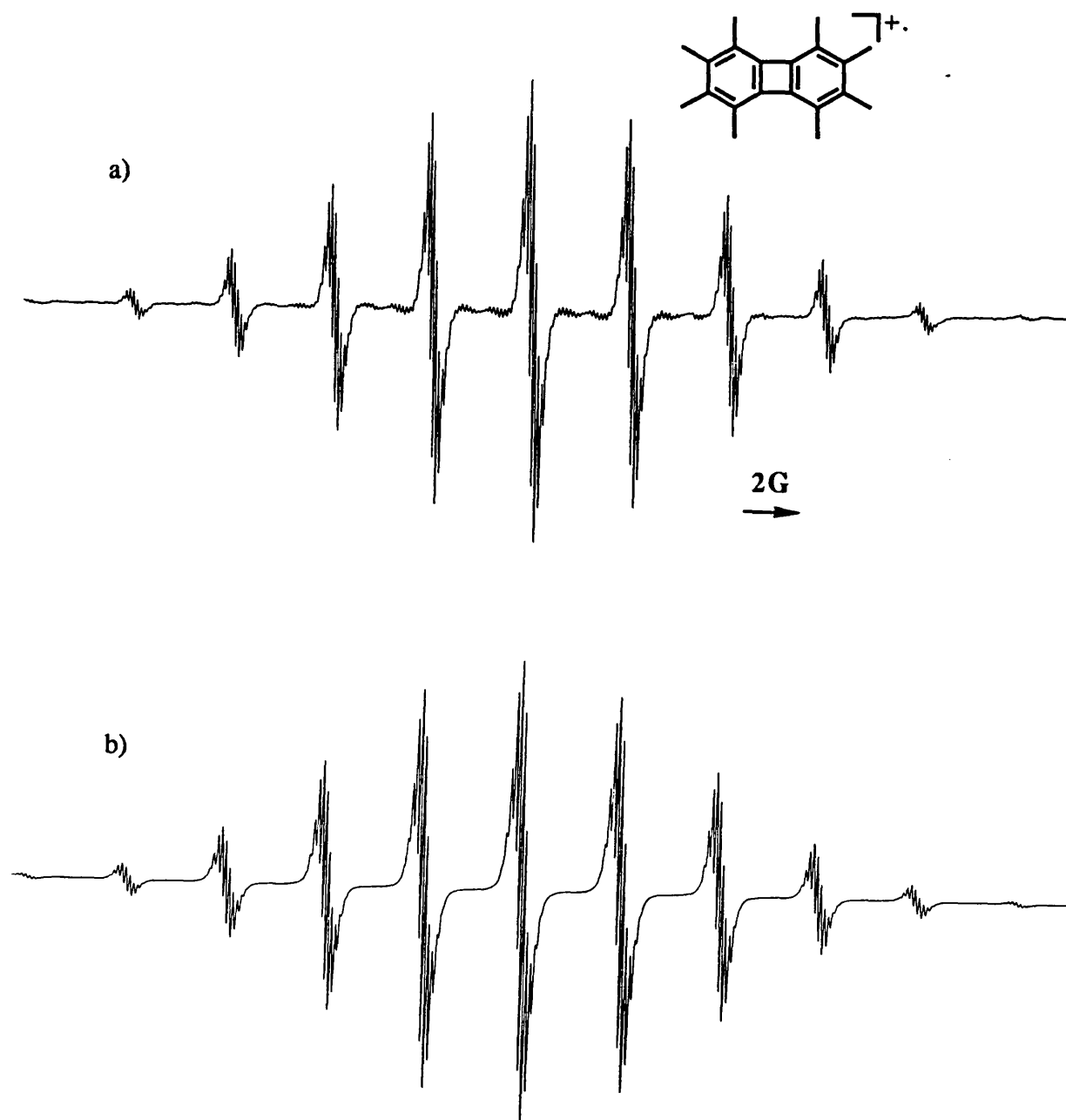


Figure 3.7 ESR Spectrum of  $(1c^{\cdot-}) K^+$  in THF at 243 K, from the photolysis of  $(1c^2)$ .



**Figure 3.8** (a) ESR Spectrum of  $(1d^+)$  in TFAH/Hg(TFA)<sub>2</sub> at 261 K. (b) Computer simulation of (a).

experiments using higher concentrations of (1d), which showed only stronger spectra of (1d<sup>+</sup>). It is likely that extensive methylation prevents dimer formation.

The radical anion was prepared by treating a solution of (1d) in THF with lithium at room temperature. The deep blue solution shows the ESR spectrum of (1d<sup>-</sup>) which is illustrated in Figure 3.9. Olah and Schleyer<sup>6</sup> found that the dianion showed *two* <sup>7</sup>Li NMR signals at room temperature, and at least *four* signals at -70°C, and they suggested that this was to be ascribed to the formation of oligomeric aggregates. Our ESR spectra show no evidence of aggregation, and indeed we are not aware of this phenomenon having been observed with radical anions; however our concentrations of (1d<sup>-</sup>)Li<sup>+</sup> are probably much lower than those of the (1d<sup>2-</sup>) 2Li<sup>+</sup> at which aggregation was observed.

The large hyperfine coupling to hydrogen or methyl at the β-positions, and the correspondingly small value at the α-positions, in both the radical cations and anions of the biphenylenes is in accord with the identical absolute values of the Huckel coefficients in the HOMO and LUMO of an alternate hydrocarbon. The hyperfine coupling at the β-positions in the radical cations is consistently greater than that in the same position in the corresponding radical anions; this is usual, and is ascribed to the effect of the positive charge in causing the 2p orbitals to contract.<sup>19</sup>

This positive charge effect is less obvious at the α-positions, where the coupling constants are at most 0.33 G and are sometimes undetectably small. However, the spin density at the α-positions in the different biphenylenes may vary in sign: Hart's<sup>2</sup> work shows that these signs could be obtained from the NMR spectra, but the directions of the contact chemical shifts of the relevant protons were not quoted.

### 3.2.2 Tetraphenylene and Octa-β-methyltetraphenylene

When a solution of tetraphenylene (2a) in TFAH/Hg(TFAH)<sub>2</sub> was irradiated with u.v. light filtered through Pyrex glass, it showed the spectrum which is illustrated in Figure 3.10, which we ascribe to the radical cation (2a<sup>+</sup>). The spectrum shows hyperfine coupling of 1.34 G to eight equivalent protons in the β-positions, and coupling to the other eight protons was within the line width of 0.05 G.

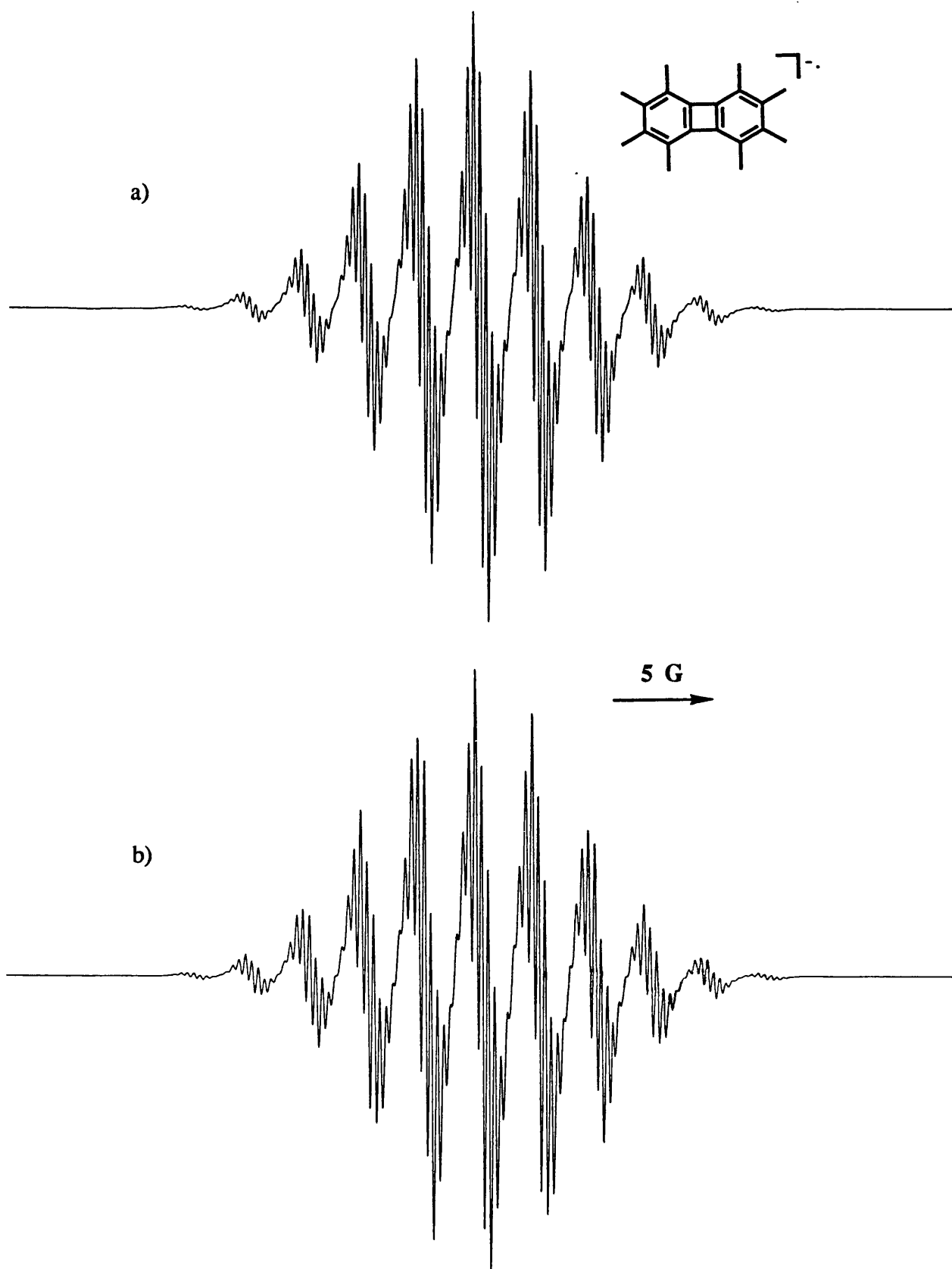


Figure 3.9 (a) ESR Spectrum of  $(1d^-)Li^+$  in THF at 243 K. (b) Computer simulation of (a).

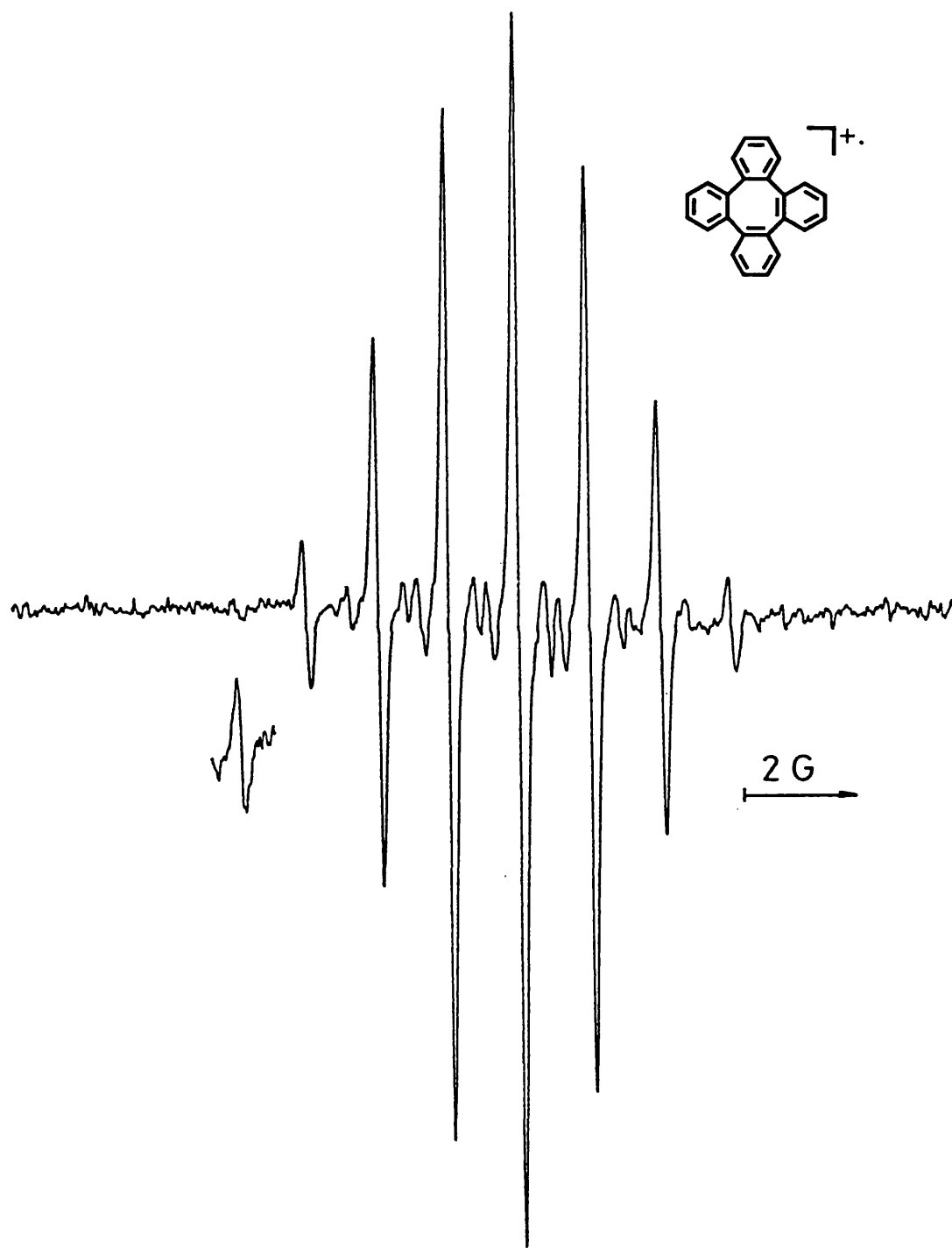
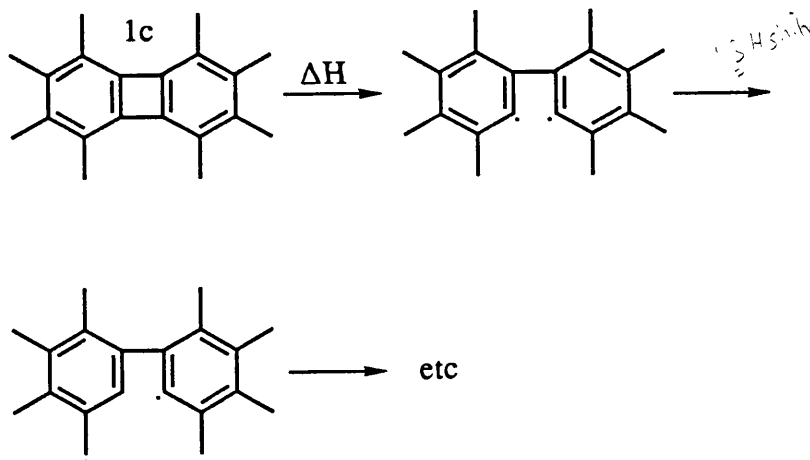


Figure 3.10 ESR Spectrum of  $(2a^{\cdot+})$  in TFAH/Hg(TFA)<sub>2</sub> at 260 K.

The ESR spectrum of the radical anion of tetraphenylene has been described by Carrington, Longuet Higgins, and Todd,<sup>8</sup> and by Huber.<sup>9</sup> By reduction with lithium in THF we obtained a strong, well resolved spectrum (Figure 3.11) with hyperfine coupling constants similar to those reported.

Tetraphenylene (2a) is formed in excellent yield by the thermolysis of biphenylene (1a) at 400 °C.<sup>11</sup> When this reaction was carried out with the methylated biphenylenes (1b), (1c), and (1d), the mass spectra of the crude product showed that the corresponding tetraphenylenes were formed in very small yield, and from the reaction of tetra- $\beta$ -methylbiphenylene (1c), the previously unknown octa- $\beta$ -methyltetraphenylene (2c) was isolated by h.p.l.c. in about 6% yield. The reaction of biphenylene (1a) has been suggested to proceed through the formation of a ring-opened diradical, and when  $\alpha$ -methyl groups are present, inter- and/or intramolecular hydrogen transfer (scheme 3.3) may detract from the yield of the tetraphenylene.



Scheme 3.3.

The central (cyclo-octatetraene) ring of tetraphenylene is non-planar, but a qualitative picture of the electron distribution can be obtained by the perturbation approach as used by Carrington, Longuet-Higgins, and Todd.<sup>8</sup>

Scheme 3.4 shows the electron distribution in the degenerate symmetric and antisymmetric bonding ( $\psi_{A1}$  and  $\psi_{S1}$ ) and antibonding ( $\psi_{A2}$  and  $\psi_{S2}$ ) orbitals of a benzene ring.



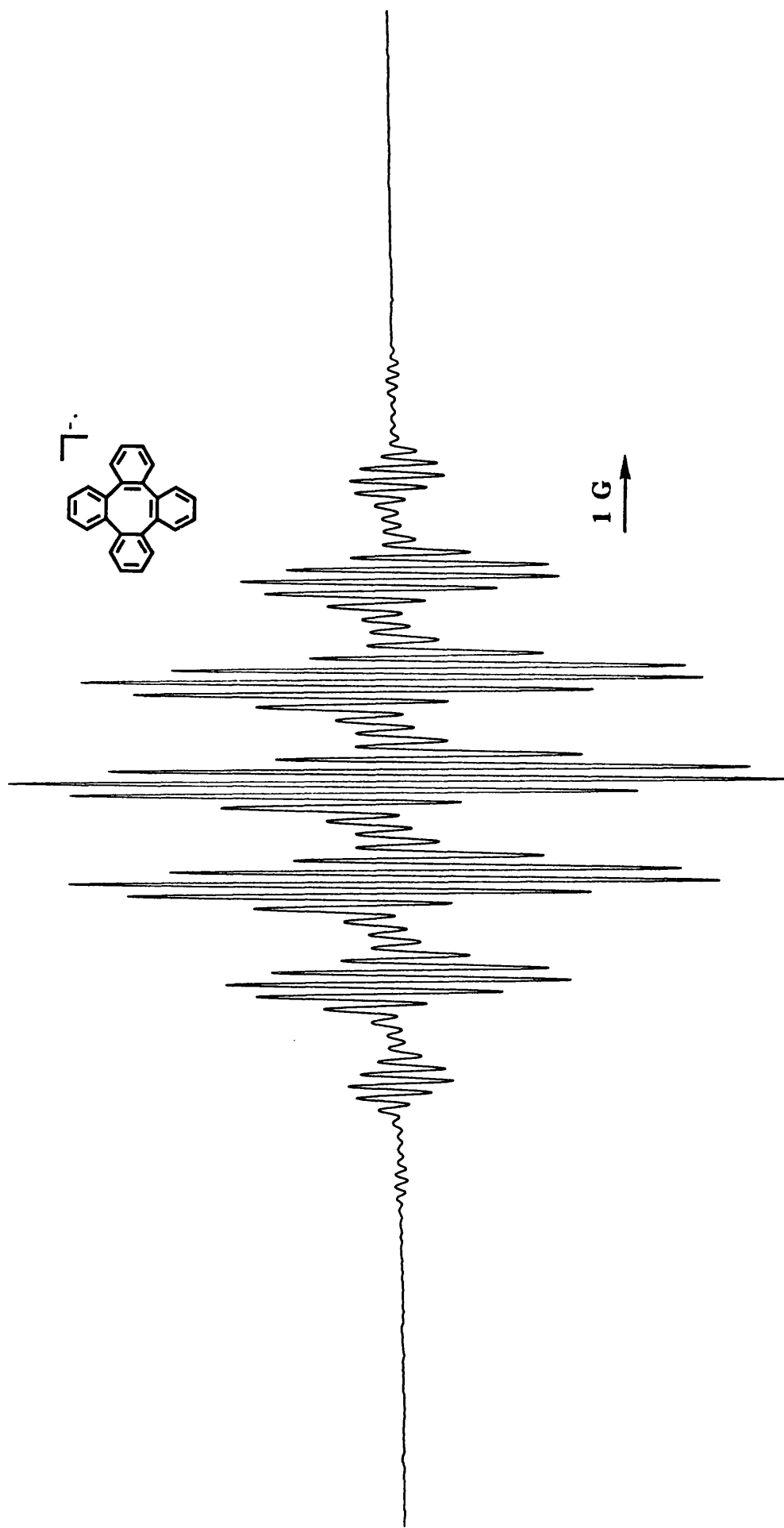


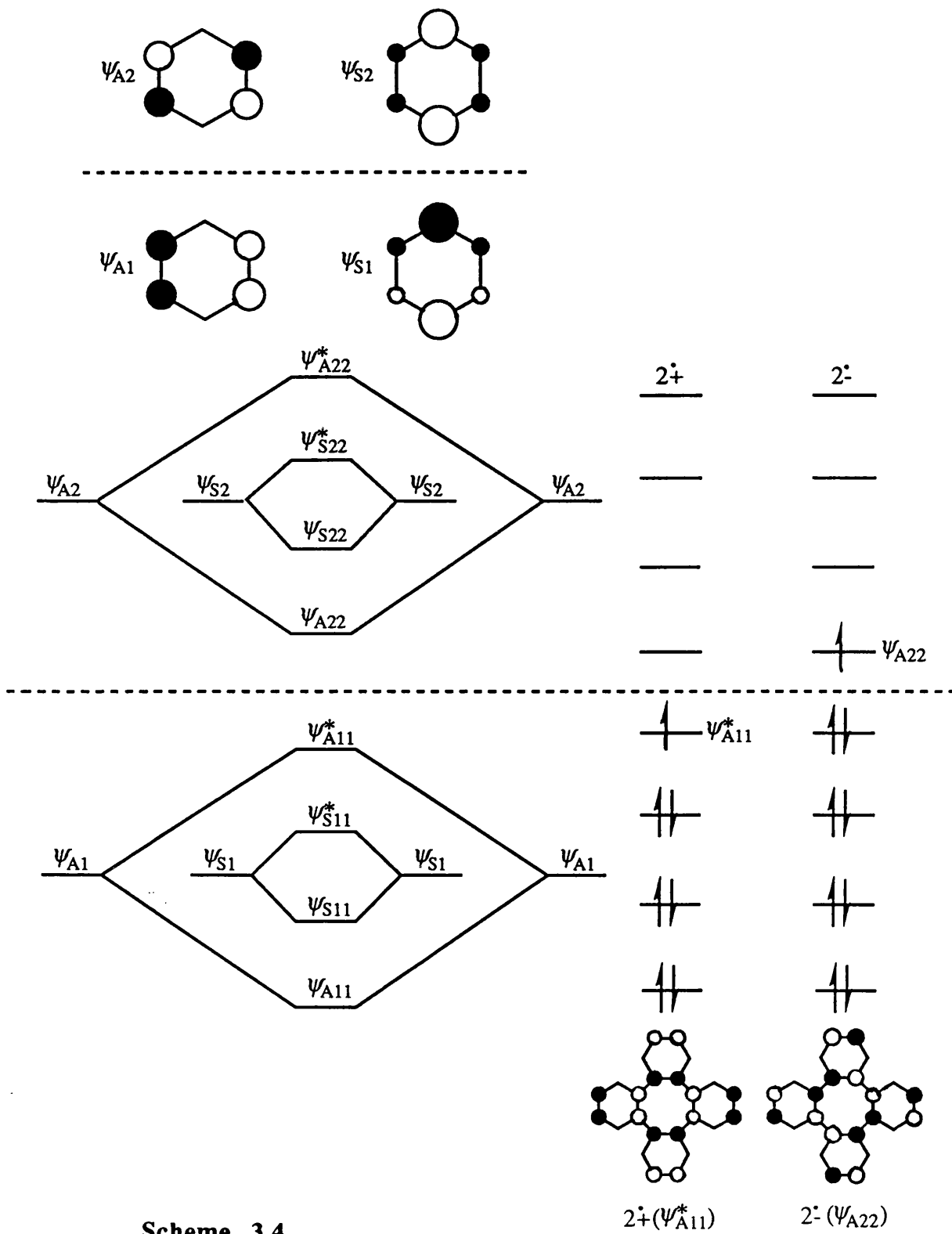
Figure 3.11 (a) ESR Spectrum of  $(2a^-)Li^+$  in THF at 243 K.

If tetraphenylene is considered to be built up from pair-wise interactions of benzene rings with a small overlap integral, the interaction between the  $\psi_A$  orbitals will be greater than that between the  $\psi_S$  orbitals because of the larger coefficients at what will be the  $\alpha$ -positions in the tetraphenylene. This is illustrated in the perturbation diagram (Scheme 3.4), which identifies the HOMO of the tetraphenylene radical cation ( $2^{\cdot+}$ ) as an antibonding combination of antisymmetric ( $\psi_{A1}$ ) orbitals, and the SOMO of the radical anion ( $2^{\cdot-}$ ) as a bonding combination of antisymmetric ( $\psi_{A2}$ ) orbitals. In both ( $2^{\cdot+}$ ) and ( $2^{\cdot-}$ ), this model predicts a large electron density at the 8  $\beta$ -positions, and a near-zero electron density at the 8  $\alpha$ -positions.

This was the basis of the argument on which the spectrum of ( $2a^{\cdot-}$ ) was analysed.<sup>8</sup> We similarly assign the hyperfine coupling in ( $2a^{\cdot+}$ ) of  $a(8H)$  1.35 G to the protons in the  $\beta$ -positions. It is interesting that this is slightly *less* than the corresponding value of 1.39 G in ( $2a^{\cdot-}$ ). We are not aware of any other example of an alternant hydrocarbon in which the positive charge does not have the reverse of this effect, but we note that if ( $2a^{\cdot+}$ ) and ( $2a^{\cdot-}$ ) remain non-planar like ( $2a$ ), they cannot legitimately be considered as alternant hydrocarbons, and that there are other complications associated with the spectra of these species, as discussed below.

We were unable to observe any ESR spectrum when octa- $\beta$ -methylbiphenylene ( $2c$ ) in THF was treated with lithium or potassium with or without sonication in the absence or presence of 18-crown-6. However, treatment of ( $2c$ ) in TFAH/Hg(TFA)<sub>2</sub> gave a light yellow solution which showed the strong spectrum of ( $2c^{\cdot+}$ ) which is illustrated in Figure 3.12. This simulates as a 25-plet of nonets; the <sup>13</sup>C hyperfine coupling could be observed but could not be analysed because of the small value of  $a(24H)$ , and the complication which results from the  $a(8H)$  coupling.

The spectrum of the radical cation of octa- $\beta$ -methyltetraphenylene ( $2c^{\cdot+}$ ) which shows a large hyperfine 25-plet coupling to the  $\beta$ -methyl groups and a small nonet coupling to the  $\alpha$ -hydrogen atoms confirms the predicted electron distribution.



Scheme 3.4

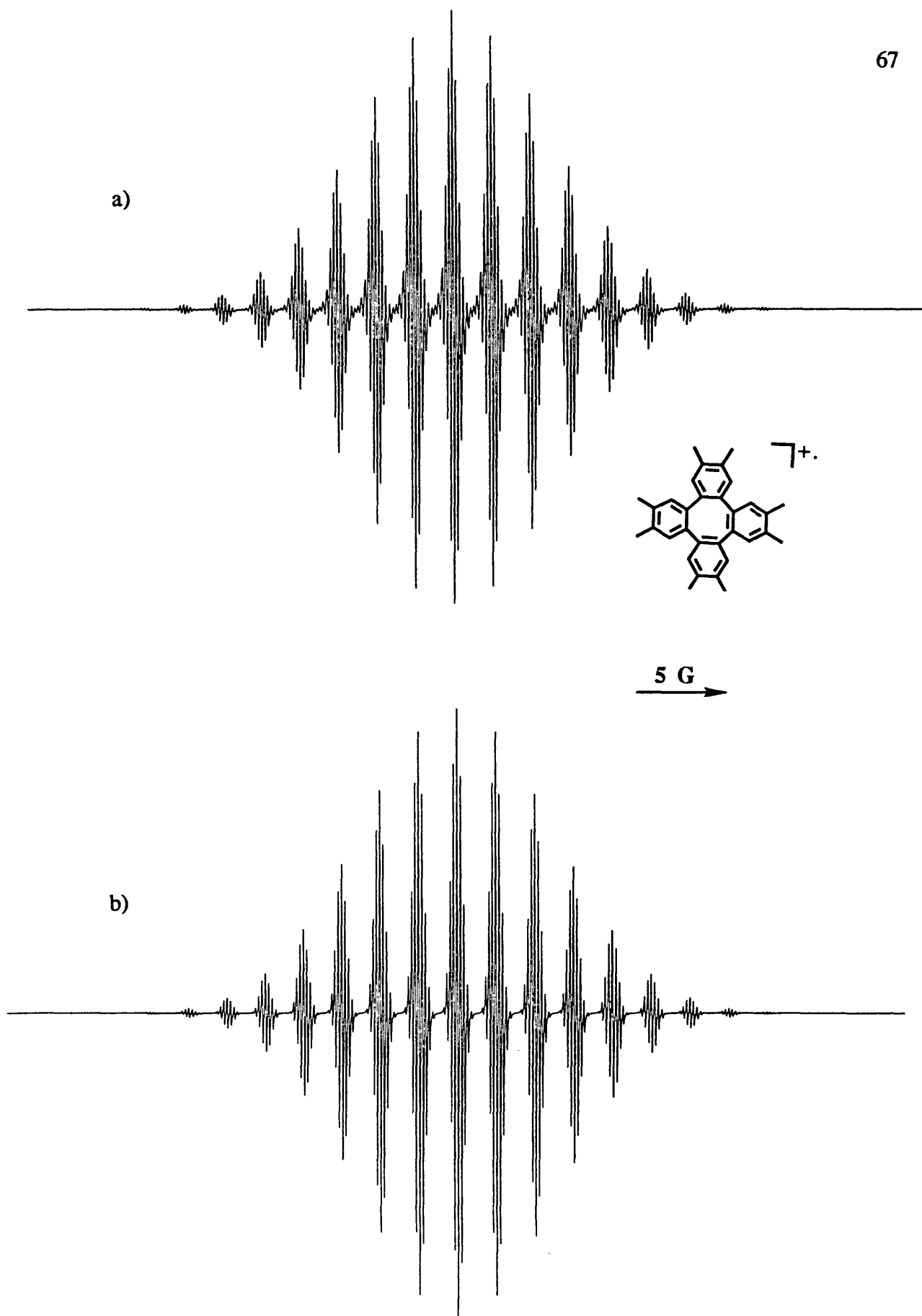
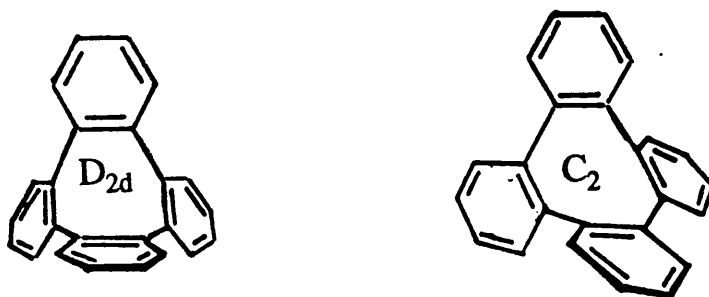


Figure 3.12 (a) ESR Spectrum of ( $2c^+$ ) in TFAH/Hg(TFA) $_2$  at 261 K. (b) Computer simulation of (a).

We were unable to detect the spectrum of the radical anion ( $2c^{\cdot-}$ ) when (2c) was treated with lithium or potassium, with or without sonication. This can be rationalised on the grounds that, if interaction between the benzene rings is small, each ring can be regarded as being analogous to durene for which we have been similarly unable to observe the formation of a radical anion, probably because electron repulsion by the methyl groups destabilises the radical anion.

These results can be compared with the very interesting work which has been carried out by Huber on the tetraphenylene radical anion ( $2a^{\cdot-}$ ) and dianion ( $2a^{2-}$ ).<sup>9</sup> X-Ray crystallography shows that tetraphenylene (and its inclusion complexes) is crown shaped with  $D_{2d}$  symmetry (as is cyclo-octatetraene which constitutes the central ring), and this is consistent with the fact that it shows only two  $^1\text{H}$  and three  $^{13}\text{C}$  NMR signals in solution. One-electron reduction gives the radical anion ( $2a^{\cdot-}$ ) with  $a(8\text{H})$  0.20 and 1.39 G, consistent with the same  $D_{2d}$  symmetry, but further reduction gives a dianion ( $2a^{2-}$ ) which shows not two but *eight*  $^1\text{H}$  NMR signals, and not three but *twelve*  $^{13}\text{C}$  NMR signals. Photolysis of this dianion now generates a new radical anion ( $2a'^{\cdot-}$ ) with an ESR spectrum which is more complicated than that of ( $2a^{\cdot-}$ ), and which shows  $a(4\text{H})$  1.71, 0.87, 0.22, and 0.14 G.

Huber proposed that whereas (2a) has  $D_{2d}$  symmetry, ( $2a'^{\cdot-}$ ) has only  $C_2$  symmetry, and that the radical anions ( $2a^{\cdot-}$ ) and ( $2a'^{\cdot-}$ ) retain the conformations of their closed shell precursors. Thus ( $2a^{2-}$ ) and ( $2a'^{\cdot-}$ ) can be described as being comprised of two near-planar biphenyl units which themselves are near-orthogonal, and in ( $2a'^{\cdot-}$ ) the unpaired electron is concentrated in one biphenyl moiety. These structures are illustrated in Scheme 3.5.



Scheme 3.5.

**Table 3.1** Hyperfine coupling constants (G) and *g*-values of the radical ions described in the text.

Radical ion	H $\alpha$	H $\beta$	Others	<i>g</i>	Solvent <sup>a</sup>	T/K	Ref
1a <sup>+</sup>	0.21(4H)	3.58(4H)	3.21, 2.55, 2.39( <sup>13</sup> C)	2.0025	TFAH	262	10
1a <sup>-</sup>	0.21(4H)	2.86(4H)	2.86, 2.44( <sup>13</sup> C)				
3a <sup>+</sup>	0.21(4H)	3.58(3H)	76.5( <sup>199</sup> Hg)	2.0014	TFAH	262	3
4a <sup>+</sup>	0.21(4H)	3.58(2H)		2.0007	TFAH	262	3
1b <sup>+</sup>	<0.01(12H)	3.25(4H)	3.04, 2.35, 2.25( <sup>13</sup> C)	2.0025	TFAH	260	<i>b</i>
1b <sup>-</sup>	0.18(12)	2.75(4H)	3.65( <sup>13</sup> C)	2.0011	THF	243	<i>b</i>
1b <sup>-</sup>			( <sup>7</sup> Li)	2.0011	THF	243	<i>b</i>
1b <sup>-</sup>			( <sup>39</sup> K)	2.0011	THF	243	<i>b</i>
3b <sup>+</sup>	<0.01(12H)	3.27(3H)	70.25( <sup>199</sup> Hg)	2.0014	TFAH	261	<i>b</i>
4b <sup>+</sup>	<0.01(12H)	3.23(2H)	70.95( <sup>199</sup> Hg)	2.0004	TFAH	261	<i>b</i>
1c <sup>+</sup>	0.08(4H)	4.70(12H)	3.5, 3.25( <sup>13</sup> C)	2.0024	TFAH	261	<i>b</i>
1c <sup>-</sup>		3.72(12H)		2.00 <sup>c</sup>	THF	243	<i>b</i>
1d <sup>+</sup>	0.17(12H)	4.50(12H)		2.0026	TFAH	261	<i>b</i>
1d <sup>-</sup>	0.33(12H)	3.04(12H)		2.0027	THF	243	<i>b</i>
2a <sup>+</sup>	<0.01(8H)	1.34(8H)					
2a <sup>-</sup>	0.16(8H)	1.31(8H)		2.0025	TFAH	260	<i>b</i>
2a <sup>-</sup>	0.14(4H)	1.17(4H)			THF	183	<i>b</i>
	0.22(4H)	0.8(4H)			MeTHF		9
2c <sup>+</sup>	0.19(8H)	2.15(24H)		2.0029	TFAH	261	<i>b</i>

*a* TFAH = trifluoroacetic acid  
 THF = tetrahydrofuran  
 MeTHF = methyltetrahydrofuran

*b* Present Work

*c* There is some doubt over the identification of the central line.

A similar effect might be looked for in the radical cation ( $2a^{+\cdot}$ ) as one-electron oxidation, like one-electron reduction, should strengthen the interaction between pairs of rings. We can see no sign of deviation from  $D_{2d}$  symmetry in the tetraphenylene or octamethyltetraphenylene radical cations ( $2a^{+\cdot}$ ) or ( $2c^{+\cdot}$ ). It is unfortunate that we were not able to generate the octa- $\beta$ -methyltetraphenylene radical anion and dianion ( $2c^{\cdot-}$ ) and ( $2c^{2-}$ ), so these could be investigated for a similar effect. It would also be interesting to attempt to generate the tetraphenylene radical cation from the dication, and study these species in a similar way.

The tetraphenylene structure is quite rigid, and it seems surprising that it could exist in a second conformation separated from the first by a barrier which (in the dianion) prevents interconversion at 150 °C. Further, we know of no other radical ion where the electron density is unsymmetrically distributed over a symmetric structure. We have considered the alternative possibility that the reduced symmetry in ( $2a'^{\cdot-}$ ) and ( $2a'^{2-}$ ) might be result the of a specific interaction with the counteranion [although no hyperfine coupling to the metal cation is apparent in the ESR spectrum of ( $2a'^{\cdot-}$ )].

h-

We have used the MNDO method in an attempt to locate an energy minimum in which the radical anion or dianion of (2a) interacts with a lithium cation, but no such minimum could be found. Similarly the more recent AM1 and PM3 methods were unsuccessful in identifying a minimum using lithium or the appropriate "sparkle" as the counterion. The AM1 method showed that the  $D_{2d}$  structure (Scheme 3.5) represents a minimum in the energy of both the radical anion and the dianion, but we cannot exclude the possibility that the  $C_2$  structure might represent a deeper minimum.

### References

1. C. A. McDowell and J. R. Rowlands, *Canad. J. Chem.*, **1960**, *38*, 503.  
A. Carrington and J. dos Santos-Veiga, *Mol. Phys.*, **1962**, *5*, 285.  
P. R. Hindle, J. dos Santos-Veiga, and J. R. Bolton, *J. Chem. Phys.*, **1968**, *48*, 4703.
2. H. Hart, A. Teuerstein, and M. A. Babin, *J. Am. Chem. Soc.*, **1981**, *103*, 903.

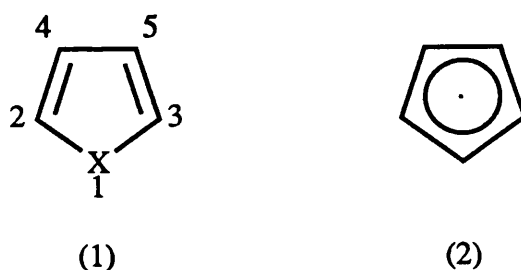
3. J. L. Courtneidge, A. G. Davies, D. C. McGuchan, and S. N. Yazdi, *J. Organometallic. Chem.*, 1988, **341**, 63.
4. G. A. Olah and G. Liang, *J. Am. Chem. Soc.*, 1977, **99**, 6045. K. Laali, *J. Chem. Res. (S)*, 1988, 378.
5. R. H. Cox, H. W. Terry, and L. W. Harrison, *Tetrahedron Lett.*, 1971, 4815. H. Gunther, H. V. Puttkamer, K. Finneiser, R. Benkem, U. Edlund, and B. Eliasson, *Helv. Chim. Acta.*, 1986, **69**, 955.
6. J. W. Bausch, P. S. Gregory, G. A. Olah, G. K. S. Prakash, P. von R. Schleyer, and G. A. Segal, *J. Am. Chem. Soc.*, 1989, **111**, 3633.
7. W. Huber, A. May, and K. Mullen, *Chem. Ber.*, 1981, **114**, 1318.
8. Carrington, H. C. Longuet Higgins, and P.F. Todd, *Mol. Phys.*, 1964, **8**, 45.
9. W. Huber, *Tetrahedron Lett.*, 1985, 181. W. Huber and K. Mullen, *Acc. Chem. Res.*, 1986, **19**, 300.
10. D. V. Avila, A. G. Davies, M. L. Girbal, and D. C. McGuchan, *J. Chem. Res., (S)*, 1989, 256.
11. M. Karplus and G. K. Fraenkel, *J. Chem. Phys.*, 1961, **35**, 1312.
12. T. Yonezawa, T. Kawamura, and H. Kato, *J. Chem. Phys.*, 1969, **50**, 3482.
13. A. G. Davies and D. C. McGuchan, unpublished work.
14. F. Gerson, 'High Resolution E.S.R. Spectroscopy', Wiley-Verlag Chemie, Berlin, 1976.
15. L. Friedman and D. F. Lindow, *J. Am. Chem. Soc.*, 1968, **90**, 2324.
16. D. Wilhelm, J. L. Courtneidge, T. Clark, and A. G. Davies, *J. Chem. Soc., Chem. Commun.*, 1984, 810.
17. A. G. Davies, J. R. M. Giles, and J. Luszyk, *J. Chem. Soc., Perkin Trans. 2*, 1981, 747.
18. O. W. Howarth and G. K. Fraenkel, *J. Chem. Phys.*, 1970, **52**, 6258.
19. J. P. Colpa and J. R. Bolton, *Mol. Phys.*, 1963, **6**, 273.



## Chapter 4. Radical Cations of Some Mono- and Bis-pyrroles and Related compounds

### 4.1 Introduction

The work described in this chapter is predominantly an investigation into the radical cations of pyrroles and their derivatives with reference to their molecular structures. Pyrrole (1;  $X = NR$ ) is an important molecule, being an integral part of haemoglobin, chlorophyll, cytochromes and many other naturally occurring molecules. Like benzene, pyrrole has 6  $\pi$ -electrons, the heteroatom contributing an electron pair, as it also does in the other hetero[5]annulenes (1;  $X = O, S, Se, \text{ or } Te$ ). The one-electron oxidation of these heteroaromatics will give a paramagnetic 5  $\pi$ -electron system, isoelectronic with the cyclopentadienyl radical (2).



The cyclopentadienyl radical has two degenerate HOMO's  $\psi_a$  and  $\psi_s$  (Figure 4.1).

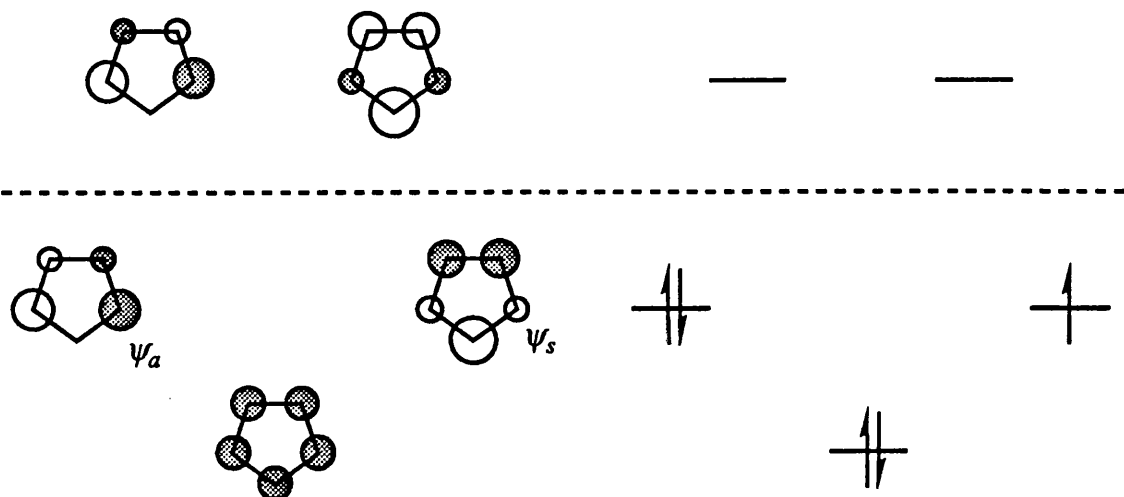


**Figure 4.1** The orbital energies and wavefunctions for the cyclopentadienyl radical.

In the heterocycles (1) the electronegative substituent X breaks the  $\psi_a/\psi_s$  degeneracy by stabilizing the  $\psi_s$  orbital which has a high electron density at the 1-position; the u.p.e. in the radical cation therefore occupies predominantly the  $\psi_a$  MO as shown in Figure 4.2.

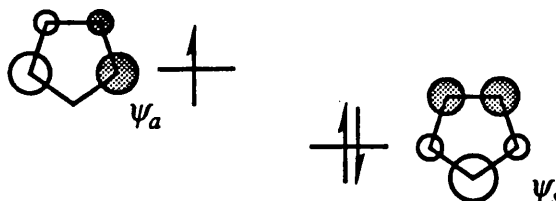


Figure 4.2 Orbital energy and occupancy in the heterocyclic radical cation ( $1^+$ ).

It is necessary to protect the 2 and 5 positions of the hetero[5]annulenes with alkyl groups when generating their radical cations in an acidic medium, or polymerisation occurs to give a paramagnetic polymer.<sup>1</sup> A result of alkylation at these positions is to destabilize further the  $\psi_s$  MO, reinforcing the energy difference between  $\psi_a$  and  $\psi_s$  due to the electronegative heteroatom. Studies have been reported by Symons,<sup>2</sup> and by Shida<sup>3</sup> of the ESR spectra of the furan, thiophene, and pyrrole radical cations generated by  $\gamma$ -irradiation in a Freon matrix. All these spectra are in accord with these predictions from MO theory, that is to say the SOMO was of the form  $\psi_a$ .

Luis Julia and Sophie Yazdi (of this research group) were the first to generate and characterise by ESR spectroscopy the radical cations of the simple alkylated furans, thiophenes, and pyrroles in fluid solution.<sup>1</sup>

This breakthrough into the radical cation chemistry of heteroaromatic molecules opens up a large field to investigation. One can look for the many different phenomena which are familiar in the homocyclic radical cations, such as the degree of coplanarity and the barrier to rotation (*e.g.* in the radical ions of Ar-Ar), substituent effects on the electron distribution, the orbital occupancy in cyclophanes, conformational mobility, dehydrodimerisation, spiroconjugation, mercurideprotonation, etc.

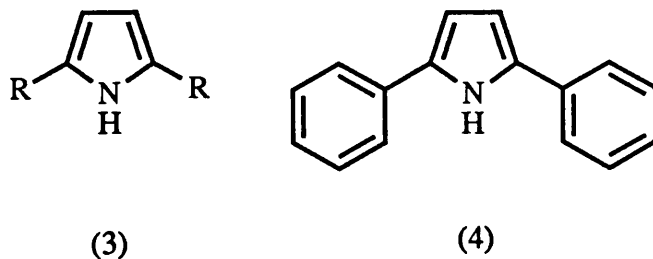
This chapter describes an extension of the studies on simple alkyl pyrroles, and attempts to identify some of these further phenomena in heteroaromatic radical cations.

We found that the pyrroles and their derivatives were best oxidized to their ESR-observable radical cations by dissolving the substrate in a nitrogen-purged solution of trifluoroacetic acid containing thallium(III) trifluoroacetate; there were only a few exceptions where the mercury(II) salt worked more readily. In general, the radical cations could be generated with both salts, the mercury salt usually requiring irradiation (see Experimental).

## 4.2 Results and Discussion

### 4.2.1 Simple *N*-Substituted Pyrroles

2,5-Di-*t*-butylpyrrole (3; R = *t*-Bu) when dissolved in  $\text{Tl}(\text{TFAH})_3/\text{TFAH}$  gave rise to its radical cation which exhibited an intense and well resolved ESR spectrum with  $a(18\text{H})$  0.62,  $a(2\text{H})$  3.58,  $a(\text{N})$  4.05, and  $a(\text{H})$  0.91 G,  $g$  2.0025 (Figure 4.3). All coupling constants and  $g$ -values are summarized in Table 4.1. We were unable to analyse the  $^{13}\text{C}$  couplings apparent in the spectrum. The couplings to the *t*-butyl and 3,4 ring protons are similar to those in the radical cations of the furan and thiophene analogues.<sup>1</sup>



The radical cations of all three compounds were long lived, and the ESR spectrum of the 2,5-di-*t*-butylpyrrole radical cation could be recorded over a week later. This is unlike the 2,5-dimethylpyrrole whose radical cation generated under similar conditions dies within 1 hour.

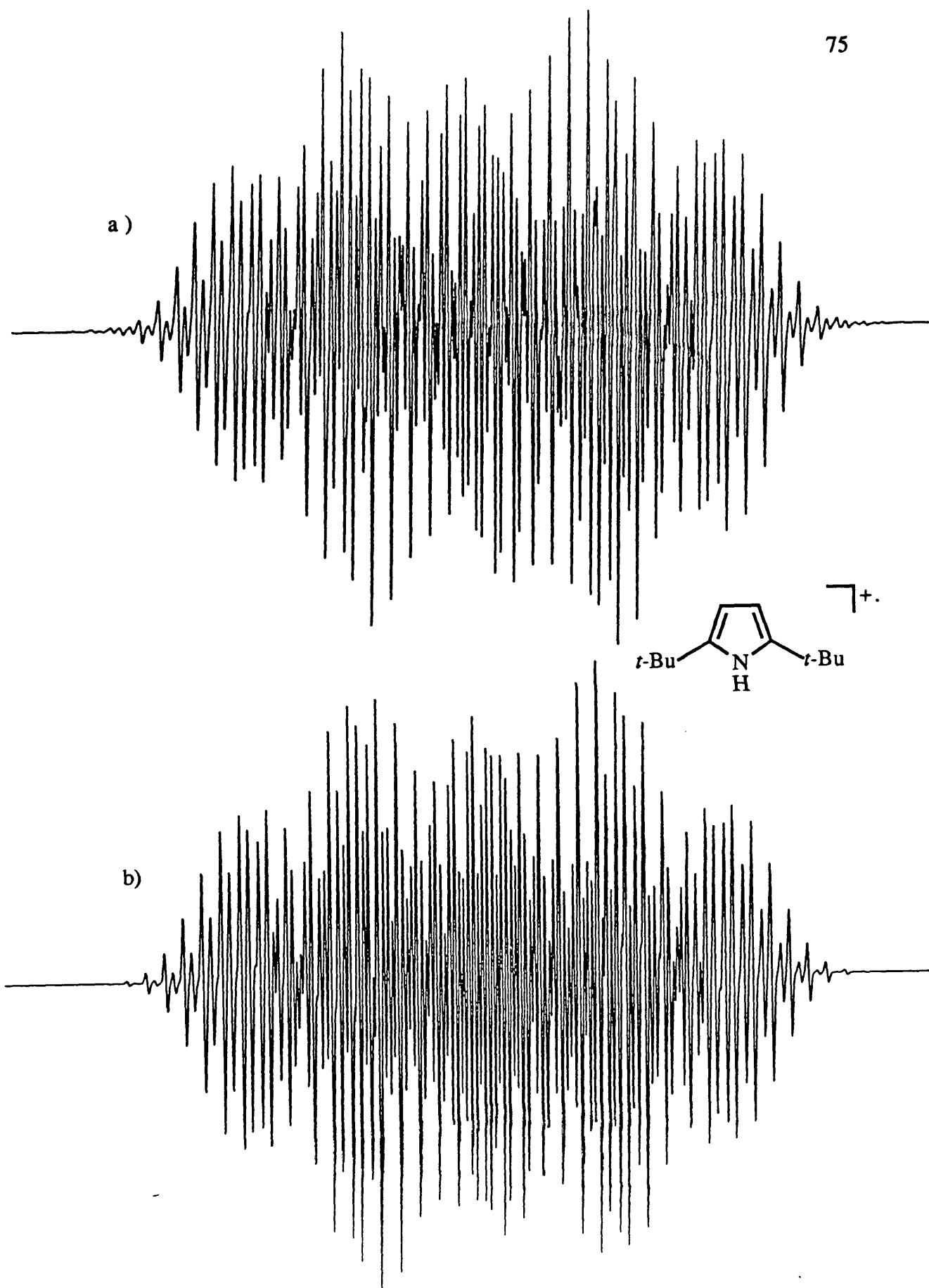
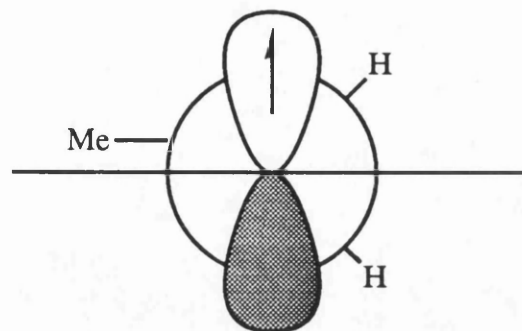


Figure 4.3 (a) ESR Spectrum of  $(3^+; R = t\text{-Bu})$  in TFAH/Tl(TFA)<sub>3</sub> at 260 K. (b) Computer simulation of (a).

The kinetic stability of the 2,5-di-*t*-butyl-furan, -thiophene, and -pyrrole radical cations is rationalised in terms of the absence of  $\beta$ -hydrogens and of steric hindrance.

One mechanism for the decay of a radical cation is the loss of a proton to leave a neutral radical, and  $\beta$ -protons will be lost more rapidly when the C-H bond subtends a small angle with the  $2p$  orbital on  $C_\alpha$ . The interaction which results will be strongest in the furan, thiophene, and pyrrole radical cations when the alkyl substituents are on the 2 and 5 positions where the electron density is highest. It is observed that for  $(1^+; X = NR, O, \text{ or } S)$  the intensities of the ESR spectra, which are proportional to the steady state concentrations, are dependent on the nature of the alkyl substituents at the positions 2 and 5. The ESR spectra of the 2,5-di-*t*-butyl derivatives of  $(1^+; X = NH, O, \text{ or } S)$  are by far the most intense, followed by the methyl and ethyl analogues. The intensity of the spectra obtained from the *t*-butyl-substituted heteroaromatics may be accounted for by the absence of  $\beta$ -hydrogens and by the steric bulk of the *t*-butyl group reducing electrophilic attack of the radical cation upon its parent.

A more subtle argument is required to accommodate the greater intensity of the ESR spectra of the radical cations of the 2,5-dimethyl substituted heterocycles over those of the diethyl derivatives. Hyperfine coupling of an u.p.e. to a  $\beta$ -proton is dependent on the dihedral angle,  $\theta$ , subtended between the C-H bond and the axis of the  $2p$  orbital on  $C_\alpha$  as shown in Figure 1.6, and  $\beta$ -proton coupling is described by the Heller-McConnell equation (Equation 1.4). The C-H bond of a freely rotating methyl group attached to a aromatic system subtends an average angle of  $45^\circ$  to the axis of the  $2p$  orbital on  $C_\alpha$ . From the  $\beta$ -proton coupling we can determine that the methyl group of an ethyl substituent prefers to lie in the nodal plane of the  $\pi$ -system (Figure 4.3) in these heterocycles, making the angle subtended between  $\beta$  C-H bonds and the  $2p$  axis *ca.*  $30^\circ$ . This results not only in a larger coupling to the  $\beta$ -protons but also in a reduced stability in the radical cations of 2,5-diethyl substituted hetero[5]annulenes.



**Figure 4.4** Orientation of a 2- or 5-ethyl substituent with respect to the adjacent  $2p_z$  orbital in the hetero[5]annulenes.

2,5-Diphenylpyrrole (4) when photolysed with Pyrex-filtered u.v. light in a solution of  $\text{Hg}(\text{TFA})_2/\text{TFAH}$  gave rise to a ESR spectrum (much stronger with  $\text{Hg}^{2+}$  as oxidant than with  $\text{Tl}^{3+}$ ) (Figure 4.5) exhibiting mercury satellites about the central feature of the spectrum. We were unable to analyse the complicated spectrum and satellites but  $a(^{199}\text{Hg}) = 64.5$  G and from the average ratio between the coupling constant of the mercury substituent and the proton it replaces (Section 1.3) we can estimate one of the proton couplings to be  $a(\text{xH})$  ca. 3.31 G.

#### 4.2.2 Oligomethylene *NN'*-Bipyrroles

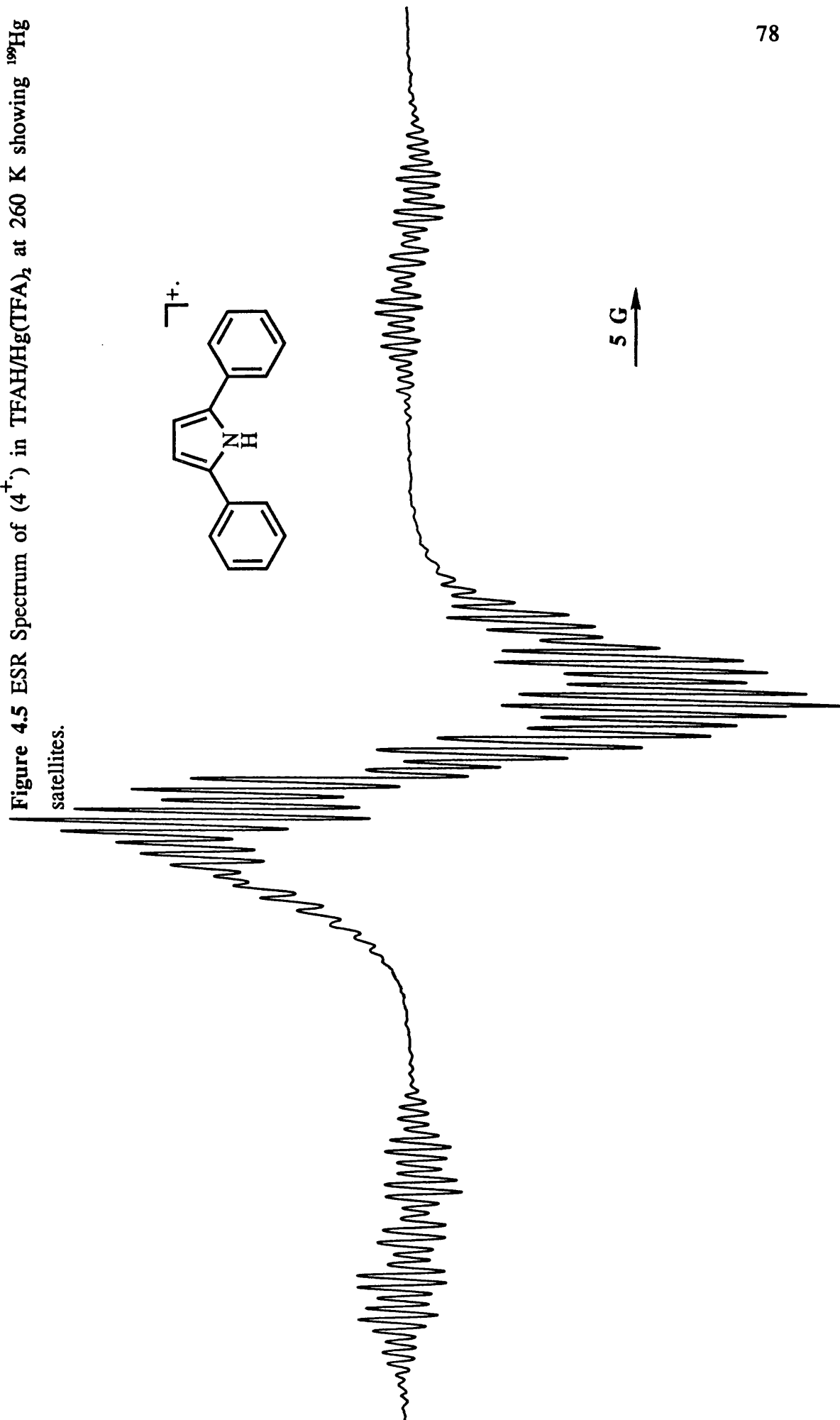
Many arene radical cations form complexes with their progenitors,  $(\text{ArH})_2^+$ , in which the u.p.e. is equally shared between two parallel ring systems; there is no example reported of the equivalent intermolecular  $\pi$ -delocalisation in radical anion chemistry.

Intramolecular through-space interaction of  $\pi$ -systems of radical ions have been reported by Huber<sup>4</sup>, Gerson<sup>5</sup>, and by Ohya-Nishiguchi.<sup>6</sup> Huber and Ohya-Nishiguchi have studied the radical anions and cations of the dianthrylalkanes (5) respectively.

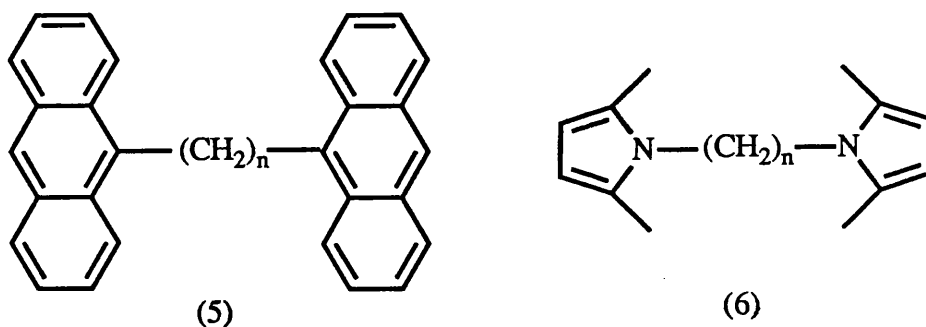
It is apparent that the synclinal face-to-face arrangement (Figure 4.6a) of the two anthracene units in the radical ions (5;  $n = 2$ ) would enforce their intramolecular through-space interaction (giving even greater interaction if synperiplanar), whereas the antiperiplanar conformation (Figure 4.6b) would not.

Huber not only modified the chain length but also varied the solvent and the counter ion. He found that the ESR spectrum of the radical anion of (5;  $n = 2$ )

Figure 4.5 ESR Spectrum of ( $4^+$ ) in TFAH/Hg(TFA)<sub>2</sub> at 260 K showing <sup>199</sup>Hg satellites.



when generated in a mixture of dimethoxyethane and hexamethylphosphorotriamide shows the u.p.e. to be delocalised over both arene units. When the radical anion was generated in methyltetrahydrofuran, which favours a tight interaction between organic ion and counter cation, the radical ion has its electron density located within one anthracene subunit.



Huber has also investigated the anions, dications, and trianions of anthrylalkanes by  $^1\text{H}$  and  $^{13}\text{C}$  NMR.

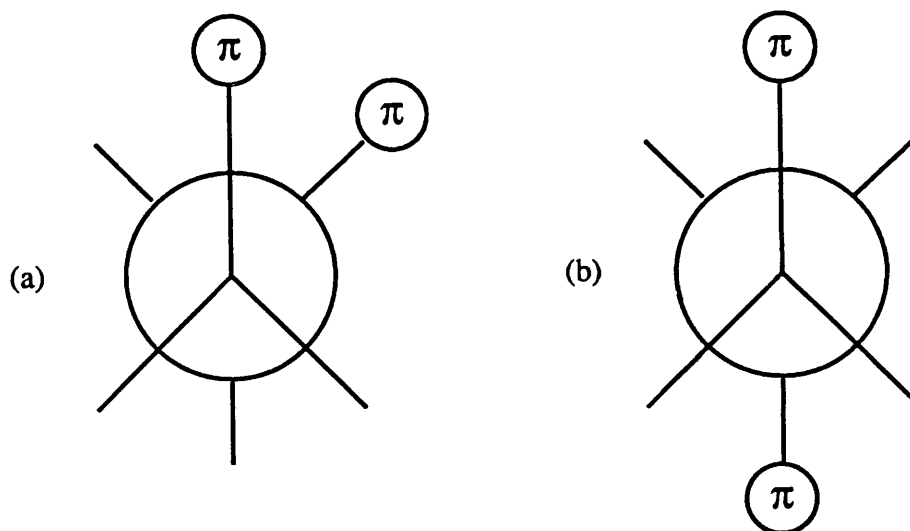
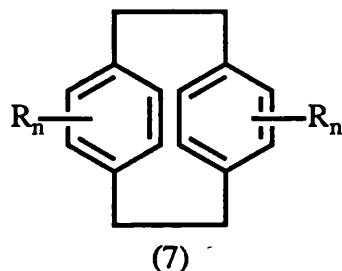


Figure 4.6 Possible conformations of dianthrylethane (5;  $n = 2$ ).



Gerson has observed the radical ions of a series of cyclophanes, finding for example that both radical cation and anion of [2.2]paracyclophane or its derivatives (7) are delocalised.



Ohya-Nishiguchi's ESR study of the radical cations of the bi-9-anthracenyl (5) derivatives showed that the u.p.e. was localised on one anthracene unit when  $n = 1, 2,$  or  $4$  but delocalised over both units when  $n = 3$ . Davies and coworkers report that in the oligomethylene-bis(2,5-dimethylpyrroles) (6;  $n = 2$  or  $3$ ) the ESR spectra of their radical cations show spin density localized in one pyrrole unit.

We have prepared similar compounds (6;  $n = 0, 1,$  and  $4$ ). Where two pyrrole units are linked by a butane chain the u.p.e. of the radical cation is localised on one ring. The ESR spectrum of ( $6^+$ ;  $n = 4$ ) is shown in Figure 4.7.

No ESR observable radical cation of methylenebis-(2,5-dimethylpyrrole) (6;  $n = 1$ ) was generated with the standard oxidizing reagents [TFAH/Tl(TFA)<sub>3</sub>, TFAH/Hg(TFA)<sub>2</sub>, TFAH/H<sub>2</sub>SO<sub>4</sub>, H<sub>2</sub>SO<sub>4</sub>, or AlCl<sub>3</sub>/CH<sub>2</sub>Cl<sub>2</sub>] with or without varying degrees of photolysis. A reason for this failure could be the distortion of  $sp^2$  hybridized atoms towards  $sp^3$  due to steric factors (see discussion on pyrrolophanes). The oligomethylene-2,5-dimethyldipyrrole (6;  $n = 2, 3,$  or  $4$ ) radical cation may not form dimer species possibly because the steric interaction by the 2,5-dimethyl substituents prevents  $\pi$ -orbital delocalization between the two aromatic units (an apparent through-space intramolecular delocalisation is discussed for the 1-phenyl-2,3,4,5-tetramethylarsole radical cation in Section 5.2). The 2,2',5,5'-tetramethylbi(*N*-pyrrolyl) (6;  $n = 0$ ) radical cation is discussed later.

#### 4.2.3 *N*-Phalimidopyrrole

The ESR spectrum of the radical cation (Figure 4.8) generated from the 1-phalimido-2,5-dimethylpyrrole (8) shows the u.p.e. localised in the pyrrole ring

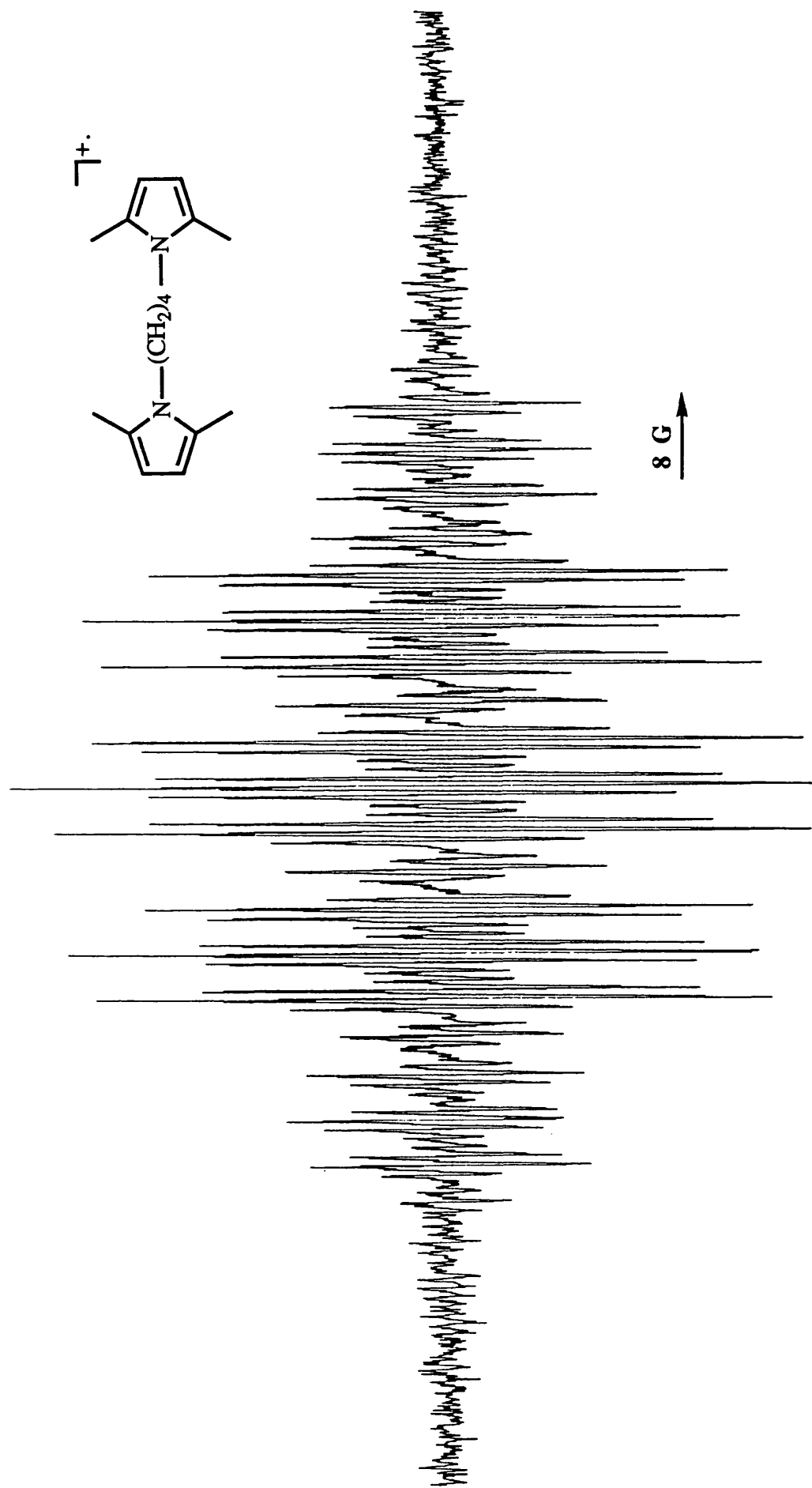


Figure 4.7 ESR Spectrum of  $(6^+; n = 4)$  in TFAH/PI(TFA)<sub>3</sub> at 260 K.

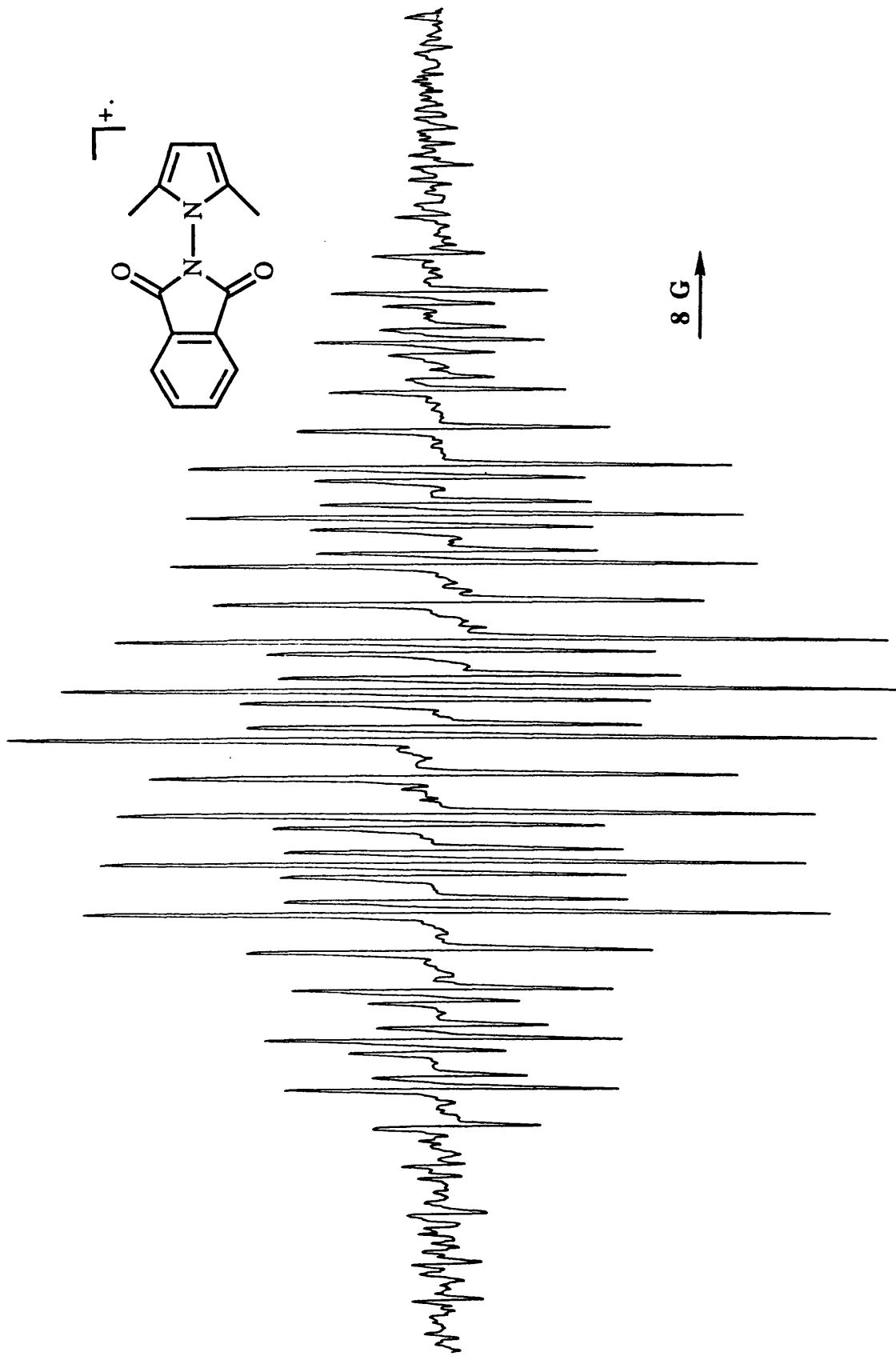
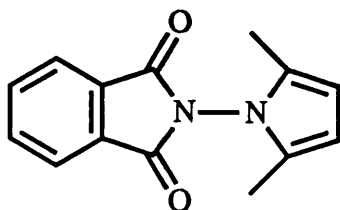


Figure 4.8 ESR Spectrum of  $(8^+)$  in TFAH/TI(TFA)<sub>3</sub> at 260 K.

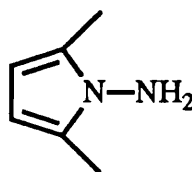
with no coupling from the phalimide moiety. This would be expected if the two units were orthogonal, because of the high IP of phthalimide.

#### 4.2.4 *N*-Aminopyrrole

The ESR spectrum (Figure 4.9) of the radical cation of 1-amino-pyrrole (9) shows the coupling constants  $a(6H)$  16.10,  $a(2H)$  3.60,  $a(N)$  4.75,  $a(N)$  1.75, and  $a(2H)$  1.75,  $g$  2.0025; this indicates that the SOMO has the form  $\psi_*$ .



(8)



(9)

#### 4.2.5 *N*-Arylpyrroles

The radical cation of *p*-phenylene-bis(2,5-dimethylpyrrole) (10; R = Me, R' = H) shows an ESR spectrum (Figure 4.10) with spin density located on one pyrrole unit. We have optimised the AM1/UHF geometry of (10<sup>+</sup>; R = Me, R' = H) which suggests that the rings are orthogonal, with the SOMO being located on the pyrrole ring, and of the form  $\psi_*$ .

Photon electron spectra and dipole moment data have been interpreted to imply that if the two rings are assumed to be orthogonal in *N*-(2,6-dimethylphenyl)-2,5-dimethylpyrrole, then there is a dihedral angle between the two rings in *N*-phenyl-2,5-dimethylpyrrole of about 60.<sup>07,8</sup> D. A. Tocher of this department determined the X-ray crystal structure of (10; R = Me, R' = H) finding that in the solid state the rings are strictly orthogonal (Figure 4.11 and Table 4.2).

If the rings are assumed to be orthogonal in solution then a comparison of the IP of 2,5-dimethylpyrrole (7.69 eV) and benzene (9.27 eV) would suggest that the u.p.e. would be localised in the pyrrole ring.

In the tetramethyl-*p*-phenylene-bis(2,5-dimethylpyrrole) (10; R = R' = Me) radical cation the u.p.e. occupies the  $\psi_*$  MO of the pyrrole ring, the tetra-alkylation not reducing the IP of the *p*-phenylene group below that of the 2,5-dimethylpyrrole. The ESR spectrum of (10<sup>+</sup>; R = R' = Me) shows second order<sup>9</sup> effects (Figure 4.12).

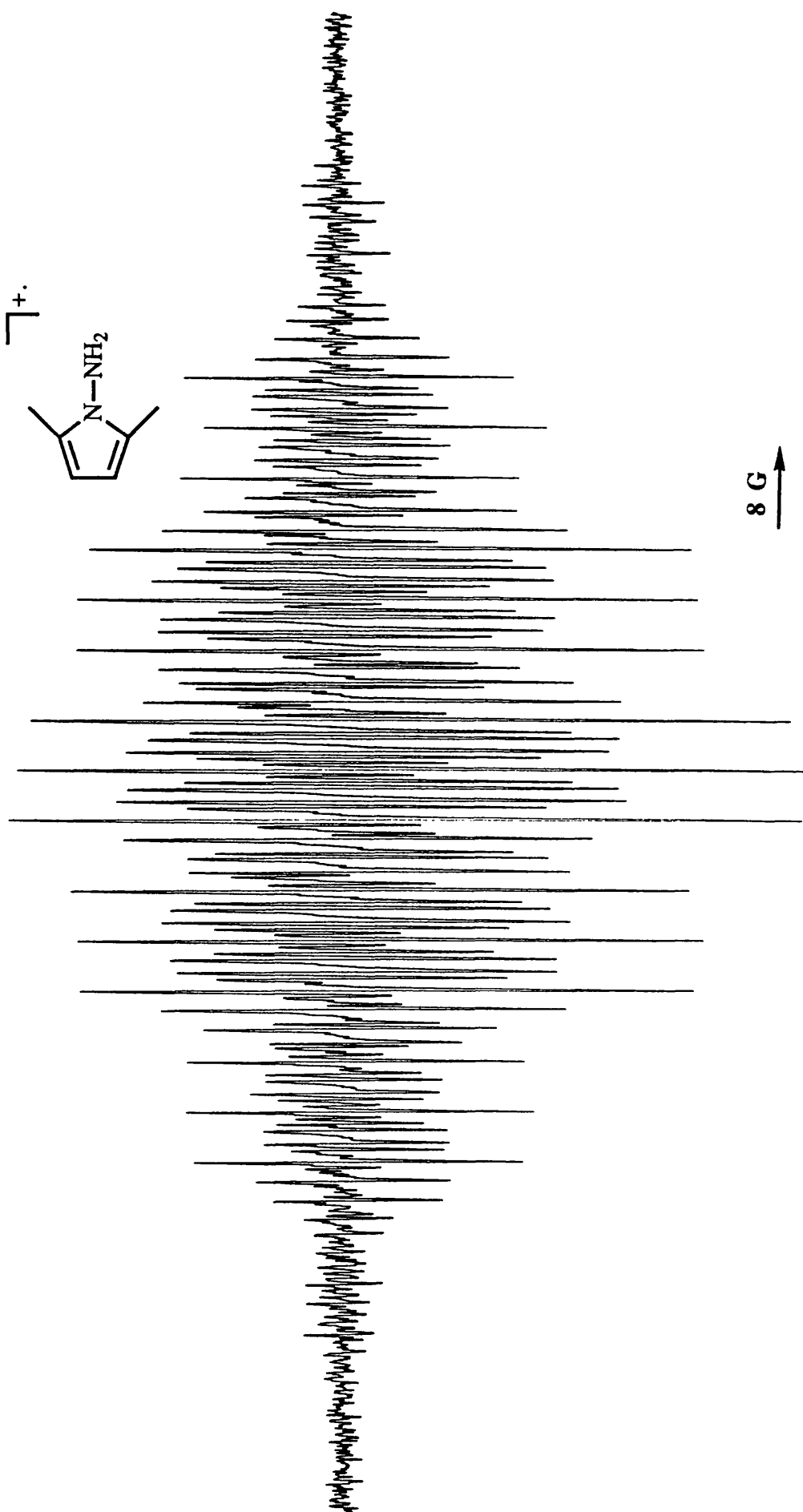
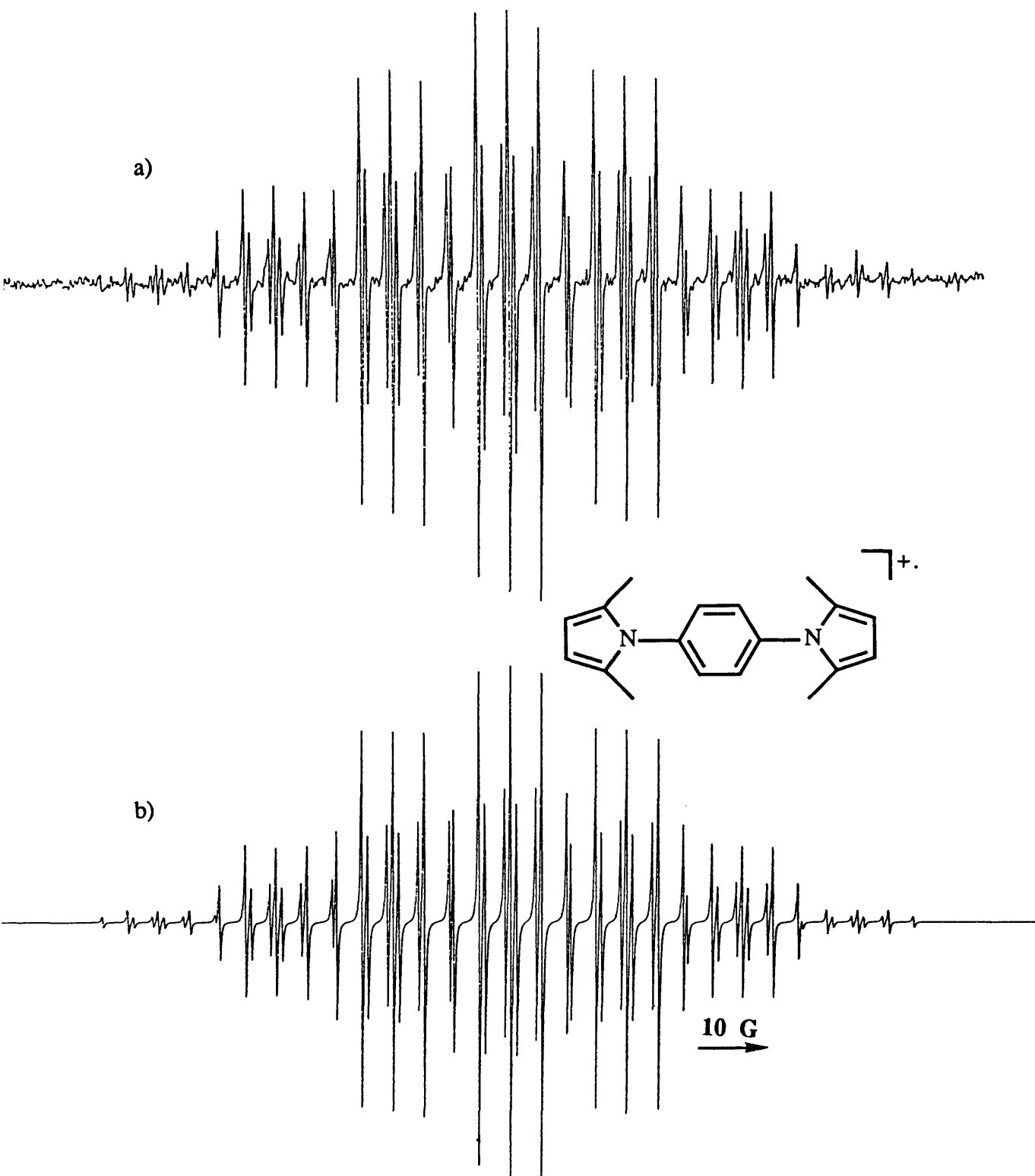


Figure 4.9 ESR Spectrum of  $(9^+)$  in TFAH/TI(TFA)<sub>3</sub> at 260 K.



**Figure 4.10** (a) ESR Spectrum of  $(10^+)$ ;  $R = \text{Me}$ ,  $R' = \text{H}$  in TFAH/Tl(TFA)<sub>3</sub> at 260 K. (b) Computer simulation of (a).

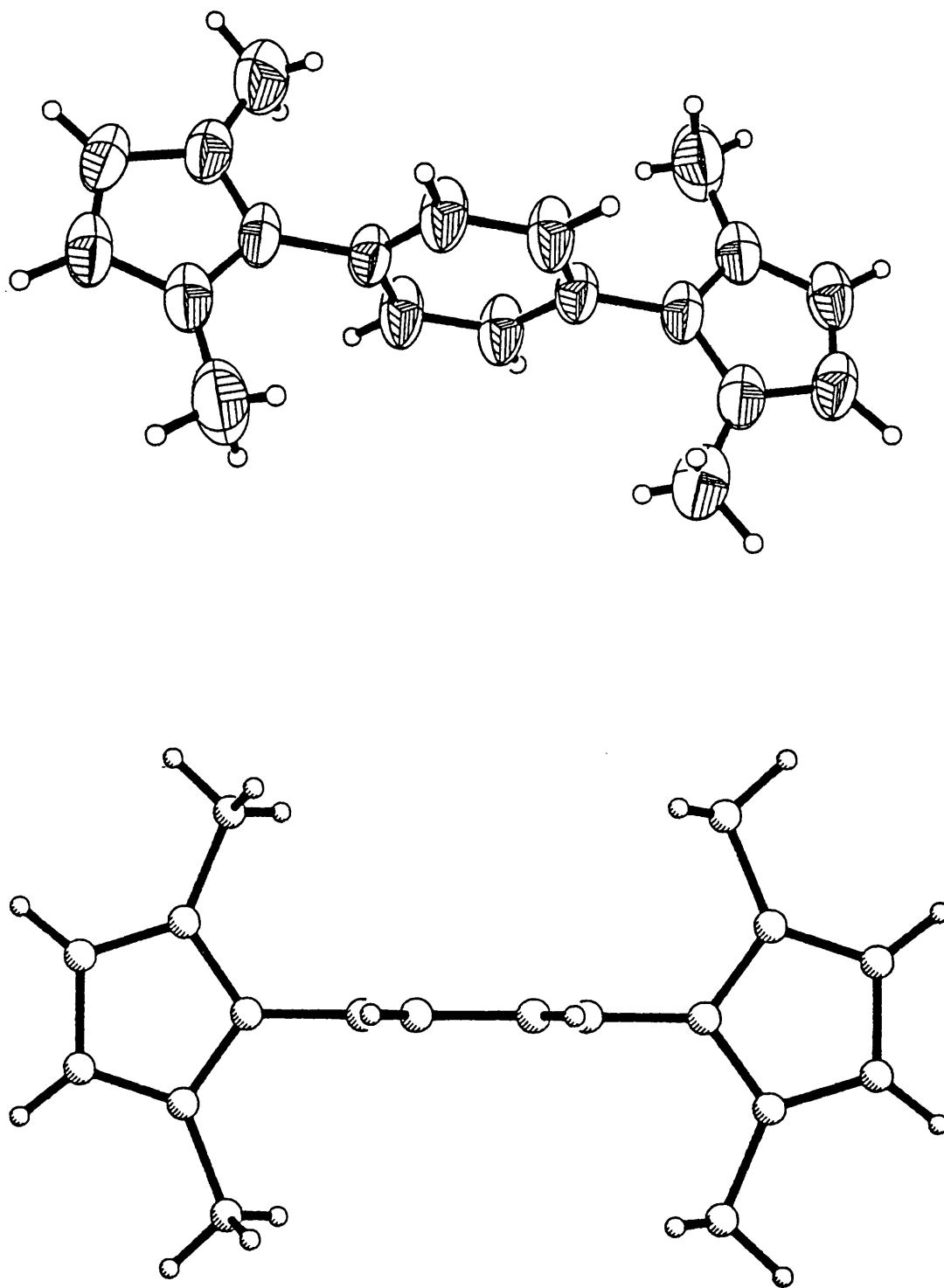
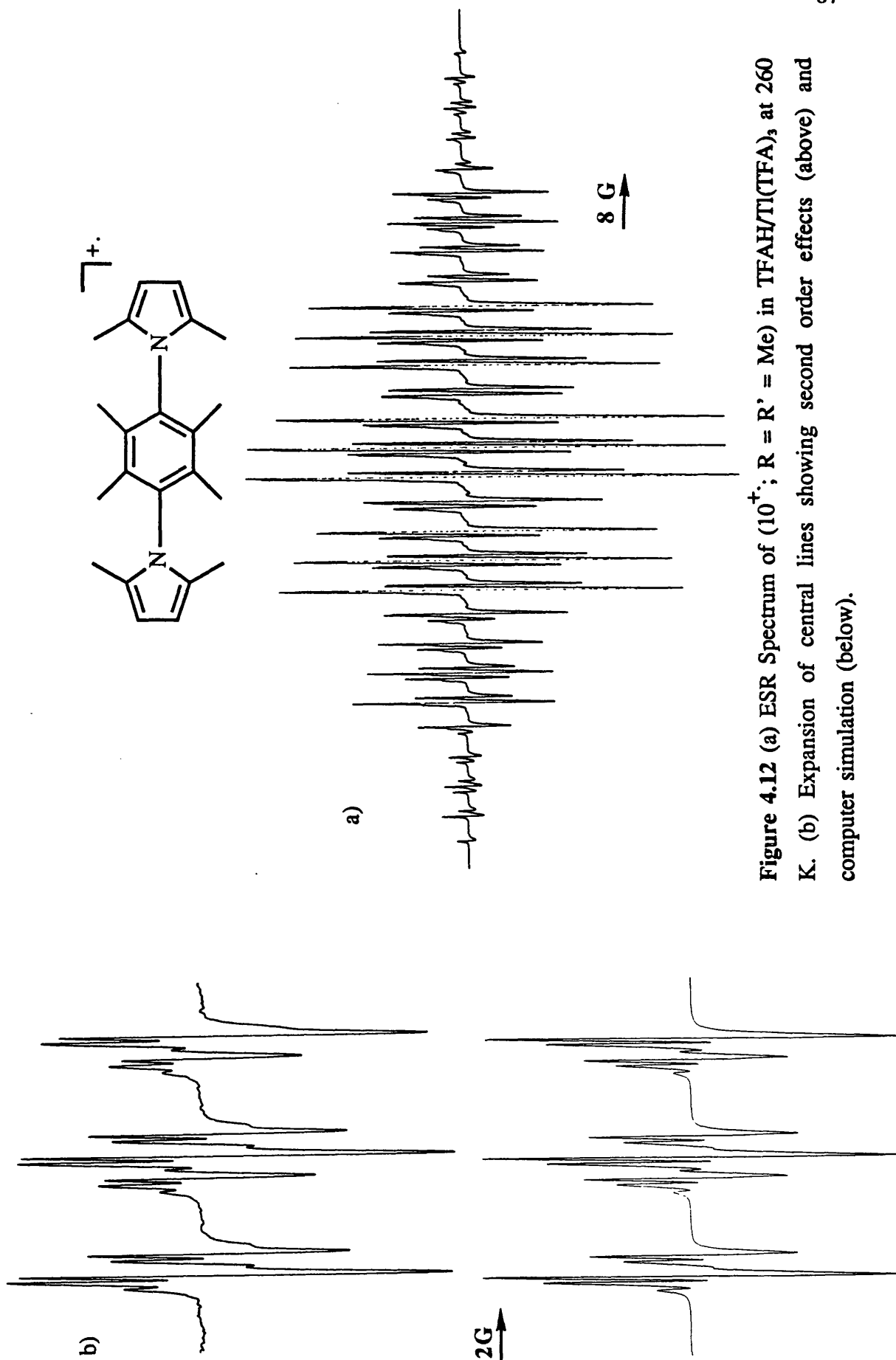
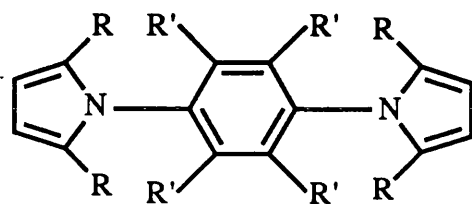


Figure 4.11 The structure of (10 ; R = Me, R' = H) (two perspectives).

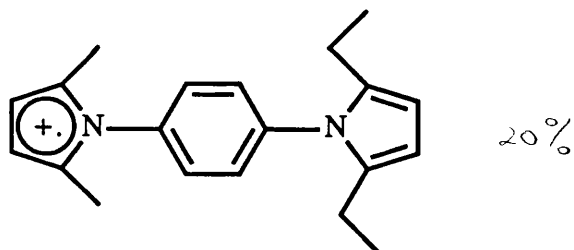




*p*-Phenylene(*N*-2,5-dimethylpyrrole)(*N*-2,5-diethylpyrrole) gives a radical cation which again shows no ESR coupling to the phenylene protons. The spectrum can now be analysed as a superposition of the spectra of the radical cations of the dimethylpyrrole (11) and diethylpyrrole (12) moieties in the ratio of 20:80 (Figure 4.13). The Boltzmann equation applied to this ratio at ca. 260 K implies that a pair of methyl groups are more effective than ethyl groups in destabilizing the SOMO, by ca. 3.0 kJ mol<sup>-1</sup>.

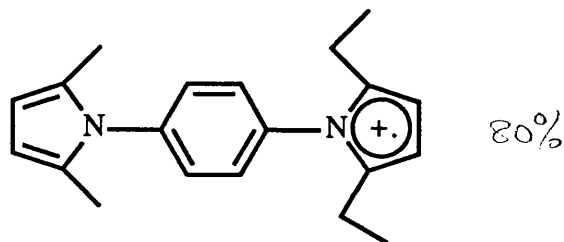


(10)



(11)

20%



(12)

80%

In the 2,5-diethyl-1,3,5-trimethylcyclopentadienyl radical, electron release by the methyl and ethyl groups is in intramolecular rather than intermolecular

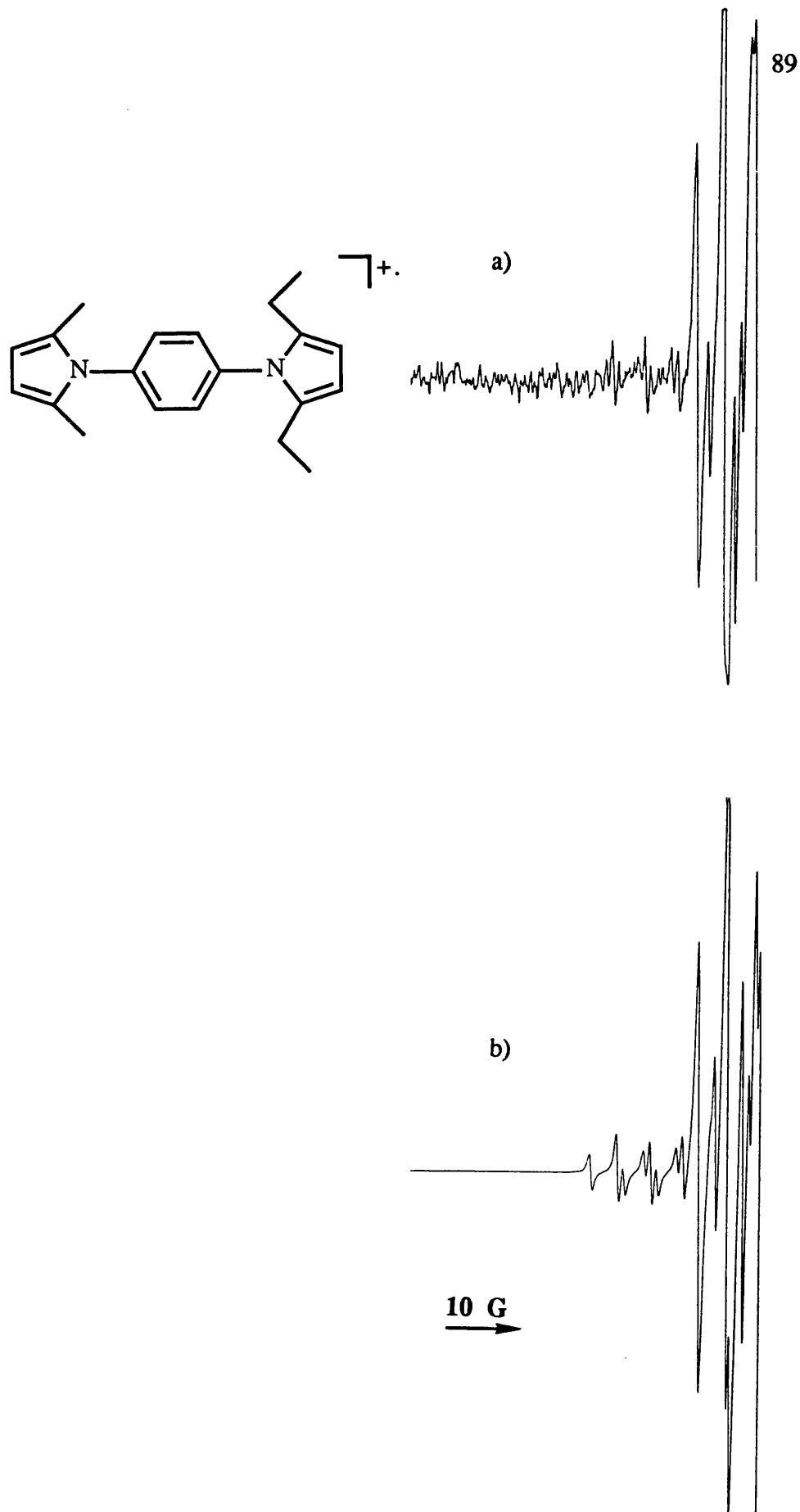
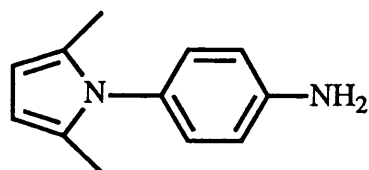


**Figure 4.13** (a) Wing line of the ESR spectra of (11 and 12) in TFAH/Tl(TFA)<sub>3</sub> at 260 K. (b) Computer simulation of (a) with contributions of (11) (*ca.* 20%) and (12) (*ca.* 80%).

competition, and from an analysis of the hyperfine coupling constants Davies *et al.*<sup>10,11</sup> have concluded that in this situation, the differential effect in the same sense between methyl and ethyl groups was 1.8 kJ mol<sup>-1</sup>. It may be that the radical cation evokes a larger hyperconjugative electron release from the alkyl substituents than does the neutral radical.

The *p*-phenylene-bis(*N*-2,5-diethylpyrrole) (10; R = Et, R' = H) radical cation exhibits an ESR spectrum (Figure 4.14) where the u.p.e. resides in one ring.

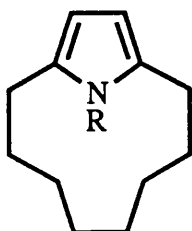
The conjugation of one amine group with a benzene ring does not lower its IP below that of the 2,5-dimethylpyrrole (IP of aniline 7.71 eV) as was demonstrated when we generated the radical cation (Figure 4.15) of 1-amino-4(*N*-2,5-dimethylpyrrole)benzene (13); the spin density was located wholly on the pyrrole unit. The IP of the  $\phi$ -NH<sub>2</sub> substituent may be higher than that of aniline. If the pyrrole and arene rings are orthogonal the mesomeric electron release by the pyrrole nitrogen lone pair (even though involved in the pyrrole aromaticity) could not occur to lower the IP the arene group. On the other hand, the electronegativity of the pyrrole nitrogen would increase the IP of the arene substituent by inductive electron attraction.



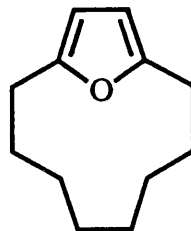
(13)

#### 4.2.6 Pyrrolophanes and Some Related Compounds

We have failed to observe any ESR spectra of the radical cations of the [8](2,5)pyrrolophanes (14; R = H or  $\phi$ ) or the [8](2,5)furanophane (15). All the standard oxidizing reagents have been used as in trying to generate ( $6^+$ ; n = 1), and also SbCl<sub>5</sub>/CH<sub>2</sub>Cl<sub>2</sub> and H<sub>2</sub>SO<sub>4</sub>/SO<sub>2</sub>.

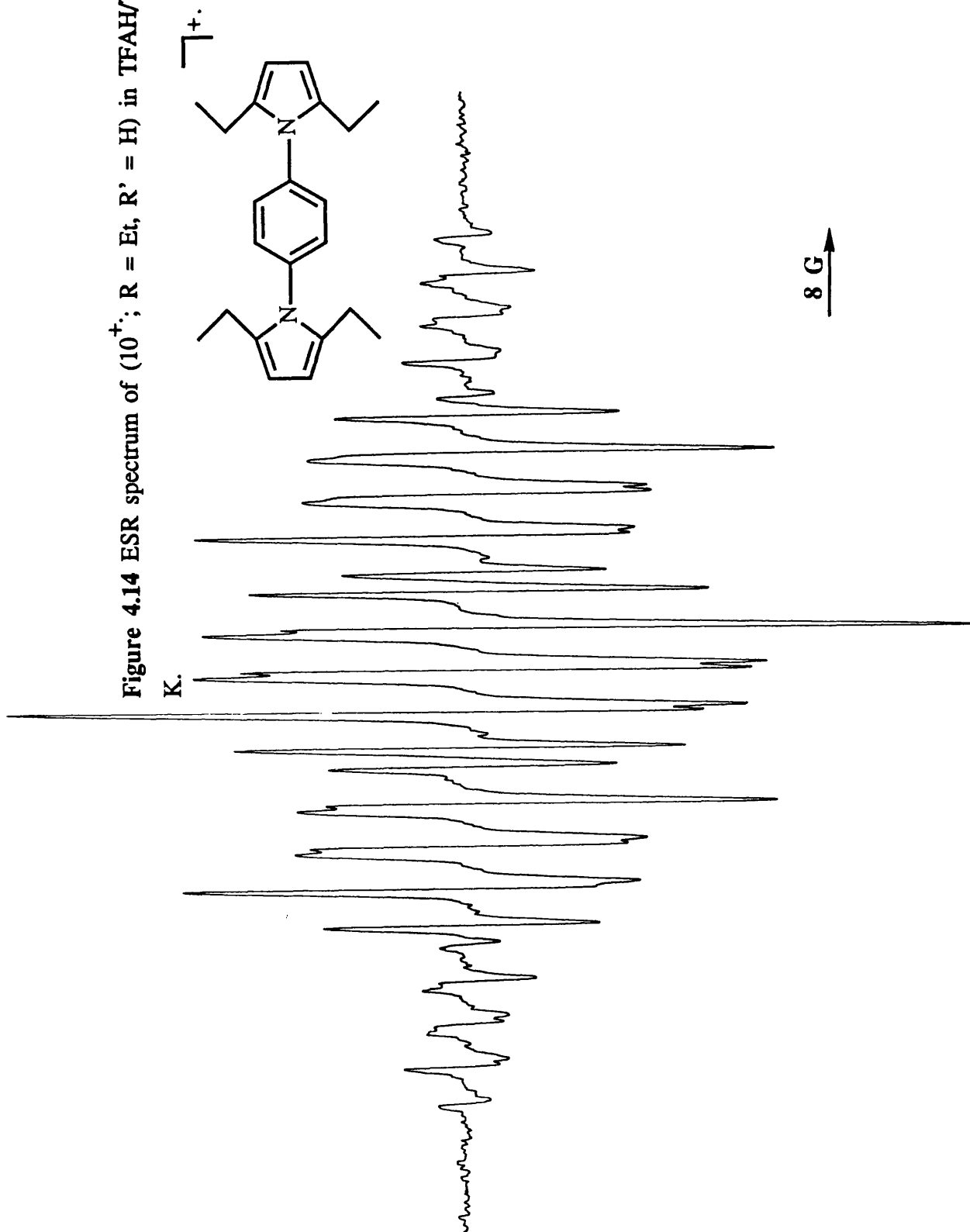


(14)



(15)

Figure 4.14 ESR spectrum of  $(10^+)$ ; R = Et, R' = H in TFAH/Tl(TFA)<sub>3</sub> at 260



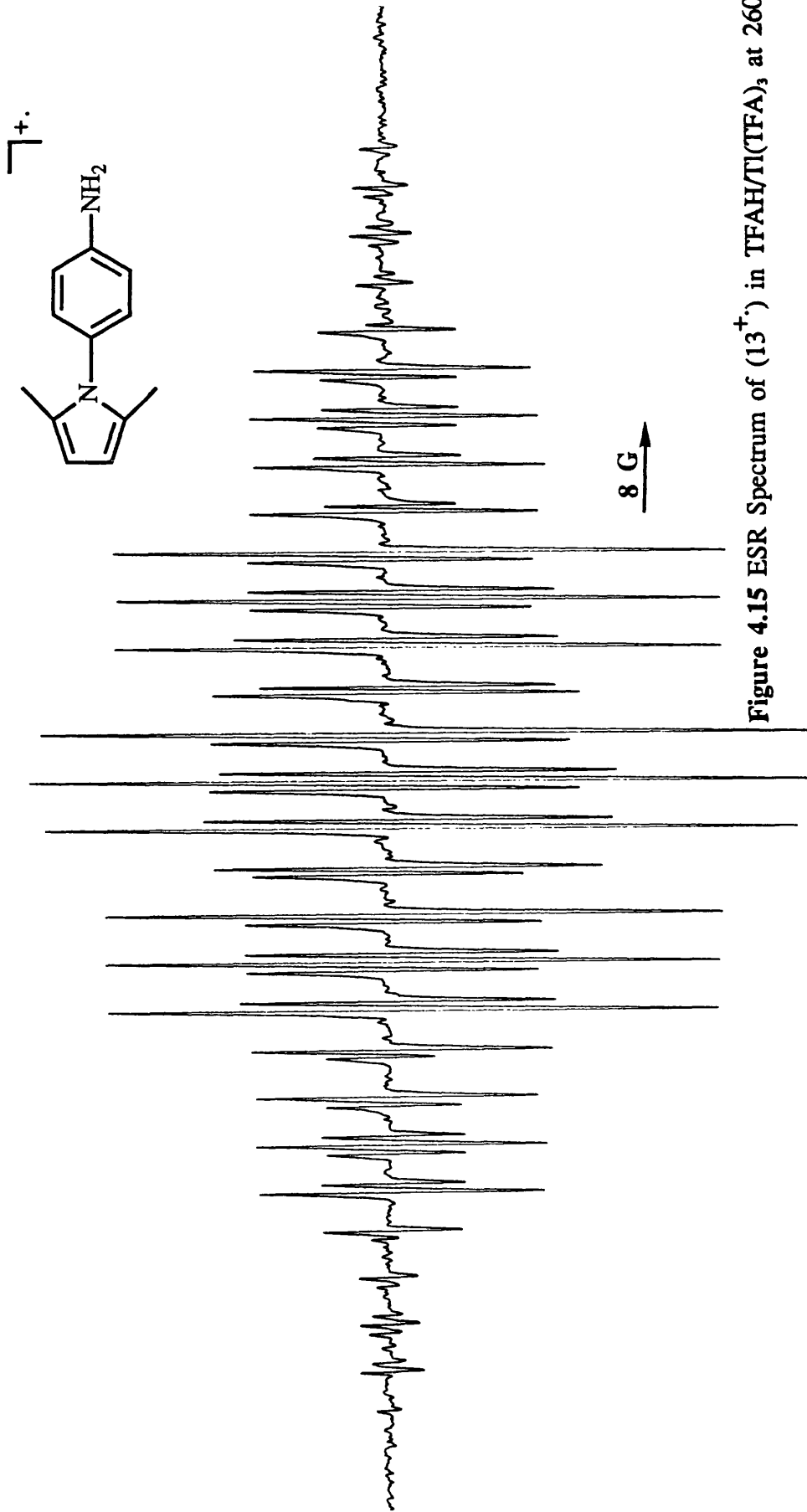
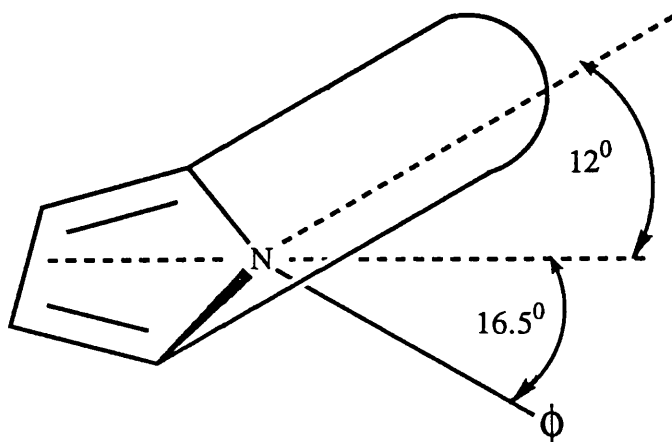


Figure 4.15 ESR Spectrum of  $(13^+)$  in TFAH/Tl(TFA)<sub>3</sub> at 260 K.

The pyrrolophanes and furanophane are reported to have a bathochromic shift of the  $\pi \rightarrow \pi^*$  absorption band compared with that corresponding 2,5-dimethylpyrrole and furan.<sup>12,13</sup> This has been taken as evidence for distortion from planarity of the pyrrole rings. D. C. Povey and G. W. Smith of Surrey University determined the crystal structure of (14; R =  $\phi$ ). The *N*-phenyl bond is bent by  $16.5^\circ$  out of the plane of the pyrrole ring, and the  $\alpha$ -methylene groups of the bridge are bent away from the ring by  $12^\circ$  in the opposite direction (Figure 4.16).



**Figure 4.16** The structure of (14; R =  $\phi$ ).

The  $\pi$ -electron system may thus resemble that of an isolated butadiene rather than a pyrrole, and Davies and coworkers find that at least tetra-alkylation of the terminal positions of butadiene is required before it is possible to oxidize butadienes to their ESR-observable radical cations by chemical methods.

#### 4.2.7 Bis(*N*-pyrrolyl)

The bis(*N*-pyrrolyl) radical cation (16) is isoelectronic with the fulvalene radical anion<sup>14</sup> (17) which has a SOMO which can be regarded as an out of phase combination of two  $\psi_r$  MO's as shown in Figure 4.17.

In pyrrole however, the  $\psi_r$  MO is lower in energy than the  $\psi_a$  MO and *ab initio* calculations<sup>15,16</sup> suggest that the HOMO of bipyrrrolyl can be represented as a combination of two  $\psi_r$  MO's to form (18).

The planar form of bipyrrrolyl is calculated to be *ca.* 5 (STO-3G) or 20 (4-31G) kcal mol<sup>-1</sup> less stable than the orthogonal form. This is in accord with the

photoelectron spectrum<sup>17</sup> of the 2,5-dimethylbipyrrolyl which resembles a superposition of the photoelectron spectra of pyrrole and 2,5-dimethylpyrrole, implying very little interaction between the two rings.

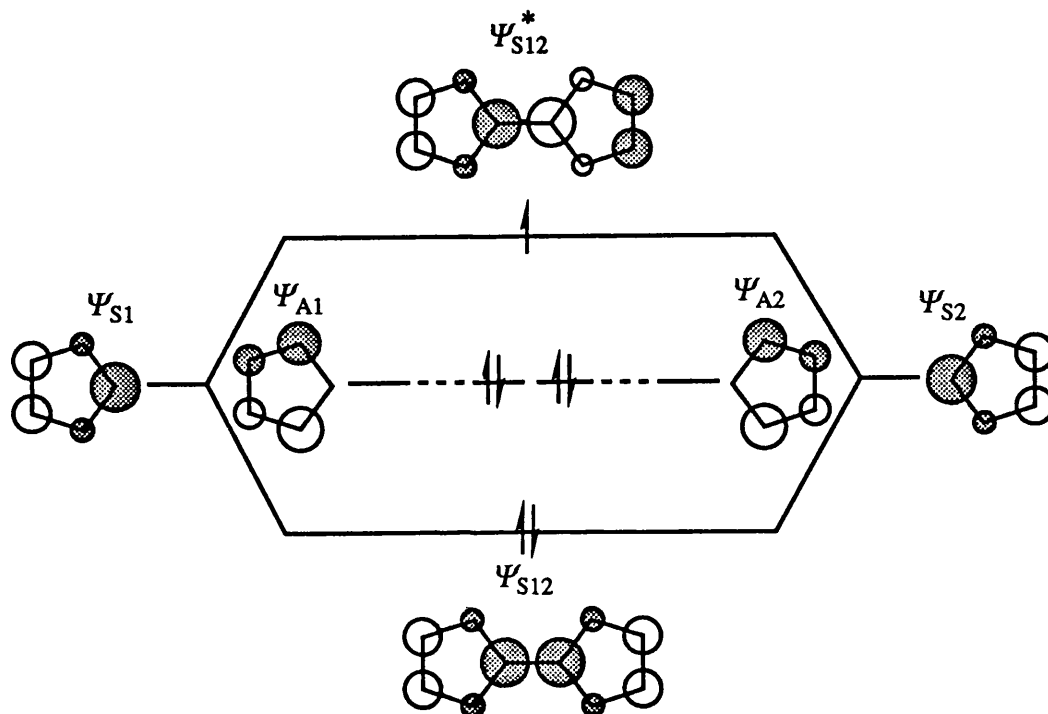
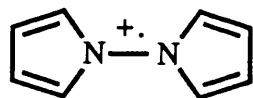
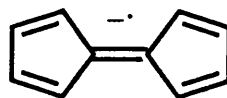


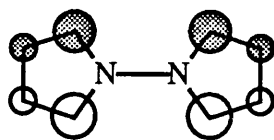
Figure 4.17 The perturbation approach as applied to the fulvalene radical anion MO.



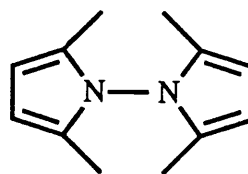
(16)



(17)



(18)



(19)

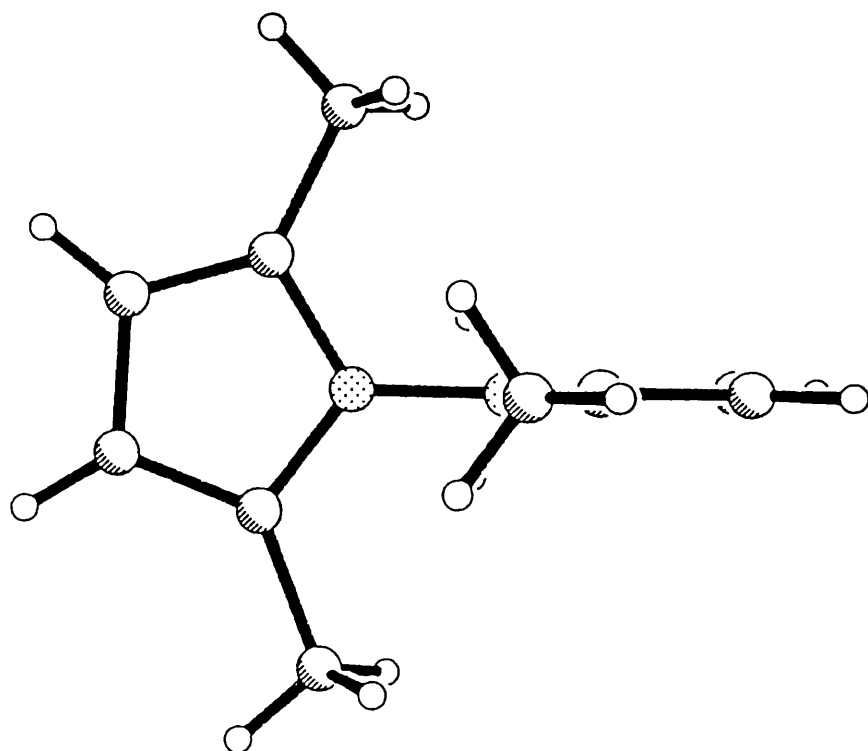
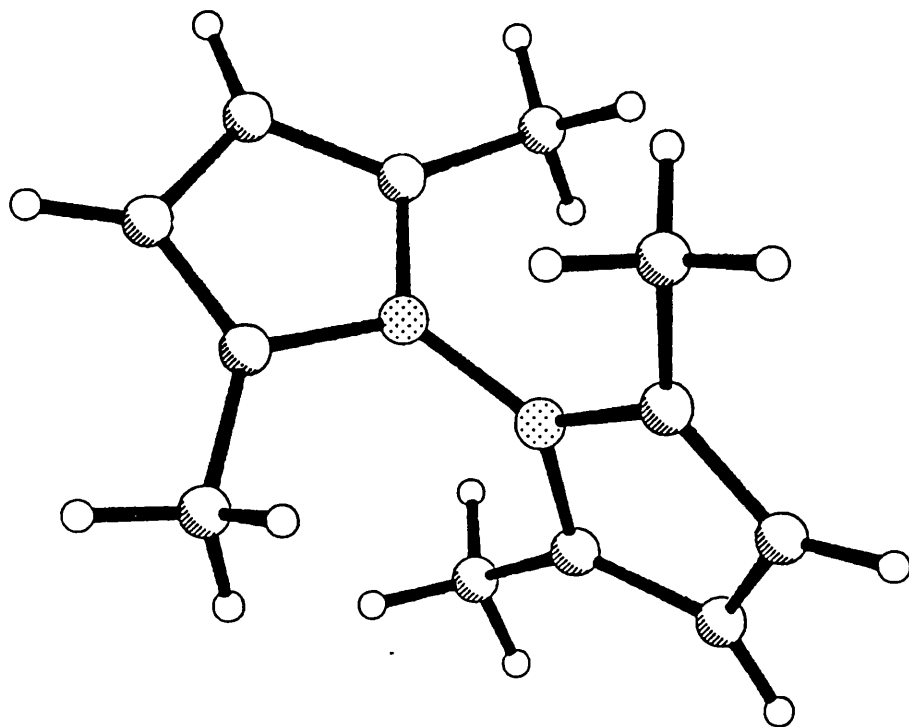
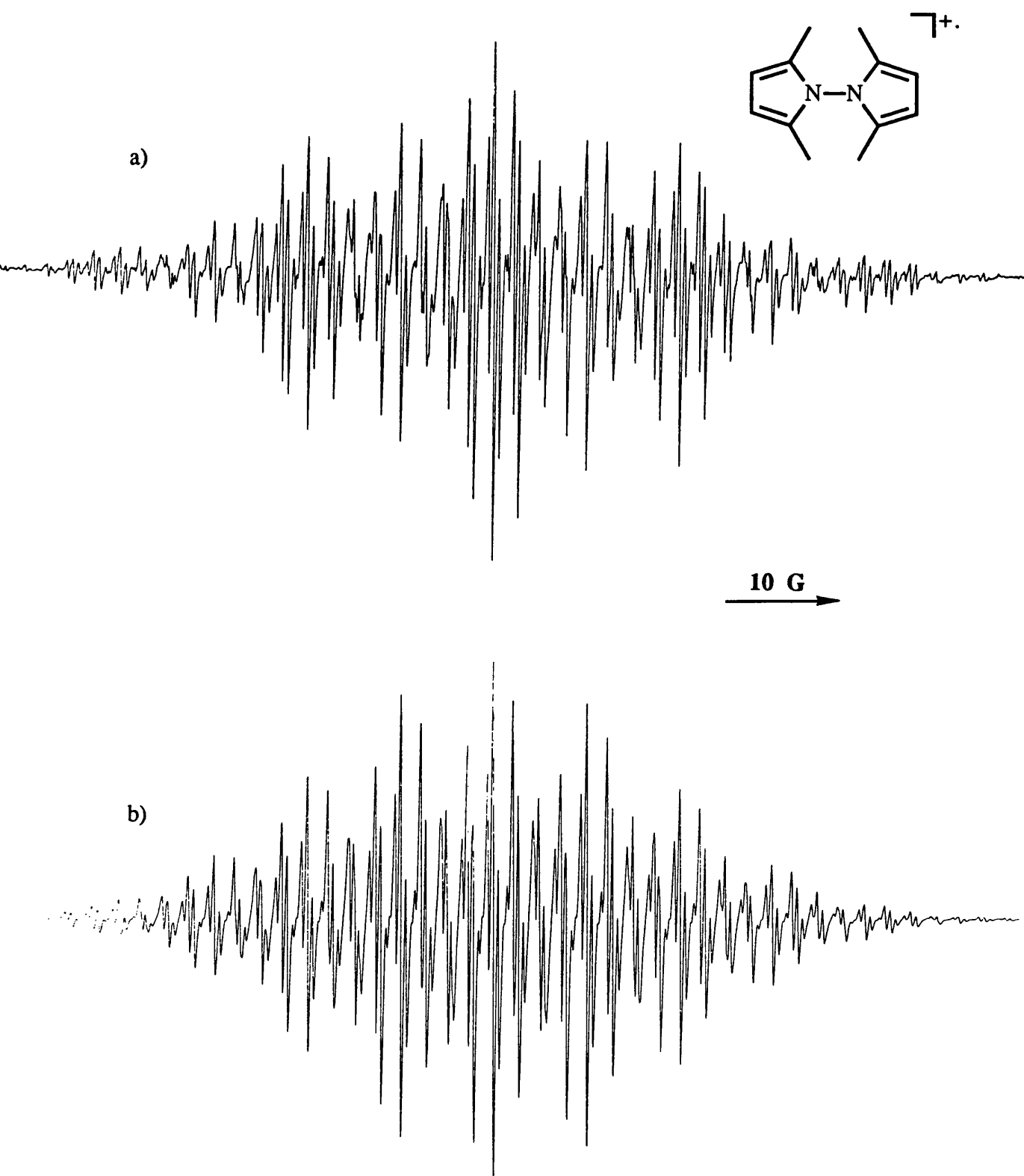


Figure 4.18 The structure of (19) (two perspectives).



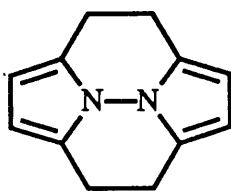


**Figure 4.19** (a) ESR Spectrum of ( $19^+$ ) in TFAH/Hg(TFA)<sub>2</sub> at 260 K. (b) Computer simulation of (a).

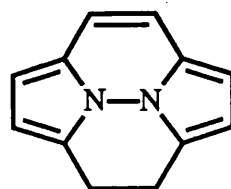
We have determined the X-ray structures of 2,2',5,5'-tetramethylbi-(*N*-pyrrolyl) (19) (Figure 4.18 and Table 4.2) and in the solid state the rings are indeed orthogonal. The orthogonality could be a result of steric interaction of the methyl groups. The ESR spectrum of (19<sup>+</sup>) (Figure 4.19) showed coupling to all magnetically active nuclei [ $a(12\text{H})$  8.35,  $a(4\text{H})$  1.79, and  $a(2\text{N})$  2.28 G,  $g$  2.0028] and is independent of temperature over the range 200-270 K. This is in accord with the u.p.e. being shared equally between two 2,5-dimethylpyrrole units in the  $\psi_s$  configuration.

#### 4.2.8 Diazapyracyclenes

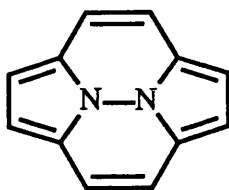
As the 2,2',5,5'-tetramethylbi-(*N*-pyrrolyl) has an orthogonal structure, we were interested in investigating a bipyrrrolyl in which the rings are held coplanar.



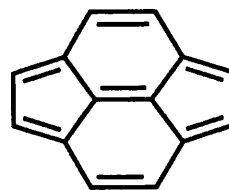
(20)



(21)



(22)



(23)

3,4,7,7-Tetrahydro-8b,8c-diazapyracyclene (20) appeared to offer such a possibility; unfortunately we were unable to observe its radical cation (all oxidizing reagents mentioned in this chapter were used). Because of this failure we determined the X-ray crystal structure of (20) (Figure 4.20 and Table 4.2). One possibility for the inability to observe (20<sup>+</sup>) by ESR spectroscopy could be that the C-H bonds of the ethylene bridges are held so that they subtend a small dihedral angle with the axis of the  $\pi$ -system, which might lead to rapid loss of a

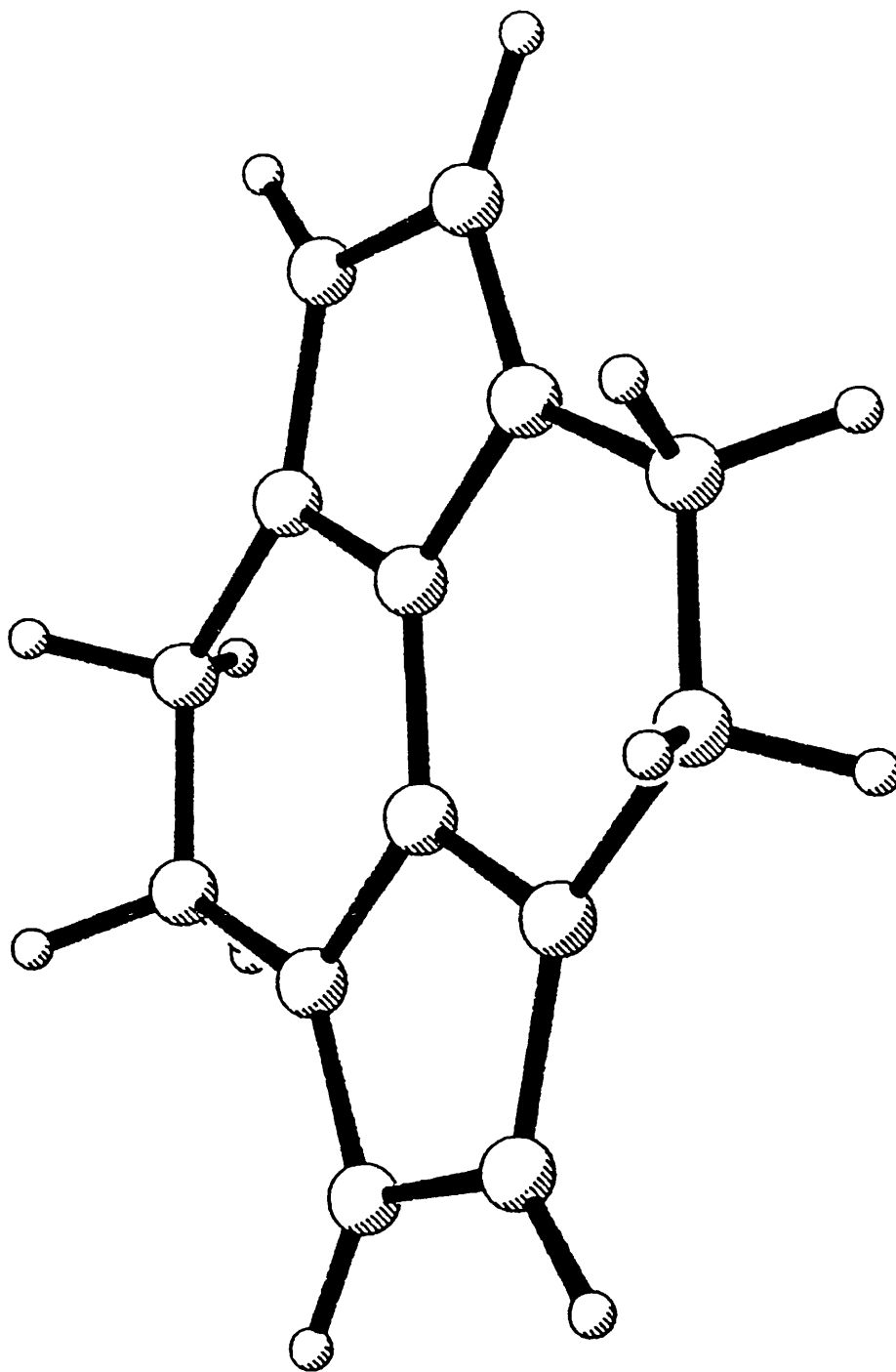
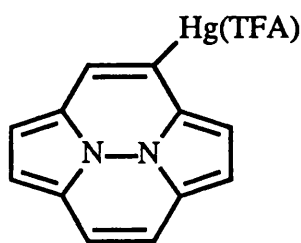


Figure 4.20 The structure of (20).

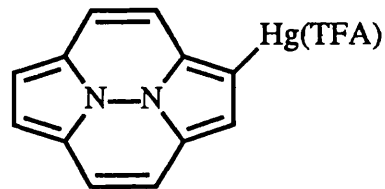
proton from the radical cation. Work-up of a solution of (20) in TFAH/Hg(TFA)<sub>2</sub> gave the tetrahydro compound (20) and the dihydro compound (21) in approximately equal amounts. It is notable that no ESR spectrum which might be assigned to the radical cation of (20) could be observed, and that no 8b,8c-diazapyracyclene (22) was formed by the loss of protons from the dihydro compound (21). We could not oxidize an authentic sample of (21) by any of the aforementioned oxidants to enable us to observe its ESR spectrum.

However 8b,8c-diazapyracyclene itself (22) readily afforded a strong ESR spectrum of (22<sup>+</sup>) (Figure 4.21) (much stronger with Hg<sup>2+</sup> as oxidant than with Tl<sup>3+</sup>) which consisted of 5 x 5 x 5 lines. The *a*(2N) coupling was assigned by examination of the outer lines of the spectrum where the appropriate 1:2:3:2:1 intensity of peaks could be observed [*a*(2N) 1.77 G]. The proton coupling constants *a*(4H) 1.77 G and *a*(4H) 2.44 G we tentively assign, on the basis of an INDO calculation, to the 1, 2, 5, and 6 positions and 3, 4, 7 and 8 positions respectively (Table 4.1). The radical anion of pyracyclene<sup>18</sup> (23), which is isoelectronic with the radical cation of diazapyracyclene (22), shows a similar electron distribution, with *a*(4H) 2.52, and *a*(4H) 1.88 G. It is interesting that attempts to generate the radical cation of pyracyclene have been unsuccessful.<sup>19</sup>

When the radical cation of the 8b,8c-diazapyracyclene is generated in TFAH/Hg(TFA)<sub>2</sub>, mercurideprotonation is observed (Figure 4.22). The satellites due to <sup>199</sup>Hg appear either side of the central feature of the main ESR spectrum, with *a*(<sup>199</sup>Hg) 48 G.



(24)



(25)

Application of the Breit-Rabbi equation to the field values of the <sup>199</sup>Hg satellites gives the central field of the mercuriated species which has *g* 2.0004. This *g*-value is, as expected, lower than that of the unmercuriated species (*g* 2.0027). As

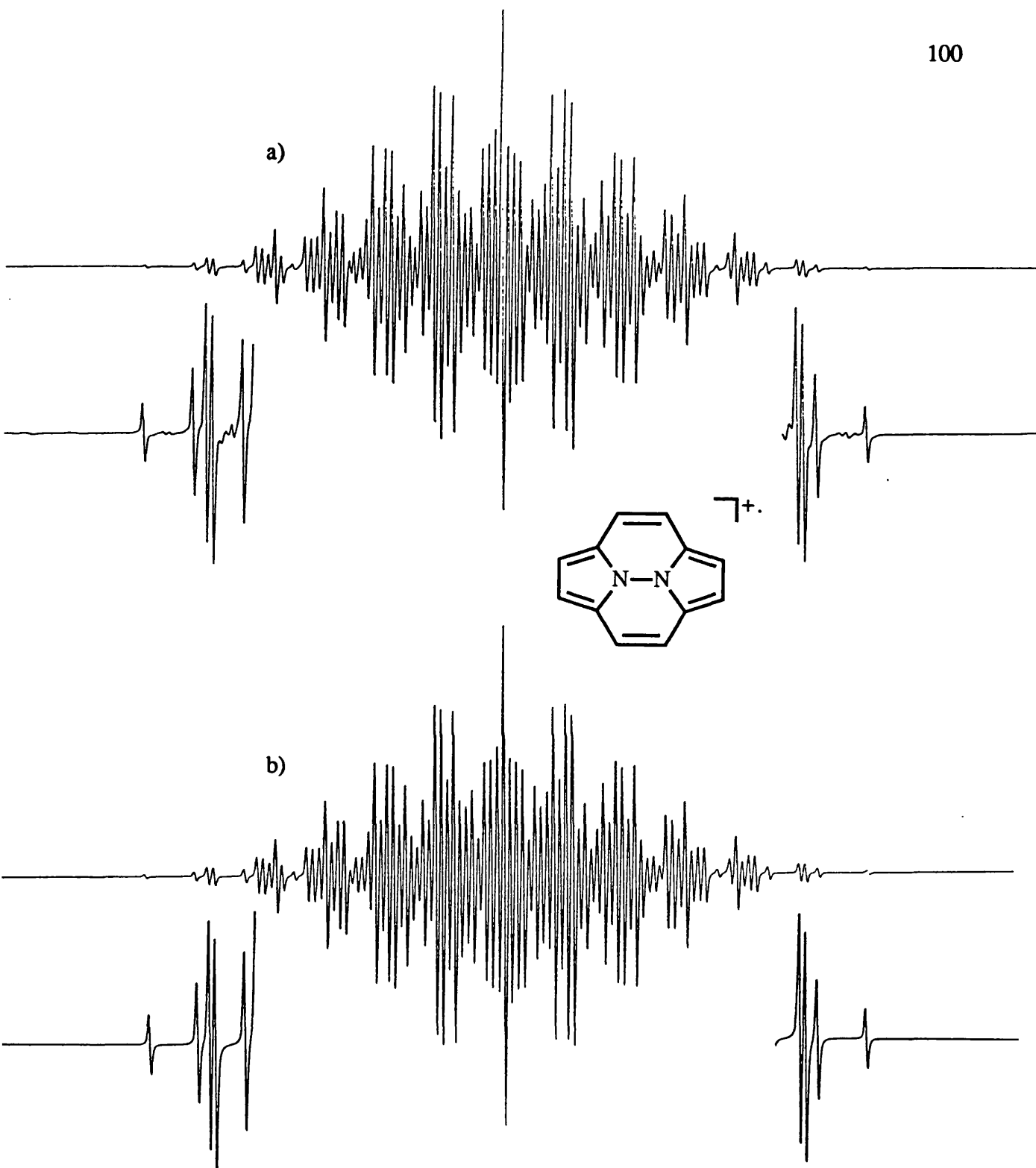


**Figure 4.21** (a) ESR Spectrum of  $(22^{2+})$  in TFAH/Hg(TFA)<sub>2</sub> at 260 K. (b) Computer simulation of (a).

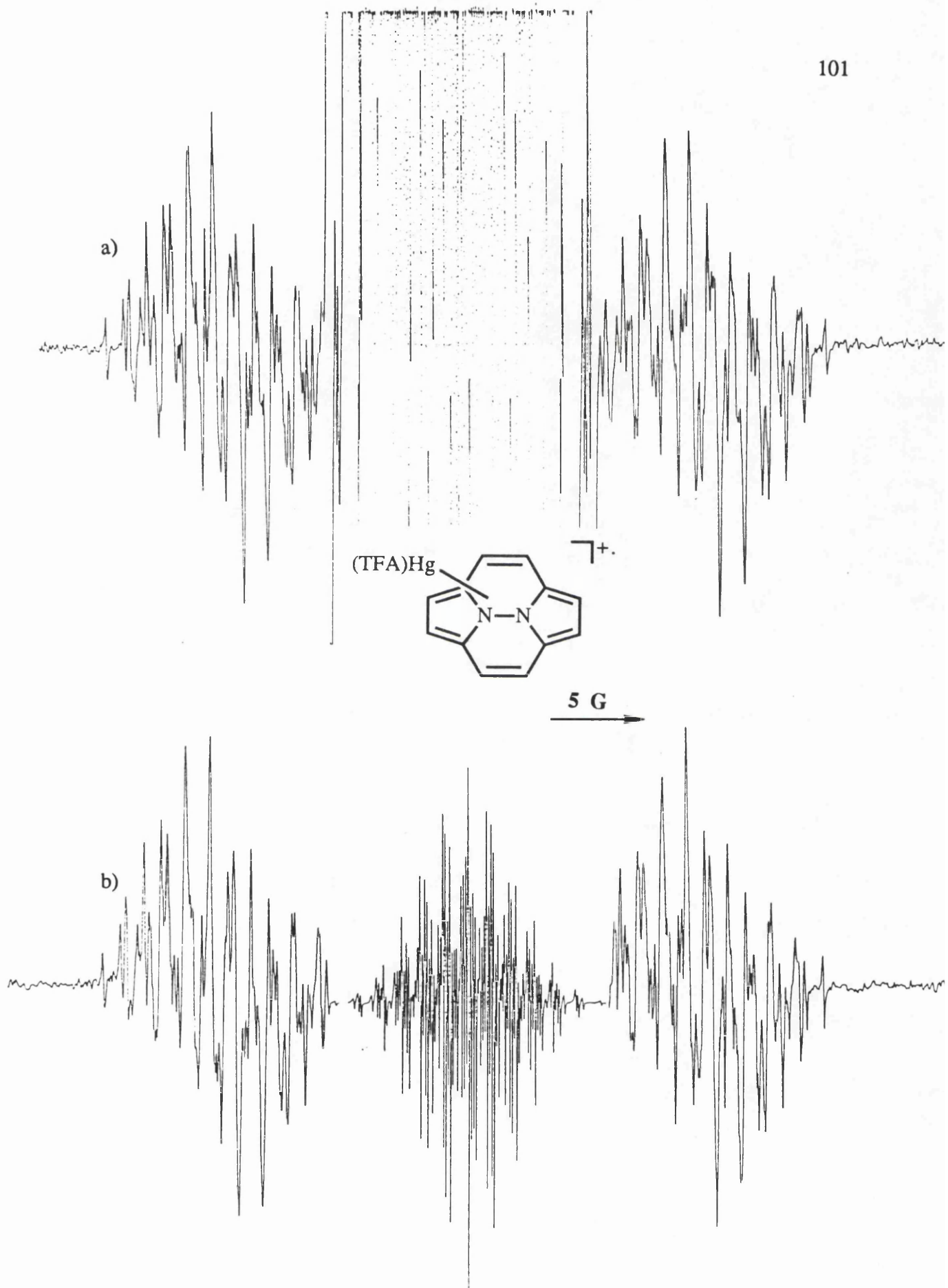
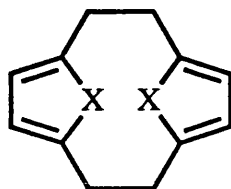


**Figure 4.22** (a) ESR Spectrum of  $(22^{+})$  in  $\text{TFAH}/\text{Hg}(\text{TFA})_2$  at 260 K showing  $(^{199}\text{Hg})$  satellites. (b) As (a), but with central feature reduced in intensity.

the electron density is fairly evenly distributed around the periphery of ( $22^+$ ), the mercuriated species are probably a mixture of (24) and (25) ( $X = \text{TFA}$ ).

#### 4.2.9 [2.2](2,5) Furano- and Thiopheno-phane

We could not oxidize [2.2](2,5)furanophane (26;  $X = \text{O}$ ) to its ESR-detectable radical cation; all the oxidizing reagents mentioned in this chapter were used.



(26)

The failure to observe ( $26^+$ ;  $X = \text{O}$ ) by ESR can be rationalized in either of two ways: distortion of the furan rings so that the  $\pi$ -systems resemble that of isolated *cis*-butadienes (Section 4.2.6), or the loss of a proton(s) due to a small dihedral angle subtended between the  $2p$  orbital on  $C_\alpha$  and the  $C_\beta\text{-H}_\beta$  bond (Section 4.2.8).

The X-ray crystal structures<sup>20</sup> of (26;  $X = \text{O}$  and S) have been reported. In (26;  $X = \text{O}$ ) the oxygens are displaced by 0.085 Å out of the plane of the 2,3,4, and 5 ring carbons which are coplanar to within  $\pm 0.002$  Å, and the  $\alpha$ -methylene groups are displaced out of the plane of the furan ring carbons by 0.4 Å (Figure 4.23). The  $\text{CH}_2\text{-CH}_2$  bonds are significantly stretched [1.569 (6) Å] giving an indication of the strain in these types of molecules. The structure of (26;  $X = \text{S}$ ) is similar in all respects but the distortions are more pronounced.

The photoelectron spectra<sup>21</sup> of (26;  $X = \text{O}$  and S) indicate that there is an intramolecular through-space interaction between the two  $\pi$ -systems; the IP's of (26;  $X = \text{O}$ ) and (26;  $X = \text{S}$ ) are 7.50 eV and 7.90 eV respectively. These IPs are lower than those of the isolated 2,5-dimethyl-furan and -thiophene moieties (IPs 7.90 and 8.02 eV respectively).

It is most likely, that upon oxidizing (26;  $X = \text{O}$ ), its radical cation decays rapidly by loss of a proton(s).

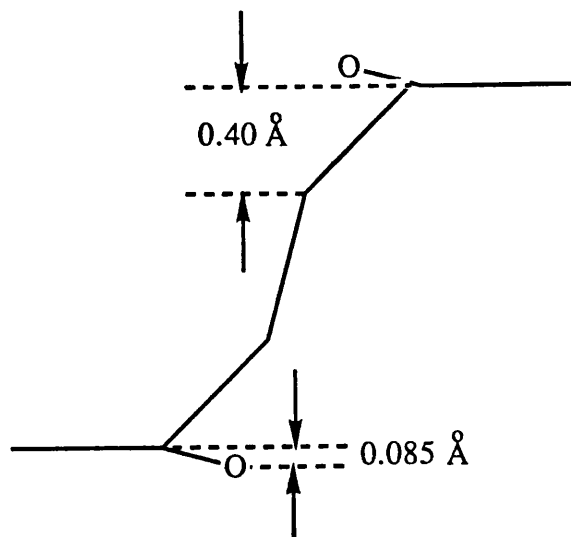


Figure 4.23 A view of the [2.2](2,5) furanophane structure.

#### 4.2.10 Dioxenes

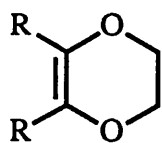
The ESR spectra of the radical cations of dioxene (27; R = H), 2,3-dimethyldioxene (27; R = Me) and benzodioxene (28) have been observed and analysed by A. G. Davies and C. J. Shields.<sup>22</sup> In all the cationic species, the pseudo-axial and pseudo-equatorial protons of the methylene groups in the half chair dioxene rings were distinguished by different hyperfine coupling constants, and computer simulation of the spectra over a range of temperatures gave the Arrhenius parameters for the ring inversion.

We proposed to extend the study of these systems to include dioxene rings attached to 5-membered heterocycles, and prepared 2,3-dihydro-5,7-dimethylfuro[3,4b]-*p*-dioxin (29). We could not oxidize (29) to any ESR-observable species using TFAH/Tl(TFA)<sub>3</sub>, TFAH/Hg(TFA)<sub>2</sub>, TFAH/H<sub>2</sub>SO<sub>4</sub>, H<sub>2</sub>SO<sub>4</sub>, AlCl<sub>3</sub>/CH<sub>2</sub>Cl<sub>2</sub>, or HFSO<sub>4</sub>/SO<sub>2</sub>. This is in contrast to the 2,5-dialkylated furans and the dioxenes (27; R = H or Me and 28) which are readily oxidized and give strong and well resolved ESR spectra. In all the dioxene radical cations characterised by ESR, a large spin density resides on the *sp*<sup>2</sup> carbons adjacent to the dioxene oxygens. We would predict a small electron density at these positions in (29).

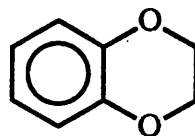
A derivative of (29) was prepared, namely 2,3,4,7-tetrahydro-5,7-dimethyl-5,7-dimethoxy-[3,4]-*p*-dioxin (30) which did not oxidize to yield any ESR-



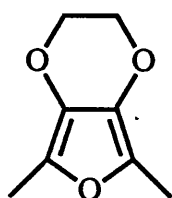
detectable species with any of the reagents used on (29).



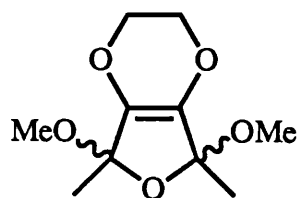
(27)



(28)



(29)

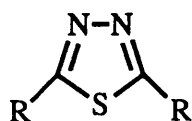


(30)

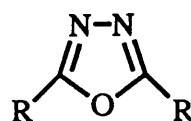
It is notable that (29) and (30) are both hygroscopic and react with atmospheric oxygen.

#### 4.2.11 1,3,4-Thiadiazoles and 1,3,4-Oxadiazoles

We could not oxidize any of the alkylated thiadiazoles (31; R = Me, Et, *i*-Pr, and *t*-Bu) or oxadiazoles (32; R = Me) to their ESR-observable radical cations. These compounds were the first to be studied by the author of this thesis and it is now clear why they can not be oxidized readily. The IP of 1,3,4-thiadiazole is 11.23 eV<sup>23</sup> and this is not within the range of our chemical oxidants.



(31)



(32)

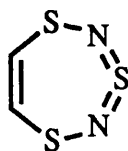
The 1,3,4-thiadiazoles have relatively low electron densities at carbon (positions 2 and 5) and relatively high electron densities at the electronegative nitrogen (positions 3 and 4)<sup>24</sup> causing the heterocycle to have a higher IP than

would other wise be expected. Hyperconjugative electron release by two alkyl substituents only lowers the IP of pyrrole by *ca.* 0.5 eV and electron release into the  $\pi$ -system of this heterocycle by alkyl groups will be smaller than it is in the 2,5-dialkylated pyrroles.

We have calculated the IPs of (31; R = H), (32; R = H) and pyrrole (3; R = H) using the PM3 Hamiltonian and find the vales 10.81, 10.92, and 8.65 eV respectively. The experimental<sup>25</sup> IP of pyrrole is 8.23 eV.

#### 4.2.14 1,3 $\lambda^{\delta^2}$ ,5,2,4-Trithiadiazepine

1,3 $\lambda^{\delta^2}$ ,5,2,4-Trithiadiazepine was provided by C W Rees of Imperial College. 1,3 $\lambda^{\delta^2}$ ,5,2,4-Trithiadiazepine (33) was oxidized to its ESR-observable radical cation by photolysing a solution of the substrate in HFSO<sub>4</sub>/SO<sub>2</sub> with Pyrex-filtered u.v. light at 175 K (Tl<sup>3+</sup> and Hg<sup>2+</sup> were unsuccessful as oxidants). The spectrum (Figure 4.24) was weak but clearly shows a triplet arising from the two equivalent protons, *a*(2H) 2.80 G, *g* 2.0155. The high *g*-value is indicative of a radical with high electron density at sulphur atoms, and these results are confirmed by PM3 calculations. The calculated IP (8.59 eV) suggests that the radical cation should be readily generated. Large u.p.e density coefficients in the radical cation, obtained from an unrestricted calculation are found at S(1) (0.383), S(3) and S(5) (0.525), and C(6) and C(7) (-0.385), and a negligible value is found at N(2) and N(4) (-0.056).



(33)

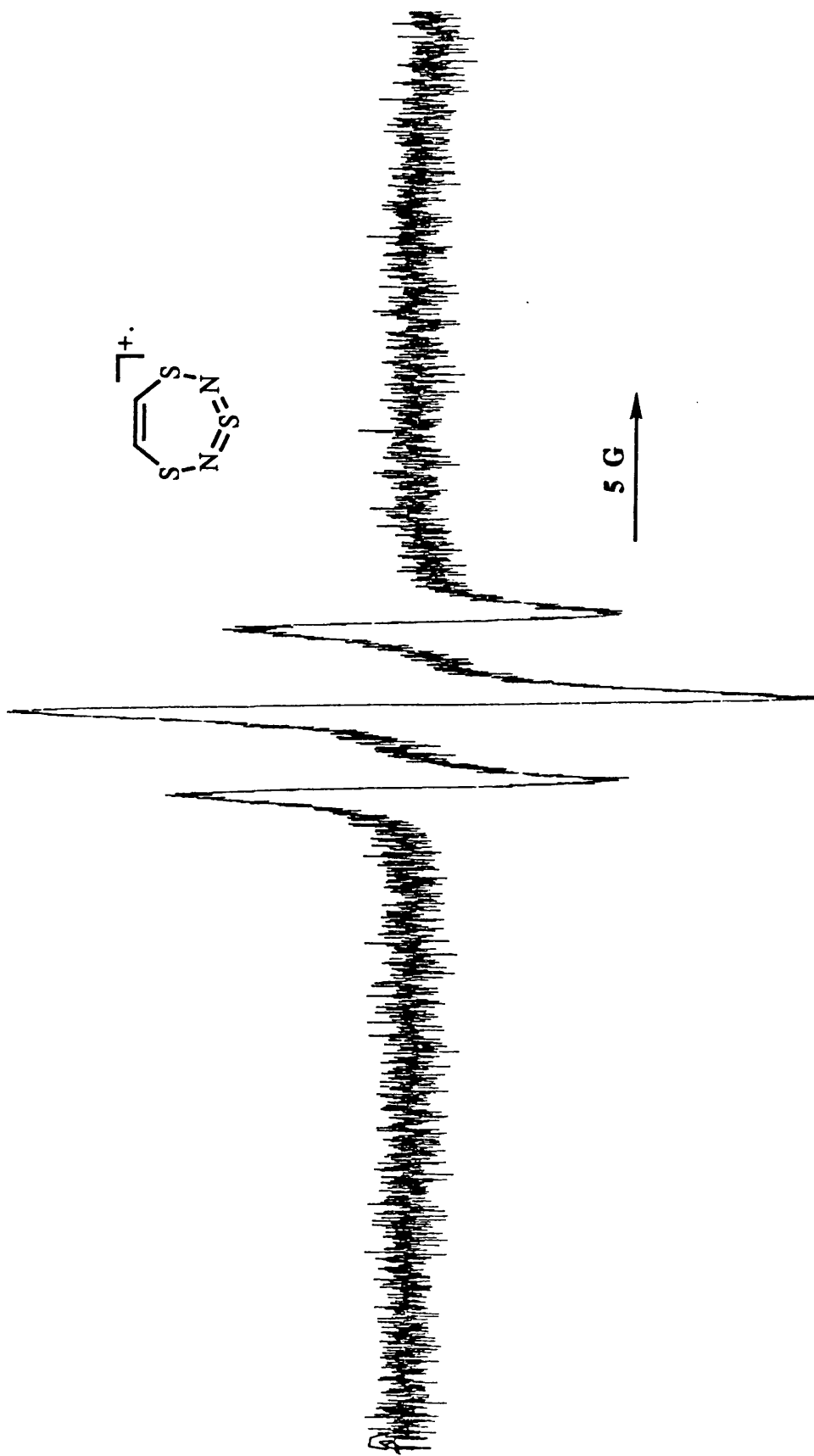
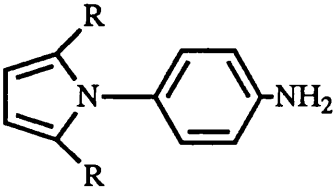
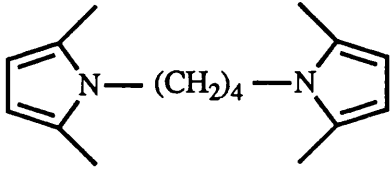
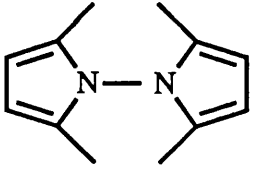
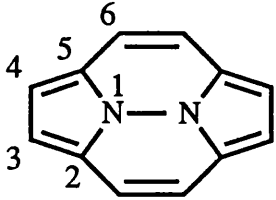


Figure 4.24 ESR Spectrum of  $(33^+)$  in  $\text{HFSO}/\text{SO}_2$  at 175 K.

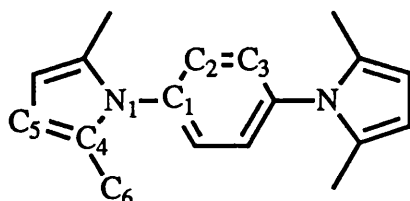
**Table 4.1** Hyperfine coupling constants (G) and *g*-values of radical cations described in the text. INDO-Derived couplings are given in parenthesis.

	2,5	3,4	N	1	<i>g</i>
t-Bu	0.62(18H) (1.48)	3.58 (2H) (2.44)	4.05 (3.70)	0.91(1H) (2.05)	2.0025
φ		64.5 ( <sup>199</sup> Hg)	(Position uncertain)		2.0004
Me	16.44 (6H)	3.52 (2H)	4.70	 No coupling	2.0024
Me	16.10 (6H) (22.48)	3.30 (2H) (2.42)	4.75 (5.36)	<sup>NH<sub>2</sub></sup> 1.75 (N) 1.75 (2H) (1.49) (2.29)	2.0025
R = R'' = Me	Me 16.20 (6H) (21.91)	3.50 (2H) (2.67)	4.32 (3.57)	R' = H No coupling	2.0025
	Me 16.40 (6H)	3.52 (2H)	4.28	R' = Me No coupling	2.0025
Et	17.24 (4H) R = R'' = Et	3.60(2H)	4.22	R' = H No coupling	2.0026
	R = Me and R'' = Et				
ca. 80%	Et 17.24 (4H)	3.60(2H)	4.22	R' = H	2.0026
ca. 20%	Me 16.20 (6H)	3.50(2H)	4.32	No coupling	

Table 4.1 Continued.

				
2,5	3,4	N	1	<i>g</i>
Me 16.40 (6H)	3.54 (2H)	4.36	$\phi$ -NH <sub>2</sub> No coupling	2.0025
				
Me 15.92 (6H)	3.40 (2H)	3.40	0.90 (2H)	2.0026
				
Me 8.32 (12H) (22.18) (6H)	1.79 (4H) (2.36) (2H)	2.28 (2N) (4.72) (N)		2.0028
				
6	3,4	N		
2.44 (4H) (1.86)	2.22 (4H) (1.63)	1.77 (2N) (1.22)		2.0027
48.0 ( <sup>199</sup> Hg)	(Position uncertain)			2.0004

**Table 4.2** Selected bond lengths and angles of structures (10; R = Me, R' = H), (19), and (22).<sup>26</sup>

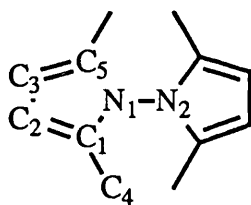


Bond lengths (Å)

N <sub>1</sub> - C <sub>1</sub>	1.435 (4)
C <sub>1</sub> - C <sub>2</sub>	1.369 (5)
C <sub>4</sub> - C <sub>5</sub>	1.357 (4)
N <sub>1</sub> - C <sub>4</sub>	1.374 (3)
C <sub>2</sub> - C <sub>3</sub>	1.375 (5)

Bond Angles (°)

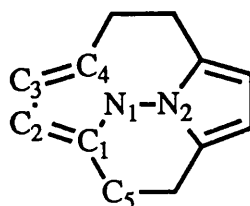
C <sub>4</sub> - N <sub>1</sub> - C <sub>1</sub>	125.2 (2)
C <sub>3</sub> - C <sub>2</sub> - C <sub>1</sub>	120.5 (4)
C <sub>5</sub> - C <sub>4</sub> - N <sub>1</sub>	107.0 (3)
C <sub>6</sub> - C <sub>4</sub> - C <sub>5</sub>	130.7 (3)
C <sub>2</sub> - C <sub>1</sub> - N <sub>1</sub>	120.5 (3)
C <sub>6</sub> - C <sub>4</sub> - N <sub>1</sub>	122.3 (3)



N <sub>1</sub> - C <sub>1</sub>	1.362 (15)
N <sub>1</sub> - N <sub>2</sub>	1.378 (18)
C <sub>1</sub> - C <sub>4</sub>	1.476 (21)
C <sub>1</sub> - C <sub>2</sub>	1.333 (17)
C <sub>2</sub> - C <sub>3</sub>	1.406 (21)

C <sub>1</sub> - N <sub>1</sub> - C <sub>5</sub>	110.7 (10)
C <sub>1</sub> - N <sub>1</sub> - N <sub>2</sub>	123.2 (9)
N <sub>1</sub> - C <sub>1</sub> - C <sub>4</sub>	120.7 (11)
N <sub>1</sub> - C <sub>1</sub> - C <sub>2</sub>	106.6 (11)
C <sub>1</sub> - C <sub>2</sub> - C <sub>3</sub>	108.4 (12)

Table 4.2 Continued.



Bond lengths (Å)

N <sub>1</sub> - C <sub>1</sub>	1.348 (11)
N <sub>1</sub> - N <sub>2</sub>	1.367 (10)
C <sub>1</sub> - C <sub>5</sub>	1.471 (18)
C <sub>2</sub> - C <sub>2</sub>	1.396 (17)
C <sub>3</sub> - C <sub>4</sub>	1.360 (11)

Bond Angles (°)

C <sub>1</sub> - N <sub>1</sub> - C <sub>4</sub>	113.2 (7)
C <sub>4</sub> - N <sub>1</sub> - N <sub>2</sub>	123.8 (8)
N <sub>1</sub> - C <sub>1</sub> - C <sub>5</sub>	116.3 (8)
C <sub>1</sub> - C <sub>2</sub> - C <sub>3</sub>	108.6 (8)
N <sub>1</sub> - C <sub>1</sub> - C <sub>2</sub>	104.2 (9)

## References

1. A. G. Davies, L. Julia, and S. N. Yazdi, *J. Chem Soc., Perkin Trans. 2*, **1989**, 239.
2. D. N. Ramakrishna Rao and M. C. R. Symons *J. Chem. Soc., Perkin Trans. 2*, **1983**, 135.
3. M. Shiotani, Y. Nagata, M. Tasaki, J. Sohma, and T. Shida, *J. Phys. Chem.*, **1983**, 87, 1170.
4. W. Huber and K. Mullen, *Acc. Chem. Res.*, **1986**, 19, 300.
5. J. Bruhin, F. Gerson, and H. Ohya-Nishiguchi, *J. Chem. Soc., Perkin Trans. 2*, **1990**, 1045.
6. A. Terahara, H. Ohya-Nishiguchi, N. Hirota, H. Higuchi, and S. Misumi, *J. Phys. Chem* **1986**, 90, 4958.
9. R. W. Fessenden, *J. Chem. Phys.* **1962**, 37, 739.
8. W. Rettig and F. Marschner, *Nouv. J. Chem.*, **1983**, 7, 425.
7. H. Lumbroso, D. M. Bertin, and F. Marschner, *J. Molec. Struct.*, **1988**, 178, 187.
10. A. G. Davies, J. P. Goddard, E. Lusztyk, and J. Lusztyk, *J. Chem Soc., Perkin Trans. 2*, **1982**, 737.
11. A. G. Davies, E. Lusztyk, and J. Lusztyk, *J. Chem. Soc., Perkin Trans. 2*, **1982**, 729.
12. H. Nozaki, T. Koyama, T. Mori, and R. Noyori *Tetrahedron Lett.*, **1968**, 2181.
13. H. Nozaki, T. Koyama, and T. Mori, *Tetrahedron*, **1969**, 25, 5357.
14. A. G. Davies, J. R. M. Giles, and J. Lusztyk, *J. Chem Soc., Perkin Trans. 2*, **1981**, 747.
15. E. Orti, J. Sanchez-Martin, and F. Thomas, *Theochem.*, **1983**, 13, 197.
16. E. Orti, J. Sanchez-Martin, P. M. Viruela-Martin, and F. Thomas, *Chem. Phys. Lett.*, **1986**, 130, 285.
17. W. Flicht, H. Peeters, P. Rademacher and W. Schulten. *Tetrahedron*, **1978**, 34, 2301.
18. B. M. Trost, S. F. Nelsen, and D. R. Britteli, *Tetrahedron Lett.*, **1967**, 3959.

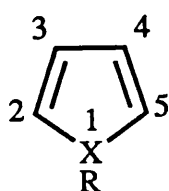


19. B. Freiermuth, S. Gerber, A. Riesen, J. Wirz, and M. Zehnder, *J. Am. Chem. Soc.*, **1990**, *112*, 738.
20. N. P. Pahor, M. Calligaris, and L. Randaccio, *J. Chem. Soc., Perkin Trans. 2*, **1978**, 42.
21. F. Bernardi, A. Bottoni, F. P. Colonna, G. Distefano, U. Folli, and P. Vivarelli, *Z. Naturforsch., Teil A*, **1978**, *33*, 959.
22. A. G. Davies, J. C. Evans, C. C. Rowlands and C. J. Shields, *Can. J. Chem.*, **1989**, *67*, 1748.
23. T. Ha, *J. Mol. Struct.*, **1979**, *51*, 87.
24. S. Castellano, H. Günther, and, S. Ebersole, *J. Phys. Chem.*, **1973**, *69*, 4166.
25. S. Cradock, R. H. Finlay, and M. H. Palmer, *Tetrahedron.*, **1973**, *29*, 173.
26. D .V. Avila, A. G. Davies, D. A. Tocher, and M. L. Truter, *Acta. Cryst. (C)*, to be submitted.

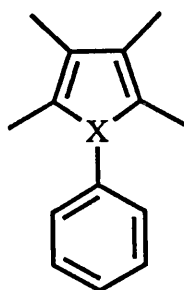
## Chapter 5. Arsoles and Some Related Compounds

### 5.1 Introduction

The most intensely investigated of the Group 5 heterocycles (1; X = N, P, As, Sb, and Bi) are the pyrroles, because of the ease of synthesis and the frequency with which the pyrrole moiety is found in naturally occurring molecules. We can find no examples of naturally occurring arsoles, stiboles or bismutholes in the literature.



(1)



(2)

Physicochemical properties of these compounds vary greatly with the nature of the heteroatom. As Group 5 is descended the  $sp^2$  hybridized orbitals become more diffuse and interact less effectively with the  $2p$  orbitals of the carbon atoms at the 2- and 5-positions. A consequence of the poor overlap is that unlike pyrrole the energy required to rehybridize the heteroatom ( $sp^3 \rightarrow sp^2$ ) is less than that gained by resonance stabilization of the five-membered ring, and the heteroatom becomes pyramidal.  $d$ -Orbitals are undoubtedly utilized, interacting with the  $2p$  orbitals on carbon in the arsoles, stiboles, and bismutholes where they are accessible.

Semi-empirical calculations of the barriers to pyramidal inversion<sup>1</sup> in which  $d$ -orbitals are omitted from the basis set have been found to be in agreement with some experimental data. As in the case of phospholes, the very small barrier to inversion in arsoles, as compared to simple arsines ( $AsR_3$ ), is attributed to the cyclic  $6\pi$ -electron system. The planar transition state is stabilized by extensive electron delocalization. The heteroatom-carbon bond lengths increase as the group is descended also affecting the degree of orbital overlap. The 30-34

kcal mole<sup>-1</sup> barriers ( $\Delta G^\ddagger$ ) to pyramidal inversion calculated for arsole and some of its derivatives are lower by *ca.* 10-15 kcal mole<sup>-1</sup> than those of simple arsines.

*Ab initio* molecular orbital theory has been used to characterize a series of Group 4 and 5 monohetero-substituted benzenes and cyclopentadienes<sup>2</sup> using the 3-21G\* basis set. The structures of the 6-membered rings suggest substantial delocalization and those of the 5-membered rings indicate that the strain arising from the larger bond angles must be weighed against  $\pi$ -delocalization in determining stabilization from the formation of the ring.

F. Mathey and coworkers,<sup>3</sup> who studied the photoelectron spectra of a some phospholes, phospholanes, and arsoles conclude that "the lone pairs in the phospholes, and very probably also in the arsole, take no part in a cyclic five-membered ring conjugation." According to these authors. "phospholes and arsoles in their ground-state conformations consist of localized diene systems and lone pairs of heteroatom electrons. In this sense phospholes and arsoles are not aromatic." The X-ray crystal structure of 1-benzylphosphole shows the phosphorus to be clearly pyramidal.<sup>4</sup>

Pyrroles are normally planar compounds with the substituent N-R bond lying in the plane of the pyrrole ring (excluding those distorted due to steric forces); this is illustrated in the molecular structure of *p*-phenylene-bis(2,5-dimethylpyrrolyl) (Figure 4.11). The type of geometry expected to be found in arsoles is shown in the molecular structure (Figure 5.1) of 2,2',5,5'-tetramethylbiarsolyl.<sup>5</sup> Compare this to that of the analogous 2,2',5,5'-tetramethylbi(*N*-pyrrolyl) (Figure 4.18).

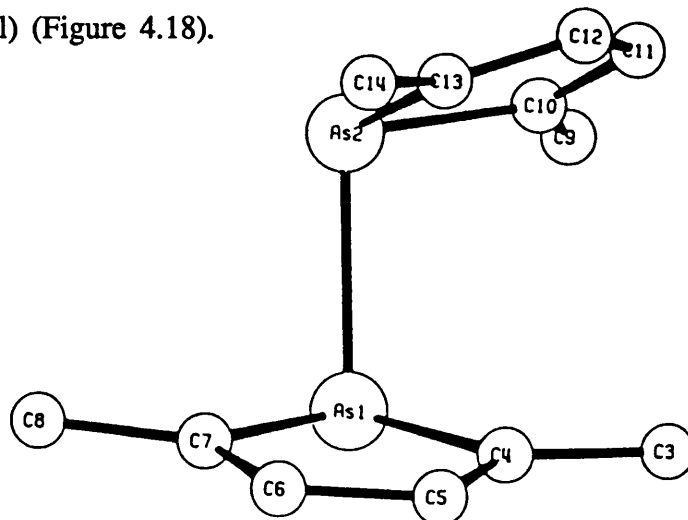


Figure 5.1 The molecular structure of 2,2',5,5'-tetramethylbiarsolyl.

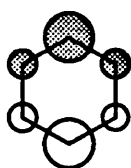
## 5.2 Results and discussion

### 5.2.1 1-Phenyl-2,3,4,5-tetramethylarsole

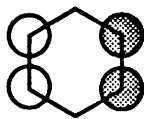
When 1-phenyl-2,3,4,5-tetramethylarsole (2; X = As) was dissolved in TFAH/Tl(TFA)<sub>3</sub>, it gave rise to a strong persistent radical cation. The ESR spectrum of 7 x 7 x 3 x 3 lines has the following characteristics:  $a(6H)$  9.37,  $a(6H)$  2.39,  $a(2H)$  3.77, and  $a(2H)$  1.37 G,  $g$  2.0024. The spectrum is in excellent accord with its computer simulation (Figure 5.2). A very low concentration of the substrate was required (*ca.* 0.1 mg in a 5 ml solution of oxidant), or the ESR spectrum was poorly resolved.

The coupling constants observed in (2<sup>+</sup>; X = As) are rationalized in terms of an intramolecular through-space interaction of the  $\pi$ -systems (Section 4.2.2) of the arene substituent and the *cis*-butadiene moiety, which are held in the appropriate conformation.

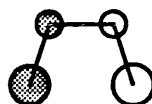
The electronegativity of arsenic (2.0) relative to carbon (2.5) should destabilize the  $\psi_3$  (3) MO of the phenyl group resulting in the HOMO being of the form  $\psi_4$  (4). The symmetry of a *cis*-butadiene HOMO (5) is of the same form as that of pyrrole (see Section 4.1).



(3)



(4)



(5)

A perturbation MO diagram can be constructed between the MO's (4) and (5) (Scheme 5.1); the new HOMO has zero electron density at the *para*-position of the phenyl group and at the heteroatom.

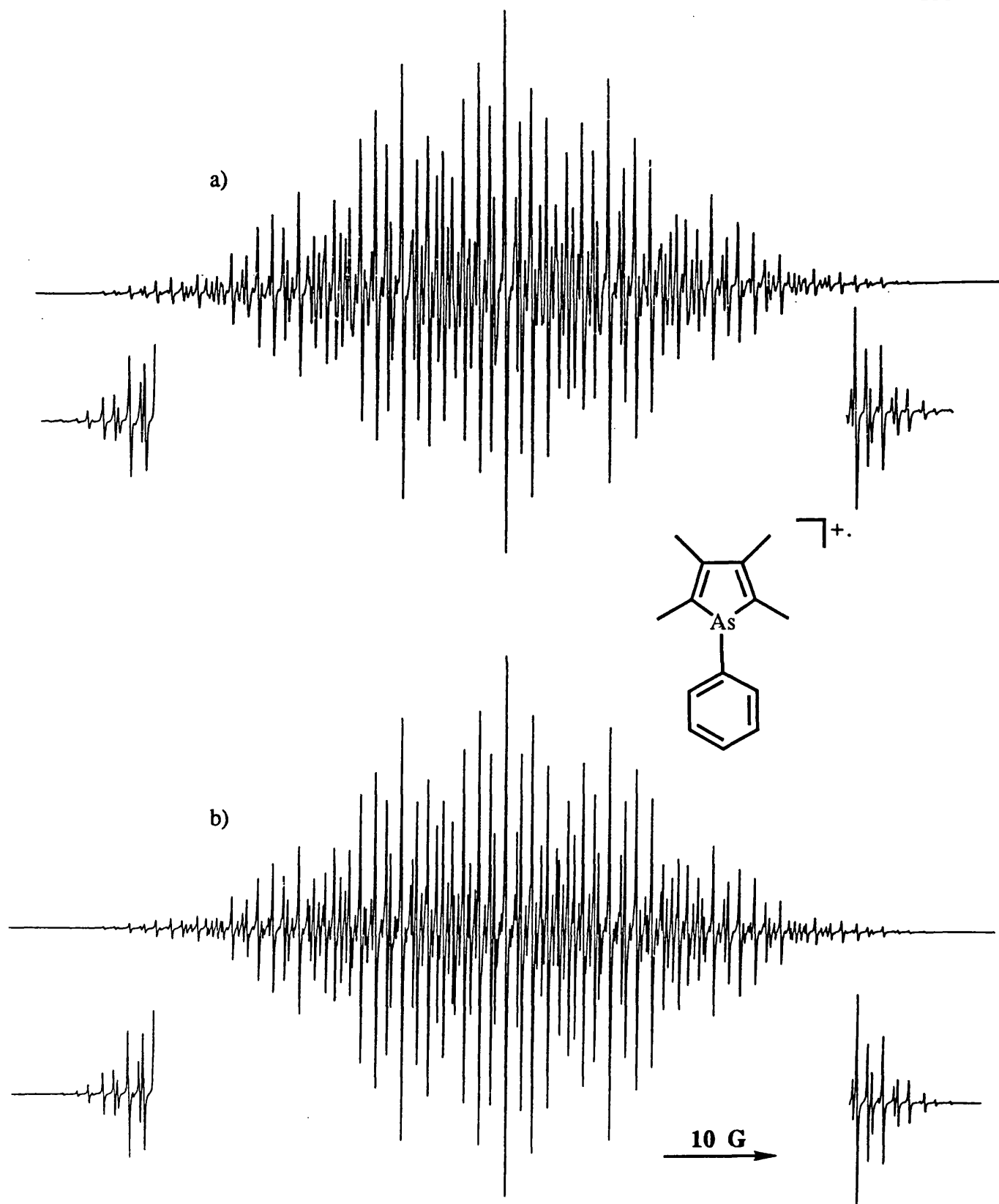
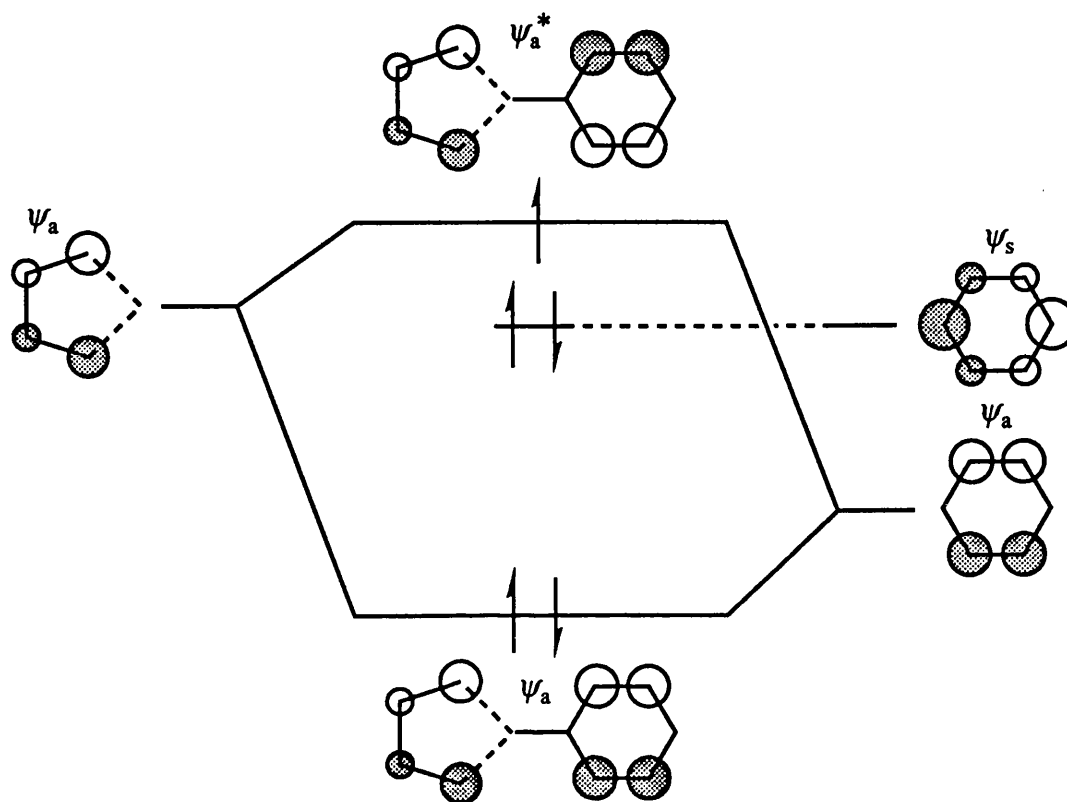


Figure 5.2 (a) ESR Spectrum of  $(2^+; X = \text{As})$  in TFAH/Tl(TFA)<sub>3</sub> at 260 K. (b) Computer simulation of (a).



Scheme 5.1

### 5.2.2 1-Phenyl-2,5-dimethylarsole

We were unable to oxidize 1-phenyl-2,5-dimethylarsole to any ESR-observable species using the oxidizing reagents TFAH/Tl(TFA)<sub>3</sub>, TFAH/Hg(TFA)<sub>2</sub>, TFAH/H<sub>2</sub>SO<sub>4</sub>, H<sub>2</sub>SO<sub>4</sub>, or AlCl<sub>3</sub>/CH<sub>2</sub>Cl<sub>2</sub> with or without varying degrees of photolysis.

The photoelectron spectra of the 1-phenyl-2,5-dimethyl-arsole and -phosphole are reported to show "that there is no conjugative interaction between the 5- and 6- membered rings."<sup>3</sup> It would be interesting to see if the same were true for 1-phenyl-2,3,4,5-tetramethylarsole, for which we postulate a through-space delocalization in the radical cation.

### 5.2.3 1-Phenyl-2,3,4,5-tetramethyl-phosphole and -stibole.

We were unable to oxidize 1-phenyl-2,3,4,5-tetramethyl-phosphole (2; X = P) and -stibole (2; X = Sb) to any ESR-observable species using the oxidizing

reagents listed above for the 1-phenyl-2,5-dimethylarsole radical cation. It may be that our success in observing ( $2^+$ ; X = As) is due to the specific geometry and the nature of the MO of (2; X = As) and that the failures possibly may be rationalized in terms of the absence of those characteristics in the other compounds.

### References

1. J. D. Androse, A. Rauk, and K. Mislow, *J. Am. Chem. Soc.*, **1974**, *96*, 6904.
2. K. K. Baldrige and M. S. Gordon, *J. Am. Chem. Soc.*, **1988**, *110*, 4208.
3. W. Schäfer, A. Schweig, G. Märkl, H. Hauptmann, and F. Mathey, *Angew. Chem., Int. Ed. Engl.*, **1973**, *12*, 145.
4. P. Coggon, J. F. Engel, A. T. McPhail, and L. D. Quin, *J. Am. Chem. Soc.*, **1970**, *92*, 5779
5. A. J. Ashe, W. M. Butler, and T. R. Diephouse, *Organometallics*, **1983**, *2*, 1005.

## Chapter 6. Experimental

### 6.1 Synthesis

#### 1,2,3,4-Tetramethyl-5,6,7,8-tetrahydronaphthalene

This compound was prepared in 10% yield by treating a mixture of 1,2,3,4-tetramethylbenzene and aluminium chloride with 1,4-dichlorobutane; m.p. 77-78 °C (lit.,<sup>1</sup> 78-79 °C),  $\delta_{\text{H}}$  (200 MHz;  $\text{CDCl}_3$ ) 1.72-1.81 (m, 4H,  $\beta\text{CH}_2$ ), 2.17 (s, 6H, Me), 2.24 (s, 6H, Me), and 2.62-2.72 (m, 4H,  $\alpha\text{CH}_2$ ).

#### 9,10-Dibromo-1,2,3,4,5,6,7,8-octahydroanthracene

This compound was prepared by treating 1,2,3,4,5,6,7,8-octahydroanthracene with bromine; m.p. 201 °C (from  $\text{CHCl}_3/\text{EtOH}$ ) (lit.,<sup>2</sup> 200-201 °C),  $\delta_{\text{H}}$  (60 MHz;  $\text{CCl}_4$ ), 1.50-1.80 (m, 8H,  $\beta\text{CH}_2$ ), 2.47-2.80 (m, 8H,  $\alpha\text{CH}_2$ ), and H.R.M.S. m/z Found 341.9689. Calc for  $\text{C}_{14}\text{H}_{16}\text{Br}_2$  341.9615.

#### 9-Bromo-10-methyl-1,2,3,4,5,6,7,8-octahydroanthracene

A solution of 1,9-dibromo-1,2,3,4,5,6,7,8-octahydroanthracene (1.5 g, 4.36 mmol) in THF (50 ml) was cooled to below -70 °C under  $\text{N}_2$ , and treated with n-butyl-lithium (1.74 ml, 2.5 molar). After warming the mixture to *ca.* 20 °C and treatment with methyl iodide (0.62 g, 4.36 mmol) in THF (10 ml), water was added. The mixture was extracted with diethyl ether (3 x 50 ml), the combined organic extracts dried with sodium sulphate, filtered, and stripped of solvent to yield the title compound (1.15 g, 72%), m.p. 152 °C (from  $\text{EtOH}/\text{CHCl}_3$ ). Found: C, 64.27; H, 7.01.  $\text{C}_{15}\text{H}_{19}\text{Br}$  requires C, 64.52; H, 6.86%.  $\delta_{\text{H}}$  (400 MHz;  $\text{CDCl}_3$ ) 1.72-1.80 (m, 8H,  $\beta\text{CH}_2$ ), 2.08 (s, 3H, Me), 2.23-2.80 (m, 8H,  $\alpha\text{CH}_2$ ), and H.R.M.S. m/z Found 278.0634. Calc. 278.0671.

#### 9,10-Dimethyl-1,2,3,4,5,6,7,8-octahydroanthracene<sup>3</sup>

A solution of 9-bromo-10-methyl-1,2,3,4,5,6,7,8-octahydroanthracene (0.70 g, 5.14 mmol) in THF (10 ml) was cooled to below -70 °C under  $\text{N}_2$ , and treated with n-butyl-lithium (2.05 ml, 2.5 molar). The reaction mixture was warmed to *ca.* 20 °C and treated with methyl iodide (0.73 g, 5.14 mmol) in THF (10 ml), and



water (100 ml) was added. Work-up of the mixture was similar to that of 9-bromo-10-methyl-1,2,3,4,5,6,7,8-octahydroanthracene yielding the title compound (0.57 g, 52%) m.p. 135.5 °C (from EtOH),  $\delta_{\text{H}}$ (400 MHz;  $\text{CDCl}_3$ ) 1.74-1.80 (m, 8H,  $\beta\text{CH}_2$ ), 2.09 (s, 6H, Me), 2.70-2.64 (m, 8H,  $\alpha\text{CH}_2$ ), and H.R.M.S. m/z Found 214.1696. Calc. 214.1721.

#### **$\beta$ -Chloroethyl-(1,2,3,4-tetramethylphenyl)-ketone**

This compound<sup>4</sup> was prepared in 68% yield by treating a mixture of 1,2,3,4-tetramethylbenzene and 3-chloropropionyl chloride with aluminium chloride,  $\delta_{\text{H}}$ (60 MHz;  $\text{CCl}_4$ ) 2.19 (s, 6H, Me), 2.29 (s, 6H, Me), 2.50 (m, 2H,  $\text{CH}_2$ ), and 2.87-2.97 (m, 2H,  $\text{CH}_2\text{Cl}$ ).

#### **4,5,6,7-Tetramethylindan-1-one**

This compound was prepared in 6% yield by treating  $\beta$ -chloroethyl-(1,2,3,4-tetramethylphenyl)-ketone with conc. sulphuric acid; m.p. 157 °C (from EtOH) (lit.,<sup>4</sup> 156 °C)  $\delta_{\text{H}}$ (200 MHz;  $\text{CDCl}_3$ ) 2.22 (s, 3H, Me), 2.24 (s, 3H, Me), 2.62 (s, 3H, Me), 2.63-2.68 (m, 2H,  $\text{CH}_2$ ), and 2.87-2.97 (m, 2H,  $\text{CH}_2$ ).

#### **4,5,6,7-Tetramethylindane**

This compound was prepared in 54% yield by treating 4,5,6,7-tetramethylindane-1-one with zinc amalgam and conc. hydrochloric acid; m.p. 98-99 °C (from EtOH) (lit.,<sup>4</sup> 99-100 °C)  $\delta_{\text{H}}$ (200 MHz;  $\text{CDCl}_3$ ) 1.93-2.12 (q, 2H,  $\text{CH}_2$ ), 2.20 (s, 12H, Me), and 2.71-2.97 (t, 4H,  $\text{CH}_2$ ).

#### **5-(3-Chloropropionyl)-indane**

This compound was prepared in 43.5% yield by treating a mixture of indane and 3-chloropropionyl chloride with aluminium chloride; m.p. 64 °C (from n-hexane) (lit.,<sup>5</sup> 68-69 °C),  $\delta_{\text{H}}$ (200 MHz;  $\text{CCl}_4$ ) 2.12 (q, 2H,  $\beta\text{CH}_2$ ,  $^3J = 7.6$  Hz), 2.95 (t, 4H,  $\alpha\text{CH}_2$ ), 3.44 (t, 2H,  $\text{CH}_2$ ), 3.92 (t, 2H,  $\text{CH}_2\text{Cl}$ ), 7.30 (d, 1H,  $\phi$ ), and 7.75 (d, 1H,  $\phi$ ).

#### **s-Hydrindacene-1-one**

This compound was prepared in 41% yield by treating 5-(3-chloropropionyl)-indane

with conc. sulphuric acid; m.p. 64-65 °C (from n-hexane) (lit.,<sup>5</sup> 80-81 °C),  $\delta_{\text{H}}$ (200 MHz;  $\text{CDCl}_3$ ) 2.12 (q, 2H,  $\beta\text{CH}_2$ ,  $^3\text{J} = 7.2$  Hz) 2.67-3.12 (m, 10H,  $\text{CH}_2$ ), 7.29 (s, 1H,  $\phi$ ), and 7.57 (s, 2H,  $\phi$ ).

### 1,2,3,4,5,6,7-Hexahydro-*s*-indacene

This compound was prepared in 44% yield by treating *s*-hydrindacene-1-one with zinc amalgam and conc. hydrochloric acid; m.p 51-52 °C (from EtOH) (lit.,<sup>6</sup> 52-54 °C),  $\delta_{\text{H}}$ (400 MHz;  $\text{CDCl}_3$ ) 2.03-2.11 (q, 4H,  $\beta\text{CH}_2$ ,  $^3\text{J} = 7.6$  Hz), 2.84-2.87(t, 8H,  $\text{CH}_2$ ), and 7.09 (s, 2H,  $\phi$ ).

### 4,8-Dibromo-1,2,3,5,6,7-hexahydro-*s*-indacene

A solution of *s*-hydrindacene (2 g, 12.66 mmol) in chloroform (20 ml) was treated with a solution of bromine (4.06 g, 25.23 mmol) in chloroform (20 ml) and left to stand for 12 h. The mixture was washed with sodium hydrogen carbonate (2 x 20 ml) and water (2 x 20 ml). The organic phase was dried over magnesium carbonate, filtered and stripped of solvent to yield the title compound (1.85 g, 46%), m.p. 166 °C (from EtOH/ $\text{CHCl}_3$ ). Found: C, 45.46; H, 3.73.  $\text{C}_{12}\text{H}_{12}\text{Br}_2$  requires C, 45.60; H, 3.83%.  $\delta_{\text{H}}$ (200 MHz;  $\text{CDCl}_3$ ) 2.05-2.21 (q, 4H,  $\beta\text{CH}_2$ ,  $^3\text{J} = 6$  Hz), and 2.94-3.01 (t, 8H,  $\alpha\text{CH}_2$ ).

### 4-Bromo-8-methyl-1,2,3,5,6,7-hexahydro-*s*-indacene and 4,8-Dimethyl-1,2,3,5,6,7-hexahydro-*s*-indacene

We were unsuccessful in preparing these compounds from 4,8-dibromo-1,2,3,5,6,7-hexahydro-*s*-indacene using the same experimental techniques as used for 9-bromo-10-methyl-1,2,3,4,5,6,7,8-octahydroanthracene and 9,10-dimethyl-1,2,3,4,5,6,7-octahydroanthracene.

### 2-Cyclopentylidenecyclopentanone

This compound was prepared in 60% yield by treating an ethanolic solution of cyclopentanone with sodium hydroxide; b.p. 112 °C at 5mm Hg (lit.,<sup>7</sup> 88.5-90.0 °C at 2 mmHg), and  $\delta_{\text{H}}$ (60 MHz;  $\text{CCl}_4$ ) 1.49-3.01 (m, 14H,  $-\text{CH}_2-$ ).

**1,2;3,4;5,6-Tris(trimethylene)benzene**

This compound was prepared in 4.5% yield by treating an ethanolic solution of 2-cyclopentylidenecyclopentanone and cyclopentanone with dry hydrogen chloride; b.p. 132 °C at 0.2 mmHg (lit., 238-239 at 762 mmHg), m.p. 92-93 °C (lit.,<sup>7</sup> 97-98 °C).  $\delta_{\text{H}}$ (60 MHz; CCl<sub>4</sub>) 2.2 (q, 6H,  $\beta$ CH<sub>2</sub>), and 2.7 (t, 12H,  $\alpha$ CH<sub>2</sub>).

**2-Bromo-5-nitro-*p*-xylene**

This compound was prepared in 39% yield by treating a solution of 2-bromo-*p*-xylene in acetic anhydride with a mixture of conc. sulphuric acid and fuming nitric acid; m.p. 65 °C (lit.,<sup>8</sup> 62-66 °C)  $\delta_{\text{H}}$ (60 MHz; CCl<sub>4</sub>) 2.50 (6H, s, Me), 7.61 (s, 1H,  $\phi$ ), and 7.88 (s, 1H,  $\phi$ ).

**2,3-Dibromo-5-nitro-*p*-xylene**

This compound was prepared in 70% yield by treating a sulphuric acid solution of silver nitrate and 2-bromo-5-nitro-*p*-xylene with bromine; m.p. 92-94 °C (lit.,<sup>8</sup> 92-96 °C)  $\delta_{\text{H}}$ (60 MHz; CCl<sub>4</sub>) 2.53 (s, 6H, Me), and 7.75 (s, 1H,  $\phi$ ).

**2,3-Dibromo-5-amino-*p*-xylene**

This compound was prepared in 60% yield by treating a ethanolic solution of 2,3-dibromo-5-nitro-*p*-xylene with hydrochloric acid and iron powder; m.p. 82-84 °C (lit.,<sup>8</sup> 87-89 °C)  $\delta_{\text{H}}$ (60 MHz; CCl<sub>4</sub>) 2.28 (s, 6H, Me), 5.39 (s, 2H, NH<sub>2</sub>), and 6.63 (s, 1H,  $\phi$ ).

**2,3-Di-bromo-*p*-xylene**

This compound was prepared in 62 % yield by treating the diazonium salt of 2,3-dibromo-5-amino-*p*-xylene with H<sub>3</sub>PO<sub>2</sub>; m.p. 16 °C (lit.,<sup>8</sup> 16-17 °C)  $\delta_{\text{H}}$ (60 MHz; CCl<sub>4</sub>) 2.33 (6H, s, Me), and 6.93 (2H, s,  $\phi$ ).

**1,4,5,8-Tetramethylbiphenylene**

2,3-Dibromo-*p*-xylene (8.0 g., 30 mmol) in dry tetrahydrofuran (455 ml) was treated at -78 °C with *n*-butyl-lithium (60.6 mmol) in hexane. The mixture was stirred for 2 h, then warmed to room temperature. Hydrolysis yielded 1,4,5,8-tetramethylbiphenylene which was recrystallised from methanol/dichloromethane as

pale yellow crystals (0.17 g, 5.5%), m.p. 228 °C (lit.,<sup>9</sup> 228.5-229 °C).  $\delta_{\text{H}}$  (60 MHz;  $\text{CCl}_4$ ) 2.12 (s, 12H, Me), and 6.25 (4H, s,  $\phi$ ).

#### 4-Bromo-5-iodo-*o*-xylene

This compound was prepared in 39% yield by treating 4-bromo-*o*-xylene with iodine in the presence of nitrosylsulphuric acid (from sulphur dioxide and fuming nitric acid<sup>10</sup>); m.p. 66.5 °C (lit.,<sup>11</sup> 68.5 °C)  $\delta_{\text{H}}$  (60 MHz;  $\text{CCl}_4$ ) 2.16 (s, 6H, Me), 7.24 (s, 1H,  $\phi$ ), and 7.46 (s, 1H,  $\phi$ ).

#### 2,3,6,7-Tetramethylbiphenylene

This compound was prepared in 3.2 % yield by treating 4-bromo-5-iodo-*o*-xylene (9 g, 28.8 mmol) in ether (50 ml) with magnesium (1.1 g, 45.8 mmol) in ether (50 ml) under nitrogen; m.p. 219 °C (from EtOH) (lit.,<sup>12</sup> 224-225 °C).  $\delta_{\text{H}}$  (60 MHz;  $\text{CCl}_4$ ) 2.02 (s, 12H, Me), and 6.40 (s, 4H,  $\phi$ ).

#### 1,2-Dibromo-3,4,5,6-tetramethylbenzene

This compound was prepared in 67% yield by treating 1,2,3,4-tetramethylbenzene with bromine; m.p. 208 °C (lit.,<sup>13</sup> 208 °C)  $\delta_{\text{H}}$  (200 MHz;  $\text{CDCl}_3$ ) 2.27 (s, 6H, Me), and 2.52 (s, 6H, Me).

#### 1,2,3,4,5,6,7,8-Octamethylbiphenylene

This compound was prepared in 60% yield by treating 1,2-dibromo-3,4,5,6-tetramethylbenzene with *n*-butyl-lithium; m.p. 241 °C (from MeOH/ $\text{CH}_2\text{Cl}_2$ ) (lit.,<sup>14</sup> 240-242 °C)  $\delta_{\text{H}}$  (200 MHz;  $\text{CDCl}_3$ ) 2.18 (s, 6H, Me), and 2.04 (s, 6H, Me).

#### Tetraphenylene<sup>15</sup>

Biphenylene (0.1 g) was pyrolysed in an evacuated sealed Pyrex tube for 1 h at 400 °C. The product was purified by chromatography on silica gel, but on oxidation it still showed the ESR spectrum of the biphenylene radical cation. It was therefore further purified by preparative h.p.l.c. on a 50 x 250 x 4.6 mm column of Nucleosil 5 m silica gel with a mobile phase of  $\text{CH}_2\text{Cl}_2$ /light petroleum (3:97) and a flow rate of 1.5  $\text{cm}^3 \text{min}^{-1}$ . Tetraphenylene was obtained as white crystals, m.p. 210 °C,  $m/z$  304. Calc. for  $\text{C}_{24}\text{H}_{16}$  304.

### 2,3,6,7,10,11,14,15-Octamethyltetraphenylene

2,3,6,7-Tetramethylbiphenylene (0.1 g) was sealed in a Pyrex tube under vacuum and heated at 400 °C for 1 h. Mass spectrometry showed the presence of the tetraphenylene (m/z 416), and this was isolated by h.p.l.c. as a white solid (12 mg, 6%) m.p. >290 °C.  $\delta_{\text{H}}$ (400 MHz; CDCl<sub>3</sub>) 2.20 (24 H, s, Me) and 6.90 (8H, s, ArH).  $\delta_{\text{C}}$ (400 MHz; CDCl<sub>3</sub>) 19.40 (Me), 130.75, 135.00, and 139.25 ( $\phi$ ). m/z (70 eV) 417 (42.5%), 416 (100;M<sup>+</sup>), 386 (15.8), 193 (18.7), 186 (10.9), 178 (15.3), 170 (10.8). Found: C, 92.45; H, 7.52. C<sub>32</sub>H<sub>32</sub> requires C, 92.96; H, 7.74%.

### 1,2,3,4,5,6,7,8,9,10,11,12,13,14,15,16-Hexadecamethyltetraphenylene

Pyrolysis of octamethylbiphenylene under similar conditions gave a dark brown oil. The m.s. showed that the tetraphenylene (m/z 528) was present in small amount, but we were unable to isolate it by h.p.l.c.

### Octane-3,6-dione

This compound was prepared in 52% yield by refluxing an ethanolic solution of propanal, pent-1-en-3-one, triethylamine and 3-benzyl-5-(2-hydroxyethyl)-4-methylthiazolium chloride under nitrogen; b.p. 97-99 °C at 10mmHg, (lit.,<sup>16</sup> 110-115 °C at 12 mmHg),  $\delta_{\text{H}}$ (200 MHz; CDCl<sub>3</sub>) 1.05 (t, 6H, Me, <sup>3</sup>J = 7 Hz) 2.49 (q, 4H, CH<sub>2</sub>Me), and 2.69 (s, 4H, -CH<sub>2</sub>CH<sub>2</sub>-).

### 2,2,7,7-Tetramethyloctane-3,6-dione<sup>17</sup>

This compound was prepared in 62% yield from the enolate of pinacolone, generated with lithium di-*iso*-propylamide (LDA). The enolate was oxidized with ferric chloride to yield the title compound, b.p. 60-64 °C at 0.5 mmHg,  $\delta_{\text{H}}$ (200 MHz; CDCl<sub>3</sub>) 1.17 (s, 18H, tBu), and 2.75 (s, 4H, -CH<sub>2</sub>).

### 2,5-Di-*t*-butylpyrrole

This compound was prepared in 91% yield by treating 2,2,7,7-tetramethyloctane-3,6-dione with ammonium carbonate; m.p. 32 °C, (lit.,<sup>18</sup> 32-33 °C),  $\delta_{\text{H}}$ (200 MHz; CDCl<sub>3</sub>) 7.50 (s, H, -NH) 5.74 (s, 2H, =CH-), and 1.75 (s, 18H, tBu).

### 2,5-Diphenylpyrrole

This compound was prepared in 52% yield by refluxing a solution 1,6-diphenyl-2,5-hexanedione in acetic acid with ammonium carbonate; m.p. 143 °C (lit.,<sup>19</sup> 143.5 °C)  $\delta_{\text{H}}$ (60 MHz,  $\text{CCl}_4$ ) 6.57 (s, 2H, -CH=), 7.21-7.53 (m, 10H,  $\phi$ ), and 8.57 (bs, 1H, NH ).

### N-Aminophthalimide

This compound was prepared in 43% yield by treating phthalimide with hydrazine hydrate; m.p. 203-205 °C, (lit.,<sup>20</sup> 200-205 °C). We were not able to record the NMR spectrum of this compound because of its insolubility in available solvents.

### 1-Phthalimido-2,5-dimethylpyrrole

This compound was prepared in 75% yield by treating *N*-aminophthalimide with hexane-2,5-dione in ethanoic acid; m.p. 178°C, (lit.,<sup>20</sup> 180-182 °C) (from EtOH),  $\delta_{\text{H}}$ (400 MHz,  $\text{CDCl}_3$ ) 2.05 (s, 6H, Me) 5.94 (s, 2H, -CH=) 7.86-7.89 (m, 2H,  $\phi$ ,  $^3J = 2.8$  Hz), and 7.99-8.02 (m, 2H,  $\phi$ ).

### 1-Amino-2,5-dimethylpyrrole

This compound was prepared in 28% yield by treating 1-phthalimido-2,5-dimethylpyrrole with hydrazine hydrate; m.p. 52 °C (from EtOH/ $\text{H}_2\text{O}$ ), (lit.,<sup>20</sup> 51-53 °C),  $\delta_{\text{H}}$ (400 MHz;  $\text{CDCl}_3$ ) 2.24 (s, 6H, Me) 4.22 (s, 2H, - $\text{NH}_2$ ), and 5.71 (s, 2H, -CH=).

### 1,4-Bis(2,5-dimethylpyrrolyl)benzene

This compound was prepared in 44% yield by treating an acidic ethanolic solution of 1,4-diaminobenzene with hexane-2,5-dione; m.p. 254 °C (from EtOH) (lit.,<sup>21</sup> 255-257 °C). Found: C, 81.65; H, 7.63; N, 10.60. Calc. for  $\text{C}_{18}\text{H}_{12}\text{N}_2$ : C, 81.78; H, 7.63; N, 10.60%.  $\delta_{\text{H}}$ (200 MHz;  $\text{CDCl}_3$ ) 2.08 (s, 12H, Me) 5.93 (s, 4H, -CH=), and 7.30 (s, 4H,  $\phi$ ).

### 1,4-Bis(2,5-diethylpyrrolyl)benzene

A mixture of 1,4-diaminobenzene (0.80 g, 7.02 mmol), octane-3,6-dione

(1.00 g, 7.02 mmol) and concentrated hydrochloric acid (0.1 ml) in ethanol was heated to reflux for 1 h. After cooling, the mixture was neutralized with a slight excess of sodium carbonate. The reaction mixture was taken up in ether (50 ml), washed with water (2 x 50 ml) and the solvent removed. The crude product in dichloromethane was filtered through silica. Removal of the solvent yielded the title compound (1.1 g, 49%), m.p. 278 °C (from EtOH). Found: C, 82.21; H, 8.75; N, 8.69.  $C_{22}N_{28}N_2$  requires C, 82.45; H, 8.81; N, 8.74%.  $\delta_H$ (200 MHz,  $CDCl_3$ ) 1.13 (t, 12H, Me,  $^3J = 7.6\text{Hz}$ ) 2.40 (q, 8H,  $-CH_2-$ ) 5.99 (s, 4H,  $-CH=$ ), and 7.31 (s, 4H,  $\phi$ ).

#### **1,4-Bis(2,5-dimethylpyrrolyl)2,3,5,6-tetramethylbenzene**

A mixture of 1,4-diamino-2,3,5,6-tetramethylbenzene (1.64 g, 10 mmol), hexane-2,5-dione (2.28 g, 20 mmol) and conc. hydrochloric acid (0.2 ml) in ethanol (50 ml) was heated to reflux for 1 h. The work-up was similar to that of 1,4-bis(2,5-diethylpyrrolyl)benzene yielding the title compound (1.98 g, 62%), m.p. 189 °C (from EtOH). Found: C, 82.14; H, 8.86; N, 8.80.  $C_{22}H_{28}N_2$  requires C, 82.45; H, 8.81; N, 8.74%.  $\delta_H$ (400 MHz;  $CDCl_3$ ) 1.83 (s, 6H, Me), 1.88 (s, 6H, Me), 5.96 (s, 5H,  $-CH=$ ), and H.R.M.S. m/z Found 320.222. Calc. 320.2252.

#### **1-Amino-4-(N-2,5-dimethylpyrrolyl)benzene**

A mixture of 1,4-diaminobenzene (1.89 g, 17.54 mmol), hexane-2,5-dione (1.00 g, 8.77 mmol) and conc. hydrochloric acid (0.2 ml) in ethanol (50 ml) was heated to reflux for one hour. After cooling, the mixture was neutralised with a slight excess of sodium carbonate, water (100 ml) added and the mixture was extracted with ether (3 x 50 ml). The combined organic extracts were washed with water (2 x 50 ml) and dilute hydrochloric acid (3 x 50 ml). To the combined acidic washings was added a slight excess of sodium carbonate solution. The cloudy mixture was extracted with ether (3 x 50 ml), and the extract dried over potassium carbonate. The solvent was removed and the residue was sublimed at 120 °C at 0.1 mmHg, yielding the title compound (0.74 g, 22%), m.p. 98 °C (from EtOH/ $H_2O$ ). Found: C, 77.38; H, 7.50; N, 14.83.  $C_{12}H_{14}N_2$  requires C, 77.38; H, 7.58; N, 14.83%.  $\delta_H$ (200 MHz;  $CDCl_3$ ) 1.98 (s, 6H, Me), 3.69-3.79 (s, 2H,  $NH_2$ ), 5.85 (s, 2H,  $-CH=$ ), 6.65-6.74 (m, 2H,  $\phi$ ), and 6.90-7.00 (m, 2H,  $\phi$ ).

### 1-(*N*-2,5-Diethylpyrrolyl)-4-(*N*-2,5-dimethylpyrrolyl)benzene

A mixture of 1-amino-(*N*-2,5-dimethylpyrrolyl)benzene (10.1 g, 0.53 mmol), octane-3,6-dione (0.076 g, 0.53 mmol) and concentrated hydrochloric acid (0.1 ml) in ethanol (5 ml) was heated to reflux for 1h. The-work up was similar to that of 1,4-bis(2,5-diethylpyrrolyl)benzene, yielding the title compound (0.077 g, 52%), m.p. 192 °C (from EtOH). Found: C, 81.84; H, 8.25; N, 9.54.  $C_{20}H_{24}N_2$  requires C, 82.13 ; H, 8.27; N, 9.58%.  $\delta_H$ (200 MHz;  $CDCl_3$ ) 1.10 (t, 6H, Me,  $^3J = 7.4$  Hz), 2.08 (s, 6H, Me) 2.36 (q, 4H,  $MeCH_2$ ), 5.94 [s, 2H,  $-CH=(MePy)$ ], 5.99 [s, 2H,  $-CH=(EtPy)$ ], and 7.29 (s, 4H,  $\phi$ ).

### Methylenebis-(2,5-dimethylpyrrole)

After dropwise addition of *n*-butyl-lithium (20 ml, 2.5 molar) under  $N_2$  to a stirred solution of 2,5-dimethylpyrrole (4.76 g, 50 mmol) in ether (30 ml) and HMPA (30 ml), the ether and cyclohexane (solvent from *n*-BuLi) were removed by distillation. The resulting lithium pyrrolate solution was added slowly at 25 °C to a stirred mixture of HMPA (30 ml) and dichloromethane (30 ml). After 15 h the reaction mixture was added to a two phase extracting mixture of ether and saturated aqueous sodium carbonate (1:1, 200 ml). The ethereal phase was washed with aqueous sodium carbonate (3 x 50 ml), dried over magnesium sulphate, and the solvent removed to yield the crude product. This was taken up in dichloromethane and quickly filtered through silica to yield the title compound (1.92 g, 38%) m.p. 123.5 °C (from EtOH). Found: C, 77.00; H, 8.68; N,13.88.  $C_{13}H_{16}N_2$  requires C,77.18; H, 8.97; N, 13.85%.  $\delta_H$ (400 MHz;  $CDCl_3$ ) 2.06 (s, 12H, Me), 5.73 (s,  $-CH_2-$ , 2H), and 5.78 (s,  $=CH-$ , 4H).

### Tetramethylene-(2,5-dimethylpyrrole)

1,4-Diaminobutane (0.882 g, 10 mmol) was dissolved in ether mixed thoroughly with montmorillonite clay K10 (4 g) and the solvent removed under vacuum. To this, hexane-2,5-dione (2.28 g, 20 mmol) was added dropwise with stirring at *ca.* 0 °C. After 24 h at *ca.* 20 °C, the product was extracted into dichloromethane and quickly filtered through silica. Removal of solvent yielded the title compound (2.39 g, 96%), m.p. 140 °C (from EtOH). Found: C, 78.71; H, 10.11; N, 11.43.  $C_{16}H_{24}N_2$  requires C, 78.64; H,9.90; N, 11.43%.  $\delta_H$ (400 MHz;



CDCl<sub>3</sub>) 1.62-1.67 (m, 4H, -CH<sub>2</sub>-), 2.20 (s, 12H, Me), 3.69-3.74 (m, 4H, NCH<sub>2</sub>), and 5.75 (s, 4H, -CH=).

### **2,2,5,5-Tetramethyl-1,1-bipyrrolyl**

This compound was prepared in 46% yield by treating an acidic ethanolic solution of 1-amino-2,5-dimethylpyrrole with hexane-2,5-dione, m.p. 64 °C (from MeOH), (lit.,<sup>20</sup> 62 °C). Found: C, 76.45; H, 8.45; N, 14.78. calc for C<sub>12</sub>H<sub>16</sub>N<sub>2</sub> C, 76.55; H, 8.57%. δ<sub>H</sub>(400 MHz; CDCl<sub>3</sub>) 1.91 (s, 12H, Me) and 5.85 (s, 4H, -CH=).

### **5-Methylfurfuryldimethylamine<sup>22</sup>**

This compound was prepared in 71% yield by treating an ethanoic acid solution of dimethylamine and formaldehyde with 2-methylfuran; b.p. 59-61 °C at 12 mmHg, δ<sub>H</sub>(200 MHz; CDCl<sub>3</sub>) 2.23 (s, 6H, Me), 2.26 (s, 2H, -CH<sub>2</sub>-), 5.86 (d, 1H, -CH=, <sup>3</sup>J = 2.8Hz), and 6.04 (d, 1H, -CH=, <sup>3</sup>J = 2.8Hz).

### **5,5-Ethylene-1,2-di(2-furyl)-ethane**

This compound was prepared in 59% yield by pyrolysis of the quaternary hydroxide of 5-methyl-2-furfuryltrimethylammonium iodide. The pyrolysis products were trapped in an alcoholic solution of hydroquinone below -70 °C to reduce polymerization; m.p. 187-189 °C (lit.,<sup>23</sup> 188-190 °C) (sealed capillary) δ<sub>H</sub>(60 MHz, CCl<sub>4</sub>) 2.63-2.87 (m, 4H, -CH<sub>2</sub>CH<sub>2</sub>-), and 6.12 (s, 4H, =CH-).

### **1,1,2,2-Tetramethoxytetrahydro-5,5-ethylene-1,2-di-(2-furyl)-ethane**

This compound was prepared in 81% yield by treating a methanolic solution of 5,5-ethylene-1,2-di-(2-furyl)ethane and potassium acetate below -5 °C with bromine; m.p. 160-162 °C (from AcOEt) (lit.,<sup>23</sup> m.p. 159-160 °C) δ<sub>H</sub>(60 MHz; CCl<sub>4</sub>) 2.49-2.58 (s, 8H, -CH<sub>2</sub>-), 3.34 (s, 12H, OMe), 5.92 (s, 2H, =CH-), and 6.23 (s, 2H, =CH-).

### **3,4,7,8-Tetrahydro-8b,8c-diazacyclopent[f,g]acenaphthylene**

This compound was prepared in 19% yield by treating 1,1,2,2-tetramethoxytetrahydro-5,5-ethylene-1,2-di-(2-furyl)ethane with dilute sulphuric acid.

The mixture was neutralised with sodium carbonate and treated with hydrazine hydrate. Work-up and sublimation (110 °C at 0.2 mmHg) of the residue gave white crystals, m.p. 172 °C, (lit.,<sup>24</sup> 172-173 °C),  $\delta_{\text{H}}$ (400 MHz; CDCl<sub>3</sub>) 2.94 (s, 8H, -CH<sub>2</sub>-) and 5.84 (s, 4H, -CH=).

### **8b,8c-Diazacyclopent[fg]acenaphthylene**

This compound was prepared in 22% yield by treating a solution of 3,4,7,8-tetrahydro-8b,8c-diazacyclopent[fg]acenaphthylene in toluene under nitrogen with 2,3-dichloro-4,5-dicyanobenzoquinone (DDQ). Work-up and sublimation (75 °C at 0.5 mmHg) of the residue produced purple crystals, m.p. 142 °C, (lit.,<sup>24</sup> 143-145 °C)  $\delta_{\text{H}}$ (400 MHz; CDCl<sub>3</sub>) 6.13 (s, 4H, -CH=), and 6.22 (s, 4H, -CH=).

### **3,4-Dihydro-8b,8c-diazacyclopent[fg]acenaphthylene**

This compound was prepared in 23% yield by treating 3,4,7,8-tetrahydro-8b,8c-diazacyclopent[fg]acenaphthylene with Pd/C (10%) in refluxing triethylene glycol under nitrogen. Work-up and sublimation (80 °C 0.5 mmHg) of the residue produced white crystals, m.p. 170 °C, (lit.,<sup>24</sup> 168-170 °C),  $\delta_{\text{H}}$ (400 MHz; CDCl<sub>3</sub>) 3.28 (s, 4H, -CH<sub>2</sub>CH<sub>2</sub>-), 6.82 (s, 2H, -CH=), and 6.32 (s, 4H, -CH=).

### **Bicyclo-[8.2.0]-dodecan-1-ol<sup>25</sup>**

This compound was prepared in 40% yield by irradiating a solution of cyclododecanone in cyclohexane with a high pressure mercury lamp. The product was a mixture of *cis* and *trans* isomers, b.p. 100-105 °C at 0.05 mmHg, and IR (neat) 3380 cm<sup>-1</sup> (OH).

### **$\Delta^{1(9)}$ -Bicyclo[7.2.0]undecene<sup>25</sup>**

This compound was prepared by dehydration of bicyclo[8.2.0]-dodecan-1-ol with thionyl chloride and pyridine in 22% yield; b.p. 80-86 °C at 0.01 mmHg.  $\delta_{\text{H}}$ (60 MHz; CCl<sub>4</sub>) 1.25-1.85 (m, 12H, -CH<sub>2</sub>-), 1.90-2.15 (m, 4H, -CH<sub>2</sub>-), and 2.25 (s, 4H, -CH<sub>2</sub>). The product contained bicyclo[7.2.0]undecene as an impurity.

### **1,4-Cyclodecanedione**

This compound was prepared in 27% yield by oxidative ring opening of

$\Delta^{10}$ -bicyclo[7.2.0]undecene with sodium metaperiodate. Work-up was similar to the literature, except that the organic extracts were washed with dilute aqueous potassium carbonate. This was to remove the oxidation product of bicyclo[8.2.0]undec-1-ene (carboxylic acid); m.p. 79 °C (lit.,<sup>25,26</sup> 78-79 °C) I.R (neat) 1708.2 (C=O)  $\text{cm}^{-1}$ .

### 10-Phenyl[8](2,5)pyrrolophane

This compound was prepared in 55% yield by treating 1,4-cyclodecanedione with aminobenzene; m.p. 54 °C, (lit.,<sup>27</sup> 54-55.5 °C),  $\delta_{\text{H}}$ (200 MHz;  $\text{CDCl}_3$ ) 0.30-1.81 (m, 12H,  $-\text{CH}_2-$ ), 2.26-2.73 (m, 4H,  $-\text{CH}_2-$ ), 6.05 (s, 2H,  $-\text{CH}=\text{}$ ), and 7.36 (m, 5H,  $\phi$ ).

### [8](2,5)Pyrrolophane

This compound was prepared in 73% yield by treating 1,4-cyclodecanedione with ammonium carbonate; m.p. 155 °C, (lit.,<sup>27</sup> 154-154.5 °C), (sealed capillary),  $\delta_{\text{H}}$ (200 MHz;  $\text{CDCl}_3$ ) 1.14-1.72 (m, 8H,  $-\text{CH}_2-$ ), 2.44-2.76 (m, 4H,  $-\text{CH}_2-$ ), 5.79 (m, 2H,  $=\text{CH}-$ ), and 7.85 (s, H, NH).

### [8](2,5)Furanophane<sup>27</sup>

This compound (an oil) was prepared in 68% yield by treating 1,4-cyclodecanedione with phosphorus pentoxide;  $\delta_{\text{H}}$ (200 MHz;  $\text{CDCl}_3$ ) 2.53 (m, 4H,  $-\text{CH}_2-$ ) and 5.58 (s, 2H,  $-\text{CH}-$ ).

### 2,3-Dihydro-5,7-dimethylfuro[3,4b]-*p*-dioxin

A mixture of 2,5-dimethyl-4-hydroxy-3(2H)-furanone (16.24 g, 127 mmol), ethane-1,2-diol (23.6 g, 536 mmol), *p*-toluene sulphonic acid (2.0 g, 95 mmol), and benzene (1 L) was stirred under reflux under  $\text{N}_2$  with a Dean and Stark trap. When water has ceased to collect (*ca.* 1h), the reaction mixture was reduced to half its volume, washed with saturated aqueous sodium carbonate (3 x 50 ml), filtered, and the solvent removed. Distillation gave the title compound, which is hygroscopic and air sensitive (6.64 g, 23%), b.p. 97 °C at 5 mmHg. Found: C, 62.06; H, 6.47.  $\text{C}_8\text{H}_{10}\text{O}_3$  requires C, 62.33; H, 6.54%.  $\delta_{\text{H}}$ (200 MHz;  $\text{CDCl}_3$ ) 2.12 (s, 6H, Me) and 4.12 (s, 4H,  $-\text{CH}_2\text{CH}_2-$ ).

### 2,3,5,7-Tetrahydro-5,7-dimethyl-5,7-dimethoxy-[3,4b]-*p*-dioxin

A mixture of 2,3-dihydro-5,7-dimethylfuro[3,4b]*p*-dioxin (4.0 g, 23 mmol), freshly fused potassium acetate (15.29 g, 54 mmol), and dry methanol (100 ml) were stirred and cooled to *ca.* -15 °C under N<sub>2</sub>. To this was added dropwise bromine (4.67 g, 29 mmol) and the mixture warmed to room temperature. After addition of an excess of sodium carbonate, the mixture was concentrated under vacuum. Water was added (100 ml) and the solution extracted with diethyl ether (3 x 50 ml). The combined organic extracts were dried with magnesium sulphate, filtered and stripped of solvent to yield the title compound as a diastereomeric mixture. The title compound is air-sensitive, hygroscopic, and light-sensitive (4.42g, 89%), m.p. 95-96 °C (from *n*-heptane). Found: C, 55.30; H, 7.69. C<sub>10</sub>H<sub>16</sub>O<sub>5</sub> requires C, 55.55; H, 7.46%.  $\delta_{\text{H}}$ (200 MHz; CDCl<sub>3</sub>) 1.50 (s, 6H, Me) 3.31 (s, 6H, Me) 1.60 (s, 6H, Me) 3.21 (s, 6H, MeO) and 4.19 (s, 8H, -CH<sub>2</sub>-).

### 2,5-Dimethyl-1,3,4-thiadiazole

This compound was prepared in 60% yield by treating N,N'-diacetalhydrazine with sulphur and triethylamine; m.p. 64 °C (lit.,<sup>28</sup> 64 °C)  $\delta_{\text{H}}$ (400 MHz; CDCl<sub>3</sub>) 2.74 (s, 6H, Me).

### 2,5-Di-*i*-propyl-1,3,4-thiadiazole<sup>28</sup>

This compound was prepared in 40% yield by treating N,N'-di-*i*-propylacetylhydrazine with sulphur and triethylamine;  $\delta_{\text{H}}$ (200 MHz; CDCl<sub>3</sub>) 1.42 (d, 2H, *i*-Pr, <sup>3</sup>J = 6.8 Hz) and 3.48 (septet, 12H, *i*-Pr).

### 2,5-Di-*t*-Butyl-1,3,4-thiadiazole

A mixture of trimethylacetaldehyde (12.9g, 150 mmol), ethanediol (10 ml) and ethanol (10 ml) at *ca.* 20 °C was treated with hydrazine hydrate (12 ml, 80%). After 2 h the reaction mixture was heated to *ca.* 70 °C and sulphur (4.8g, 150 mmol) and triethylamine (2.5 ml, 30% in EtOH) added; the mixture was heated for a further two days at *ca.* 90 °C. After cooling, the crude product in ether (50 ml) was filtered through silica and the filtrate washed with dilute aqueous CuSO<sub>4</sub> (2 x 25 ml) and water (2 x 25 ml). The organics were dried (MgSO<sub>4</sub>), filtered and

the solvent removed under vacuum. The residue was subjected to chromatography, to yield the title compound (5.64, 19%) m.p. 92 °C Found: C, 60.29; H, 9.25; N, 13.99. C<sub>10</sub>H<sub>18</sub>N<sub>2</sub>S required C, 60.56; H, 9.15; N, 14.12%.  $\delta_{\text{H}}$ (400 MHz; CDCl<sub>3</sub>) 1.54 (s, 18H, *t*-Bu).

### 2,5-Dimethyl-1,3,4-oxadiazole<sup>29</sup>

This compound (an oil) was prepared in 60% yield by treating a solution of *N,N'*-diacetalhydrazine in ethanoic acid with perchloric acid;  $\delta_{\text{H}}$ (60 MHz; CCl<sub>4</sub>) 2.50 (s, 6H, Me).

### 2,4-Hexadiyne

This compound was prepared in 23% yield by treating a mixture of freshly prepared sodamide and 1,4-dichloro-2-butyne in liquid ammonia with methyl iodide; m.p. 66 °C, (lit.,<sup>30</sup> 67 °C) and  $\delta_{\text{H}}$ (200 MHz; CDCl<sub>3</sub>) 2.20 (s, 6H, Me).

### Phenylarsine

This compound was prepared in 53% yield by reducing phenylarsonic acid with zinc amalgam and hydrochloric acid under nitrogen; b.p. 55 °C at 4 mmHg, (lit.,<sup>31</sup> 81-83 °C at 0.5 mmHg),  $\delta_{\text{H}}$ (400 MHz; CDCl<sub>3</sub>) 3.62 (s, 2H, -AsH<sub>2</sub>), and 7.25-7.32 (m, 5H,  $\phi$ ).

### 1-Phenyl-2,5-dimethylarsole

This compound (an oil) was prepared in 32% yield by treating a solution of 2,4-hexadiyne <sup>and phenylarsine</sup> in benzene with *n*-butyl-lithium; b.p. 80 °C at 0.5 mmHg, (lit.,<sup>31</sup> 81-83 at 0.5mmHg),  $\delta_{\text{H}}$ (200 MHz; CDCl<sub>3</sub>) 2.11 (s, 6H, Me), 6.51 (s, 2H, -CH=), and 7.22-7.34 (m, 5H,  $\phi$ ).

### Bis( $\eta^5$ -cyclopentadienyl)-2,3,4,5-tetramethylzirconacyclopentadiene<sup>32</sup>

This compound was generated in solution *in situ* by treating zirconocene dichloride in THF with *n*-butyl lithium followed by 2-butyne.

### 1-Phenyl-2,3,4,5-tetramethylarsole<sup>32</sup>

This compound (an oil) was prepared in 64% yield by treating bis( $\eta^5$ -

cyclopentadienyl)-2,3,4,5-tetramethylzirconacyclopentadiene with trichloroarsine followed by phenyl-lithium;  $\delta_{\text{H}}$ (200 MHz;  $\text{CDCl}_3$ ) 1.89 (s, 6H, Me), 1.99 (s, 6H, Me), and 7.27-7.29 (m, sH,  $\phi$ ).

### 1-Phenyl-2,3,4,5-tetramethylstibole<sup>32</sup>

This compound (an oil) was prepared in 71% yield by treating bis( $\eta^5$ -cyclopentadienyl)-2,3,4,5-tetramethylzirconacyclopentadiene with trichloroantimony followed by phenyl-lithium;  $\delta_{\text{H}}$ (200 MHz;  $\text{CDCl}_3$ ) 1.87 (s, 6H, Me), 2.05 (s, 6H, Me), 7.22-7.28 (m, 3H,  $\phi$ ), and 7.42-7.47 (m, 2H,  $\phi$ ).

### 1-Phenyl-2,3,4,5-tetramethylphosphole<sup>32</sup>

This compound (an oil) was prepared in 82% yield by treating bis  $\eta^5$ -cyclopentadienyl)-2,3,4,5-tetramethylzirconacyclopentadiene with dichlorophenylphosphine;  $\delta_{\text{H}}$ (200 MHz;  $\text{CDCl}_3$ ) 1.20 (d, 6H, Me,  $J = 3.6\text{Hz}$ ), 1.95 (d, 6H, Me,  $J = 4.2\text{ Hz}$ ), and 7.28 (m, 5H,  $\phi$ ).

## 6.2 Preparation of samples for ESR spectroscopy

All samples were prepared in silica tubes as illustrated in Figures 6.1 and 6.2.

### 6.2.1 Oxidants.

#### Mercury or Thallium Trifluoroacetate in Trifluoroacetic acid

A mixture of TFAH (1 ml) and either  $\text{Hg}(\text{TFH})_2$  or  $\text{Tl}(\text{TFA})_3$  (*ca.* 10 mg) at *ca.* 260 K was purged of oxygen by bubbling nitrogen through the mixture (*ca.* 2 min). The substrate (0.05-10 mg) in TFAH or  $\text{CH}_2\text{Cl}_2$  was added to the oxidizing mixture and the nitrogen passed through the mixture for a further minute.

#### Aluminium Chloride or Antimony Pentachloride in Dichloromethane

A mixture of  $\text{CH}_2\text{Cl}_2$  (1 ml) and either  $\text{AlCl}_3$  or  $\text{SbCl}_5$  (*ca.* 10 mg) at *ca.* 190 K were purged of oxygen by bubbling nitrogen through the mixture (*ca.* 2 min). The substrate (0.05-10 mg) in  $\text{CH}_2\text{Cl}_2$  was added to the oxidizing mixture and the nitrogen passed through the mixture for a further minute.

#### Fluorosulphonic and Liquid Sulphur Dioxide

A mixture of  $\text{SO}_2$  (0.5 ml) and  $\text{HFSO}_4$  (0.5 ml) at ca. 190 K were purged of oxygen by bubbling nitrogen through the mixture (ca. 2 min). The substrate (0.05-10 mg) in  $\text{CH}_2\text{Cl}_2$  was added to the oxidizing mixture and the nitrogen passed through the mixture for a further minute.

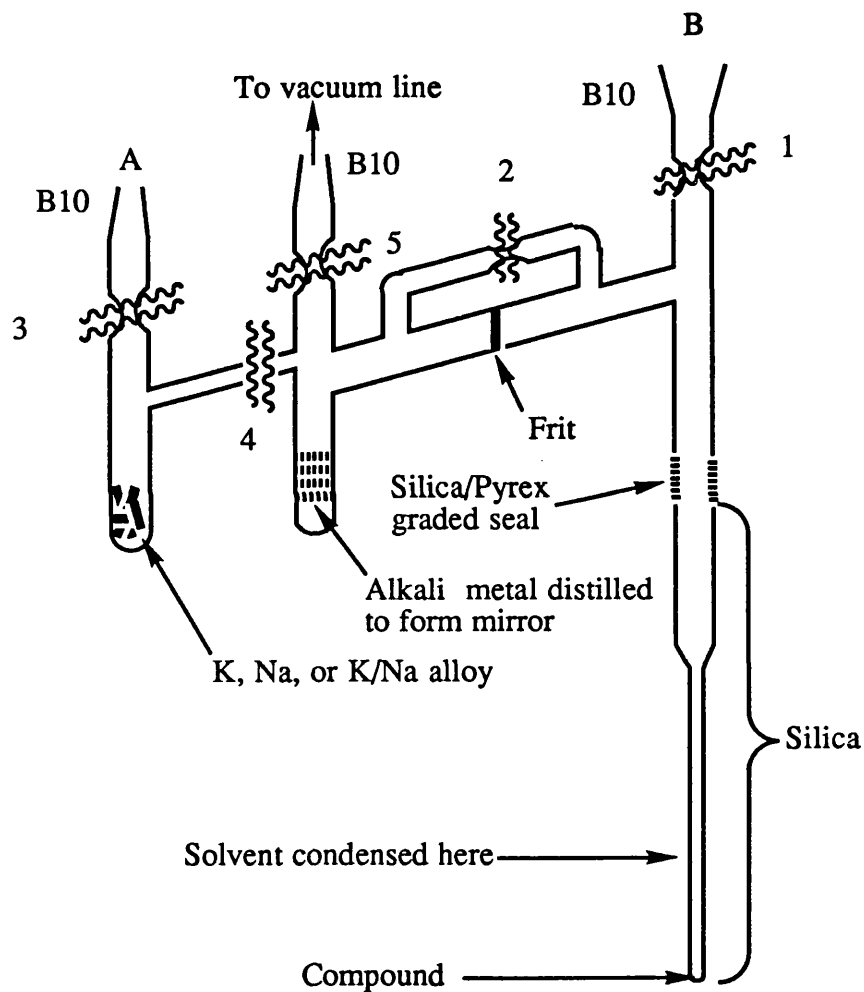


Figure 6.1 Apparatus for preparing radical anions.

### 6.2.2 Reductants

To prepare the radical anions, the degassed solution of the substrate in THF in a sealed silica tube was brought in contact with a potassium mirror or with a slice of lithium which was in contact with a chip of silica to abrade the surface. If the reduction was slow, it was accelerated by immersing the tube in an ultrasonic cleaning bath.

Preparation of the radical anions using Na, K, or Na/K alloy was carried out in the apparatus illustrated in Figure 6.1 using the following procedures:

- 1) The apparatus was predried in an oven (*ca.* 100 °C, 24 h) and then cooled under nitrogen or argon. All further operations were conducted under an inert atmosphere.
- 2) A weighed amount of substrate, sufficient to give a *ca.*  $10^{-3}$  M solution was introduced to the silica tube and joint B was stoppered.
- 3) Freshly cut K, Na or Na/K alloy was washed with dry *n*-pentane and placed in vessel A and joint A was closed off using a small flask.
- 4) The apparatus was evacuated to *ca.*  $10^{-2}$  mmHg; volatile or sublimable samples were prefrozen in liquid nitrogen.
- 5) Points 1 and 3 were sealed and cut and a portion of the metal was carefully distilled over. Point 4 was then sealed and cut.
- 6) Predried solvent (THF or DME) was condensed into the silica tube from the vacuum line.
- 7) Point 2 was sealed and point 5 was sealed and cut.
- 9) When ready, the solution of the compound was brought into contact with the alkali metal.

### 6.3 ESR spectroscopy

ESR spectra were recorded using a Varian E109 or Bruker ESP300 instrument operating in the microwave region *ca.* 9.1 GHz. The spectrometer was fitted with a 500 W high pressure mercury lamp, focused on the cavity using a fused silica condensing lens. The intensity of the light was attenuated with neutral (metal gauze 3, 10, and 30% transmittance ) and glass filters (soda and Pyrex



glass).

The difference in field between the magnetic probe and the sample was determined by measuring the  $g$ -value of the pyrene radical anion<sup>33</sup> ( $g$  2.002710). The unknown  $g$ -value of the radical could then be calculated from the resonance condition given below.

$$h\nu_0 = g\beta B_0$$

$h$  Is Planck's constant,  $\nu_0$  is the microwave frequency,  $\beta$  is the Bohr magneton, and  $B_0$  is the field at the centre of resonance.

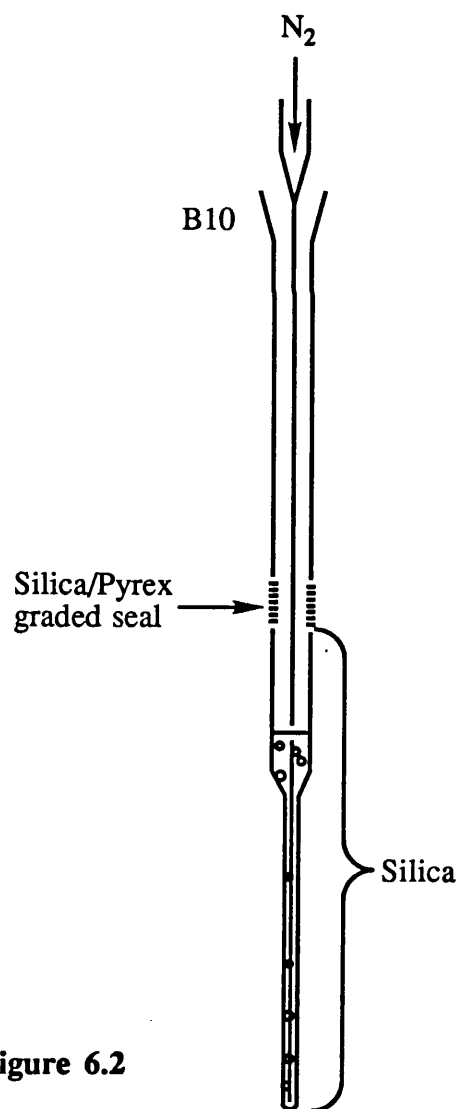


Figure 6.2

Computer simulations of experimental spectra were carried out with the Bruker EPR-Calc program, a modified version of ESRSPEC2<sup>34</sup> or using the ESRXN<sup>35</sup> program for kinetic spectra.

#### 6.4 NMR-Spectroscopy

NMR-spectra were recorded on either a Varian VXR 400, a Varian XL 200, a Perkin Elmer R12 or a Jeol PMX 60 spectrometer.

#### 6.5 Semi-empirical MO and Molecular Mechanics Calculations

Calculations were carried out on a Vax 6310 computer using the MOPAC 5,<sup>36</sup> INDO,<sup>37</sup> and the MM2<sup>38</sup> programs.

#### 6.6 X-Ray Crystallography

Crystal structure data were collected using a Nicolet R3v/m automatic four circle diffractometer. The structures were solved by routine application of direct methods.

All calculations were carried out using a MicroVax 2 computer running SHELXS 86.

#### References

1. D . Hausigh, *Synthesis*. **1971**, *6*, 307.
2. G. Schroeter, *Chem. Ber.*, **1927**, *60*, 2035.
3. D. M. Singleton, *Tetrahedron, Let.*, **1973**, *15*, 1933.
4. R. Criegee, F. Förg, B. A. Brune, and D. Schönlebet, *Chem. Ber.*, **1964**, *97*, 3461.
5. Z. J. Vejdelek, M. Bartosova, and M. Protiva, *Collect. Czech. Chem. Commun.*, **1976**, *41*, 2020.
6. R. T. Arnold and E. Rondestvedt, *J. Am. Chem. Soc.*, **1945**, *45*, 1265.
7. R. Mayer, *Chem. Ber.*, **1956**, *89*, 1443.
8. S. Gronowitz and G. Hanson, *Arkiv. fur. Kemi.*, **1967**, *27*, 145.
9. H. Hart, A. Teuerstein, and M. A. Babin, *J. Am. Chem. Soc.*, **1981**, *103*,

- 903.
10. Fieser and Fieser, 'Reagents for Organic Synthesis', Wiley, New York, 1967, p. 755.
  11. P. S. Varma and K. S. V. Raman, *J. Indian Chem. Soc.*, **1935**, *12*, 245.
  12. P. R. Constantine, G. E. Hall, C. R. Harrison, J. F. W. McOmie, and R. J. G. Searle, *J. Chem. Soc. (C)*, **1966**, 1767.
  13. L. I. Smith and C. L. Moyle, *J. Am. Chem. Soc.*, **1933**, *55*, 1676.
  14. H. Hart and A. Teuerstein, *Synthesis*, **1979**, 693.
  15. L. Friedman and D.F. Lindow, *J. Am. Chem. Soc.*, **1968**, *90*, 2324.
  16. A. G. Davies, L. Julia, and S. N. Yazdi, *J. Chem. Soc. Trans. 2*, **1989**, 239.
  17. R. H. Frazier Jr., and R. L. Harlow, *J. Org. Chem.*, **1980**, *19*, 5408.
  18. R. Ramasseul and A. Rassat, *J. Chem. Soc. Chem. Commun.*, **1965**, 453.
  19. S. Soedigo, and J. M. Patterson, *J. Org. Chem.*, **1968**, *33*, 2057.
  20. W. Flicht, U. Krämer, and H. Zimmermann, *Chem. Ber.*, **1969**, *102*, 3268.
  21. H. Kofod, L. E. Sutton, and J. Jackson, *J. Chem. Soc.*, **1952**, 1467.
  22. *Org. Synth. Coll. Vol. 5*, **1963**, 626.
  23. H. E. Winberg, F. S. Fawcett, W. E. Mochel, and C. W. Theobald, *J. Am. Chem. Soc.*, **1960**, *82*, 1428.
  24. J. L. Atwood, D. C. Hrcir, C. Wong, and W. W. Paulder, *J. Am. Chem. Soc.*, **1974**, *96*, 6132.
  25. K. Matsui, T. Mori, and H. Nozaki, *Bull. Chem. Soc. Jpn.*, **1971**, *44*, 3440.
  26. K. Matsui, T. Mori, and H. Nozaki, *Bull. Chem. Soc. Jpn.*, **1970**, *43*, 231.
  27. K. Matsui and T. Mori, *Tetrahedron*, **1969**, *25*, 5357.
  28. H. Hagen, R. D. Kohler, and H. Fleig, *Liebigs Ann. Chem.*, **1980**, 1216.
  29. G. V. Boyd and S. R. Dando, *J. Chem. Soc. (C)*, **1970**, 1397.
  30. L. Brandsma, "Preparative Acetylene Chemistry" Elsevier, 1972.
  31. G. Markl, H. Hauptmann, and A. Merz, *J. Organomet. Chem.*, **1983**, *249*, 335.
  32. P. J. Fagan and W. A. Nugent, *J. Am. Chem. Soc.*, **1988**, *110*, 2310.
  33. B. Segal, M. Kaplan and G. K. Fraenkel, *J. Chem. Phys.*, **1965**, *43*, 4191.
  34. QCPE no. 210.

35. QCPE no. 209.
36. QCPE no. 455
37. QCPE no. 274
38. QCPE no. 423

*f*